

**LIQUID PHASE MICROEXTRACTION OF HALLUCINOGENIC  
COMPOUNDS FROM HUMAN URINE SAMPLES BASED ON  
SINGLE HOLLOW FIBRE FOLLOWED BY CHROMATOGRAPHIC  
DETERMINATION**



By

Somandla Ncube

A dissertation submitted to the Faculty of Science, University of the  
Witwatersrand in fulfilment of the requirements for the degree of  
Master of Science

University of the Witwatersrand, Johannesburg, March 2016

## **DECLARATION**

I declare that this dissertation is my own, unaided work. It is being submitted for the degree of Master of Science at the University of the Witwatersrand, Johannesburg. It has not been submitted before for any degree or examination at any university

---

(Signature of candidate)

17<sup>th</sup> day of May 2016

## ABSTRACT

A liquid phase microextraction based on single hollow fibre followed by liquid chromatographic determination was developed for the extraction and quantification of the hallucinogenic muscimol and its two precursors, tryptophan and tryptamine from urine samples. A multivariate design of experiment was used in which a half fractional factorial approach was applied to screen six potential factors (donor phase pH, acceptor phase concentration, supported liquid membrane composition, stirring rate, extraction time and salt content) for their extent of vitality on the extraction of muscimol, tryptophan and tryptamine using the developed method. Four factors were identified as essential for an enhanced enrichment of each of the three research analytes from diluted urine samples.

The paired vital factors were then optimized using central composite designs where empirical quadratic response models were used to visualize the response surface through contour plots, surface plots and optimization plots of response output. When the muscimol-based optimum factor levels were applied for the simultaneous extraction of the three research analytes, a composite desirability of 0.687 was obtained implying that the set conditions were ideal for a combined extraction of the analytes from the donor phase into the acceptor phase across a supported liquid membrane impregnated with a carrier molecule. This was an acceptable result considering that only the optimized muscimol factor levels were set as universal factor values. Muscimol was the analyte of interest in this research.

The composite desirability value was predicted by setting the extraction conditions to 20% (w/w) di-(2-ethylhexyl) phosphoric acid (DEHPA) in dihexyl ether (DHE) supported on the walls of a hollow fibre into a 200 mM HCl acceptor phase inside the hollow fibre from a 20% (v/v) diluted urine donor phase spiked in the 0.1 – 10  $\mu\text{g mL}^{-1}$  analyte concentration range maintained at pH 4 and stirred at 800 rpm for 60 mins. Experimentally, average enrichments of 4.1, 19.7 and 24.1 were obtained for muscimol, tryptophan and tryptamine, respectively.

The complexity of urine and the anionic nature of the carrier molecule embedded on the supported liquid membrane resulted in interfering peaks that could not be completely resolved from the analyte peaks. Thus matrix-based calibration curves were used to address matrix effects.

Various statistical approaches were used to validate suitability of the developed method for its potential use in quantifying muscimol and its precursors from urine samples. These validation measures were used as a way of determining the method's ability to maintain the extraction process at equilibrium over a specific range of analyte concentrations over a period of analyte existence in a urine sample. The  $r^2$  values of the matrix-based linear regression prediction models ranged from 0.9933 to 0.9986. The linearity of the regression line of the matrix-based calibration for each analyte was directly linked to the analyte enrichment repeatability. Simultaneous analyte enrichment repeatability over a 0.1 – 10  $\mu\text{g mL}^{-1}$  analyte spiking concentration ranged from an RSD value of 8.3% to 13.1%. Limits of detection were 0.021  $\mu\text{g mL}^{-1}$ , 0.061  $\mu\text{g mL}^{-1}$  and 0.005  $\mu\text{g mL}^{-1}$  for muscimol, tryptophan and tryptamine, respectively.

Other validation parameters that were considered included specificity (and selectivity), accuracy, robustness, extraction range and system suitability. The accuracy of the developed method was reported as the reproducibility of enrichment factor values over six spiking concentrations used in constructing matrix-based calibration curves. System suitability was limited to an HPLC-UV approach. Method suitability was addressed through a comparative summary in which the LOD, LOQ and  $r^2$  values for the developed method were compared to other methods that have been used to extract muscimol from urine samples. The relevance or acceptability of the enrichment factor values obtained for the extraction of the three analytes was achieved by comparison with enrichment factor values of several compounds with similar polarity that have been extracted from urine samples using carrier-mediated hollow fibre liquid phase microextraction.

## **ACKNOWLEDGEMENTS**

First and foremost I would like to thank my supervisors Prof. Luke Chimuka and Prof. Ewa Cukrowska at the University of the Witwatersrand for grooming me towards finding innovative solutions to environmental challenges through research in sample preparation, method development and chromatographic instrumentation for quantification of organic analytes in biological and environmental samples. I appreciate all the contributions of time, ideas and funding to make my MSc productive and stimulating.

Thanks also go to the National Research Fund of South Africa (Innovation Scholarships Grant number: 94860) and the University of the Witwatersrand postgraduate merit award for financial support.

The Post Graduate students in the Environmental Analytical Chemistry research group have contributed immensely to my personal and professional growth. The group has been a source of friendship with invaluable moral support and intellectual guidance.

Last but not least, I would like to thank my family for all their love and encouragement. To my son (Iminathi), his mom (MaFuzani) and my mom (MaNdlovu), thank you for realizing my love for science and supporting me in all my pursuits. To my late sister Sithabile and my brother Pritchard and their families, thank you so much for the encouragement and financial support. Audrey Sharon, ingqobe isingeyakho mtshana wami.

## TABLE OF CONTENTS

DECLARATION .....	ii
ABSTRACT .....	iii
ACKNOWLEDGEMENTS .....	v
TABLE OF CONTENTS .....	vi
LIST OF FIGURES .....	ix
LIST OF TABLES .....	xiii
LIST OF ABBREVIATIONS .....	xvi
1 INTRODUCTION .....	1
2 LITERATURE REVIEW.....	4
2.1 Hallucinogenic compounds .....	4
2.1.1 Definition .....	4
2.1.2 Mushrooms: history, uses and abuses .....	5
2.1.3 Pharmacokinetics and physiological effects of psilocin and muscimol.....	6
2.1.4 Hallucinogenic research: the past, the present and the future .....	10
2.2 HF-LPME sample preparation .....	12
2.2.1 Principle of the HF-LPME .....	12
2.2.2 Advantages of the HF-LPME .....	12
2.2.3 Critical parameters in HF-LPME .....	14
2.2.4 Carrier-mediated three phase HF-LPME for polar compounds.....	15
2.3 Quantification of Muscimol in urine samples .....	17
2.4 Multivariate approaches to design of experiments.....	18
2.4.1 Multivariate design of experiments.....	18
2.4.2 Multivariate Data Analysis Software .....	19
2.4.3 Factorial Designs.....	19
2.4.4 Response surface designs for main factor optimization.....	23
2.4.5 Desirability functions .....	27
2.5 Method application to human body fluids.....	29
2.5.1 Urine samples.....	29
2.6 Matrix-based calibration curves .....	29

2.7	Method validation parameters .....	30
2.7.1	Linearity .....	30
2.7.2	Limits of detection and quantification .....	31
2.7.3	Other method validation parameters .....	32
3	RESEARCH OBJECTIVES .....	34
3.1	General objectives .....	34
3.2	Specific objectives.....	34
3.3	Justification .....	34
4	RESEARCH METHODOLOGY.....	36
4.1	Chemicals and reagents .....	36
4.2	Instrumentation.....	36
4.3	Preparation of standard solutions and buffered mobile phase.....	37
4.4	Chromatographic conditions .....	38
4.5	Calibration of the HPLC-UV.....	39
4.6	Hollow fibre preparation .....	39
4.7	HF-LPME procedure .....	42
4.8	Efficiency of the method .....	43
4.9	Multivariate optimization of the HF-LPME parameters .....	45
4.9.1	Screening experiments using a half fractional factorial design .....	45
4.9.2	Optimization experiments using central composite designs .....	49
4.9.3	Applying optimized method to spiked water samples .....	57
4.10	Method application to human urine .....	58
4.10.1	Urine collection.....	59
4.10.2	Urine preparation, spiking and extraction of analytes .....	59
4.10.3	Calculating matrix effects .....	60
4.10.4	Constructing matrix-based calibration curves.....	60
4.10.5	Method validation .....	61
5	RESULTS AND DISCUSSION .....	63
5.1	Selection of chromatographic conditions .....	63
5.2	Instrument calibration.....	64
5.3	Screening results.....	65
5.3.1	Half fractional factorial design for tryptamine.....	65
5.3.2	Half fractional factorial design for muscimol .....	69
5.3.3	Comparing the current screening results to other related studies ...	72

5.4	Central composite design results .....	74
5.4.1	Pairing of factors essential for muscimol.....	74
5.4.2	Pairing of factors essential for tryptamine .....	76
5.4.3	Paired factor optimization for muscimol.....	77
5.4.4	Paired factor optimization for tryptophan .....	82
5.4.5	Paired factor optimization for TA .....	87
5.4.6	Paired factor optimization for psilocin.....	92
5.4.7	Quadratic response surface models for paired factor optimizations	95
5.4.8	Comparison of optimized factor levels in different articles.....	95
5.5	Comparison of Minitab-predicted EF values with experimental EF values for individual extractions under specific optimum values .....	97
5.6	Comparison of Minitab-predicted EF values versus experimental EF values for simultaneous extractions under conditions optimized for muscimol	98
5.6.1	Changes in predicted EF values and individual desirabilities.....	98
5.6.2	Compound desirability .....	101
5.7	Applying the method in urine samples .....	103
5.7.1	Spiked urine extraction results .....	103
5.7.2	Calculating matrix effects .....	105
5.7.3	Matrix-based calibration curve for tryptamine .....	108
5.7.4	Matrix-based calibration curve for muscimol .....	112
5.7.5	Matrix-based calibration curve for tryptophan .....	115
5.7.6	Differences in peak area errors and EF value errors at each analyte spiking level .....	117
5.8	EF values for the simultaneous extractions from diluted urine samples	118
5.9	Method validation.....	120
5.9.1	Limits of detection and quantification .....	122
5.9.2	Repeatability and reproducibility.....	122
5.9.3	Comparative studies .....	124
6	CONCLUSIONS AND RECOMMENDATIONS .....	127
6.1	Conclusions .....	127
6.2	Recommendations .....	128
7	REFERENCES.....	130
	APPENDIX.....	144



## LIST OF FIGURES

Figure 1 The hypnagogic <i>Amanita muscaria</i> (a), the psychedelic <i>Psilocybe cubensis</i> (b), the first ever cultivated paratrophic <i>Auricularia auricular</i> (c) and <i>Agaricus bisporus</i> at the shelves of a common supermarket in SA (d) .....	6
Figure 2 Psychedelics: psilocybin (a) and psilocin (b), and the neurotransmitter, serotonin (c) .....	7
Figure 3 Psycho-sedatives: ibotenic acid (a) and muscimol (b), and gamma-aminobutanoic acid (GABA), the neurotransmitter (c).....	8
Figure 4 Structure of DEHPA .....	16
Figure 5 The carrier-mediated extraction of MUS from an acidic donor sample to a more acidic acceptor phase.....	17
Figure 6 Available factorial designs as displayed on Minitab 16 .....	25
Figure 7 Star points for a 2 <sup>2</sup> factorial as given by $\pm\alpha$ on the axial lines. Modified from <a href="https://onlinecourses.science.psu.edu/stat503/node/59">https://onlinecourses.science.psu.edu/stat503/node/59</a> .....	25
Figure 8 Mesh contour plots showing a saddle point (a), a minimum point (b) and a maximum point (c). Modified form <a href="http://reliawiki.org/index.php/">http://reliawiki.org/index.php/</a> .....	27
Figure 9 Plots of desirability functions when the goal is to maximize the set response value (a), the goal is to minimize the set response value (b) or the goal is to set a target value for the response. ....	27
Figure 10 Chemical structures of the model compounds and their relevant physical properties .....	40
Figure 11 Schematic diagram for the HF-LPME procedure.....	44
Figure 12 Designing a spherical rotatable central composite approach. X <sub>1-4</sub> refers to the four vital factors identified from fractional factorial design.....	50
Figure 13 Retention and separation on three RP-columns at optimized conditions. Compounds: (1) Muscimol; (2) Tryptophan; (3) 3,4- Dimethoxyphenethylamine; (4) Phenethylamine; (5) Tryptamine; (6) Hordenine; (7) Psilocin. Compound numbering was based on descending polarity.....	63
Figure 14 Chromatograms when THF and MeCN were used to dilute the MeOH stock solutions for analyte injection. Compounds: (7) Psilocin; (6) Hordenine; (5) Tryptamine; (4) Phenethylamine; (3) 3, 4- Dimethoxyphenethylamine; (2)	

Tryptophan; (1) Muscimol. Muscimol and psilocin were injected at $1 \mu\text{g mL}^{-1}$ and at $0.5 \mu\text{g mL}^{-1}$ respectively .....	65
Figure 15 Pareto chart of factor effects for the extraction of TA (Alpha = 0.05, only 30 largest effects shown) .....	67
Figure 16 Normal plot of factor effects for extraction of TA (Alpha = 0.05, only 30 largest effects shown).....	68
Figure 17 Main factor effects plot for response average during extraction of TA	68
Figure 18 Pareto chart of factor effects for the extraction of MUS (Alpha = 0.05, only 30 largest effects shown) .....	70
Figure 19 Normal plot of factor effects for the extraction of MUS (Alpha = 0.05, only 30 largest effects shown) .....	71
Figure 20 Main factor effects plot for response average during extraction of MUS .....	71
Figure 21 Pareto chart of standardized effects of the main factors of MUS (Alpha = 0.05) .....	75
Figure 22 Normal plot of standardized effects of the main factors on MUS (Alpha = 0.05) .....	75
Figure 23 Pareto chart of standardized effects of TA (Alpha = 0.05).....	76
Figure 24 Normal plot of standardized effects of main factors on TA (Alpha = 0.05). .....	77
Figure 25 Contour plot of EF values of MUS versus the interrelated effect of stirring rate and DP pH .....	78
Figure 26 Surface plot of EF values of MUS versus the interrelated effect of stirring rate and DP pH .....	79
Figure 27 Optimization plot of effects of stirring rate and DP pH on enrichment of MUS.....	79
Figure 28 Contour plot of EF values of MUS versus the interrelated effect of SLM composition and AP concentration .....	80
Figure 29 Surface plot of EF values of MUS versus the interrelated effect of SLM composition and AP concentration .....	81
Figure 30 Optimization plot of effects of SLM composition and AP concentration on enrichment of MUS.....	82

Figure 31 Contour plot of EF values of TRP versus the interrelated effect of stirring rate and DP pH .....	83
Figure 32 Surface plot of EF values of TRP versus the interrelated effect of stirring rate and DP pH .....	84
Figure 33 Contour plot of effects of stirring rate and DP pH on enrichment of TRP .....	84
Figure 34 Contour plot of EF values of TRP versus the interrelated effect of SLM composition and AP concentration .....	86
Figure 35 Surface plot of EF values of TRP versus the interrelated effect of SLM composition and AP concentration .....	86
Figure 36 Contour plot of effects of SLM composition and AP concentration on enrichment of TRP .....	87
Figure 37 Contour plot of EF values of TA versus the interrelated effect of AP concentration and DP pH .....	88
Figure 38 Surface plot of EF values of TA versus the interrelated effect of AP concentration and DP pH .....	89
Figure 39 Optimization plot of effects of AP concentration and DP pH on enrichment of TA .....	89
Figure 40 Contour plot of EF values of TA versus the interrelated effect of extraction time and SLM composition.....	90
Figure 41 Surface plot of EF values of TA versus the interrelated effect of extraction time and SLM composition.....	91
Figure 42 Optimization plot of effects of extraction time and SLM composition on enrichment of TA .....	92
Figure 43 Contour plot of EF values of PSI versus the interrelated effect of extraction time and SLM composition.....	93
Figure 44 Surface plot of EF values of PSI versus the interrelated effect of extraction time and SLM composition.....	94
Figure 45 Optimization plot of effects of extraction time and SLM composition on enrichment of PSI.....	94
Figure 46 Effects of setting the stirring rate to 800 rpm on the desirability and response output for MUS .....	99

Figure 47 Effects of setting MUS-based levels of DP pH and stirring rate on the dual desirability and response output for TRP .....	99
Figure 48 Effects of setting MUS-based levels of AP concentration and SLM composition on the dual desirability and response output for TRP .....	100
Figure 49 Effects of setting MUS-based levels of DP pH and AP concentration on the dual desirability and response output for TA .....	100
Figure 50 Effects of setting MUS-based levels of SLM composition and extraction time on the dual desirability and response output for TA.....	101
Figure 51 Comparison of blank urine peaks and the 2 $\mu\text{g mL}^{-1}$ spiked urine peaks for the extraction of TA (a) and, MUS and TRP (b).....	104
Figure 52 Matrix-based calibration curve for the extraction of TA from diluted urine samples; acceptor phase had been diluted 53 fold. (n=3, SD).....	111
Figure 53 Matrix-based calibration curve for the extraction of TA from diluted urine samples assuming the AP was not diluted. (n=3, SD).....	111
Figure 54 Matrix-based calibration curve for the extraction of MUS from diluted urine samples spiked up to a concentration of 5 $\mu\text{g mL}^{-1}$ . The acceptor phase had been diluted 6 fold. (n=3; SD) .....	114
Figure 55 Matrix-based calibration curve for the extraction of TRP from diluted urine samples spiked up to a concentration of 10 $\mu\text{g mL}^{-1}$ . The acceptor phase had been diluted 6 fold.....	117

## LIST OF TABLES

Table 1 Pharmacokinetics and physiological effects of psilocin and muscimol.....	9
Table 2 Resolutions and their acceptability in predicting interactions .....	24
Table 3 Properties of the six columns used.....	41
Table 4 Dilution of acceptor phases for injection into the HPLC system.....	43
Table 5 Summary of a fractional factorial design used.....	45
Table 6 Lower and upper levels for the six factors .....	46
Table 7 Alias structure of the $2^{6-1}$ fractional factorial design for six factors .....	47
Table 8 Design of experiment summary showing uncoded randomized runs when a $2^{6-1}$ fractional factorial was designed with each factor having two levels; a lower level and an upper level.....	48
Table 9 Factor levels that were entered into Minitab when creating the CCD for the main factors .....	51
Table 10 Actual factor levels of the main factors that were experimentally investigated .....	51
Table 11 Randomized central composite design for the essential factors at $\alpha = 2$	52
Table 12 Randomized uncoded central composite design for the essential factors for TA.....	54
Table 13 Factor levels for the investigation of the combined effect of DP pH and stirring rate in the extraction of MUS .....	55
Table 14 Factor levels for the investigation of the combined effect of AP concentration and SLM composition in the extraction of MUS .....	55
Table 15 Factor levels for the investigation of the combined effect of DP pH and AP concentration in the extraction of TA .....	55
Table 16 Factor levels for the investigation of the combined effect of SLM composition and extraction time in the extraction of TA .....	56
Table 17 Factor levels for the investigation of the combined effect of donor phase pH and stirring rate in the extraction of TRP.....	56
Table 18 Factor levels for the investigation of the combined effect of AP concentration and SLM composition in the extraction of TRP .....	56

Table 19	Factor levels for the investigation of the combined effect of SLM composition and extraction time in the extraction of PSI.....	57
Table 20	Summary of instrument calibration results for the four analytes.....	65
Table 21	One-way ANOVA results for extraction of TA (n=3).....	66
Table 22	One-way ANOVA results for extraction of MUS (n=3) .....	69
Table 23	Comparison of essential factors identified through fractional designs	73
Table 24	Summary of quadratic response surface models for two factor interactions using uncoded data. ....	96
Table 25	Summary of optimum levels for non-analyte related factors.....	97
Table 26	Experimental versus Minitab 16-predicted EF values under optimum conditions for extracting TA, MUS and TRP individually. ....	98
Table 27	Comparison of predicted and experimental EF values when TA, MUS and TRP were extracted simultaneously under universal factor levels.....	102
Table 28	EF values for simultaneous extraction of TA, MUS and TRP using 200 mM HCl as the acceptor phase (n=3).....	103
Table 29	Average peak areas for extraction of MUS from 2 $\mu\text{g mL}^{-1}$ spiked diluted urine solutions using 200 mM HCl as acceptor phase (n=3) .....	105
Table 30	Comparison of EF values of TA, MUS and TRP in water and diluted urine samples spiked at 2 $\mu\text{g mL}^{-1}$ (n=3).....	106
Table 31	Percentage matrix effects on extraction of TA, MUS and TRP from a 2 $\mu\text{g mL}^{-1}$ spiked diluted urine sample using 200 mM HCl as the acceptor phase (n=3, RSD).....	106
Table 32	Summary of percentage reductions in EF values when TA, MUS and TRP were extracted from spiked diluted urine compared to spiked water samples .....	107
Table 33	Comparison of matrix peak areas in EF values for TA, MUS and TRP in spiked diluted urine samples .....	107
Table 34	Summary of data for calculating EF values for extracting TA from six different spiking concentrations (n=3, RSD) .....	110
Table 35	Single Factor ANOVA for blank and 0.1 $\mu\text{g mL}^{-1}$ spiked results. ....	112
Table 36	Summary of data for calculating EF values for extracting MUS from six different spiking concentrations (n=3, RSD) .....	113

Table 37	Single Factor ANOVA for blank and 0.1 $\mu\text{g mL}^{-1}$ spiked result. ....	115
Table 38	Summary of data for calculating EF values for extracting TA from six different spiking concentrations (n=3, RSD) .....	116
Table 39	Summary of errors when three extractions were performed per analyte spiked concentration (n=3).....	119
Table 40	Summary of EF values for the simultaneous extraction of MUS, TRP and TA from diluted urine sample spiked in the 0.1 – 10 $\mu\text{g mL}^{-1}$ .....	120
Table 41	Summary of method validation parameters. ....	121
Table 42	Comparison of $r^2$ values, LODs and LOQs for the matrix-based calibration and the standard solution-based calibration. ....	121
Table 43	Reproducibility of EF values of TA, MUS and TRP extracted from the 2 $\mu\text{g mL}^{-1}$ spiked urine solution after 24 hrs.....	123
Table 44	Comparison of LODs and LOQs, repeatability and reproducibility, and $r^2$ values for different methods that have used to extract MUS from urine samples. ....	125
Table 45	EF values of polar compounds with $X \log P_3 \leq 1.6$ that have been extracted from urine using carrier-mediated HF-LPME.....	126

## LIST OF ABBREVIATIONS

Aliquat 336	N-Methyl-N,N,N-trioctylammonium chloride
ANOVA	Analysis of variance
AP	Acceptor phase
CCD	Central composite design
DEHPA	Di-(2-ethylhexyl) phosphoric acid
DHE	Dihexyl ether
DOE	Design of experiment
DP	Donor phase
EF	Enrichment factor
GABA	Gamma-aminobutanoic acid
HCl	Hydrochloric acid
HF	Hollow fibre
HF-LPME	Hollow fibre-Liquid phase microextraction
HILIC	Hydrophilic interaction liquid chromatography
HPLC-UV	High performance liquid chromatography – ultra violet
LC-MS	Liquid chromatography – mass spectroscopy
LOD	Limit of detection
LOQ	Limit of quantification
LSD	Lysergic acid diethylamide
LPME	Liquid phase microextraction



MeCN	Acetonitrile
MeOH	Methanol
MUS	Muscimol
NaCl	Sodium chloride
OFAT	One-factor-at-a-time
PSI	Psilocin
$R^2$ or $r^2$	Coefficient of determination
(R)SD	(Relative) Standard deviation
SLM	Supported liquid membrane
TA	Tryptamine
TEHP	Tris(2-ethylhexyl) phosphate
THF	Tetrahydrofuran
TRP	Tryptophan

# 1 INTRODUCTION

Hallucinogenic compounds are of particular interest because of their documented pharmacokinetics and physiological effects if consumed at elevated levels. Literature reports and anecdotal evidence on the continued intentional consumption of hallucinogenic mushrooms for their mind enhancing effect and the accidental poisoning is a cause for concern (Tsujikawa et al., 2007; van Amsterdam et al., 2011). It is therefore necessary to analyse body fluids from individuals suspected to be under the influence of hallucinogens so as to prospectively curb the possibility of unsocial behaviour and where possible break causalities. Such results can be used as legal evidence in forensics and in food toxicology.

Development of analytical methods for quantification of hallucinogenic compounds in urine samples of individuals suspected to have consumed hallucinogenic mushrooms whether intentionally or by mistake is essential in toxicology and criminology. The reliability of results for legal investigation of culprits or victims depends solely on the validity and the accuracy of the method used for quantification. Muscimol (MUS) is a hallucinogenic compound found in *Amanita* mushrooms and its quantification in urine can be used to prove prior exposure to *Amanita* mushrooms. It is excreted unchanged in urine. Very few publications have been reported for quantifying MUS in human body fluids. Solid phase extraction has been reported by Hasegawa et al. (2013) to extract MUS from blood serum (Hasegawa et al., 2013). NMR-NOESY spectroscopy, capillary electrophoresis coupled with electrospray tandem mass spectrometry and cation exchanger with GC-MS with derivatization have also been reported (Deja et al., 2014; Ginterová et al., 2014; Stříbrný et al., 2012).

Sample preparation is still seen as crucial and critical in any analytical determination and can be viewed as ‘rate determining’ in any analytical procedure (Abadi et al., 2012; Chimuka et al., 2011). Currently simple, cheap and environmental friendly sample preparation techniques especially those based on liquid phase microextractions (LPME) are favoured in which sampling,

extraction, and enrichment concentration are all integrated into a single extraction unit (Lin et al., 2013; Pena-Pereira et al., 2010a, 2010b).

Since the publication of the first paper on liquid phase microextraction (LPME) in 1996, different approaches have been developed as an attempt to improve recoveries, facilitate automation and miniaturize organic solvents used. One of these techniques is single hollow fibre liquid phase microextraction (HF-LPME) (Chimuka et al., 2011; Dadfarnia and Shabani, 2010; Dziarkowska et al., 2008; Lin and Chen, 2006; Pena-Pereira et al., 2010a, 2010b; Poliwoda et al., 2010). HF-LPME was first introduced by Pedersen-Bjergaard and Rasmussen in 1999 as a viable fabrication to conventional flat fiber membrane sample preparation modules for chromatographic and electrophoretic analysis of trace amounts of ionizable analytes (Abadi et al., 2012; Al Azzam et al., 2010; Lee et al., 2008; Pena-Pereira et al., 2010a). Other LPME techniques include single drop microextraction introduced by Liu and Dasgupta and dispersive liquid-liquid microextraction designed to eliminate use of the micro-syringe (Asensio-Ramos et al., 2011; Lin et al., 2013).

The HF-LPME technique is based on compound dissolution from a small volume of aqueous sample solution, the donor phase (DP) into a supported liquid membrane (SLM), usually a low polarity organic solvent that is impregnated in the pores of a hydrophobic porous hollow fibre (HF). The analyte is then back extracted into a micro-volume acceptor phase (AP) placed inside the lumen of the fiber through ionization and diffusion processes (Chimuka et al., 2011, 2010; Ebrahimpour et al., 2011a). For very polar analytes or analytes that exist in their charged state in the entire pH working range, a carrier molecule can be impregnated into the SLM to aid transfer (Asensio-Ramos et al., 2011; Chimuka et al., 2011; Ebrahimpour et al., 2011a).

The AP now containing the analyte is directly injected into the analytical instruments for identification and quantification (Asensio-Ramos et al., 2011). Reverse phase columns tend to fail in separation of polar compounds leading to the advent of hydrophilic interaction liquid chromatography (HILIC) columns.

HILIC columns continue to find application in extraction and separation of polar analytes from complex biological samples.

A robust experimental design is one that considers interdependence of design elements and provides a full insight of interaction between the factors that affect the response output most. Multivariate experimental approaches allow designers to target those factors that are more important than others. The most common factor screening design in experimental research is the factorial approach where there are multiple factors and the researcher is interested in the combined effect on the response output and the need to simultaneously investigate them. The objective of these designs is to identify factors that have a significant effect on the response among factors that have been predicted to have an impact on an experimental response. Once the power factors have been identified, their interrelationships that maximize the response output are predicted using response surface designs. The two common approaches in response surface designs are the central composite design (CCD) and the Box-Behnken design (Atkinson et al., 2007; Cox and Reid, 2000). Where a simultaneous extraction and quantification of several analytes is needed, a desirability function is used to measure how the universal factor values satisfy the targeted response output of a design.

As far as this research is concerned, nothing has been published on extraction of muscimol and ibotenic acid or psilocin and psilocybin using HF-LPME. The present work targeted extraction of muscimol and its two precursors, tryptophan (TRP) and tryptamine (TA) using HF-LPME in conjunction with HPLC-UV technique. This technique is attractive because unlike solid phase extraction, it is simple, environmentally friendly and inexpensive. It does not require a further clean-up or preconcentration step. HF-LPME technique can also be selective if all the critical parameters for an effective HF-LPME extraction are carefully optimised. Multivariate approaches to experimental design are a solution in this regard.

## **2 LITERATURE REVIEW**

### **2.1 Hallucinogenic compounds**

#### **2.1.1 Definition**

A hallucinogen is a pharmacologically psychoactive agent that alters the state of the mind by either enhancing one's consciousness, perception, emotion and thought or inducing new non-ordinary psychological experiences that lead to an exaggerated freedom of thought (Nichols, 2004). The experience may be pleasant and stimulating as exemplified in euphoria and activated sensory awareness, or hypnagogic and depressant. This reinforcing effect of psychoactive substances has been utilized for illicit recreational purposes, to purposefully augment one's consciousness, or as entheogens (Hasler et al., 2004). Either case, individuals tend to use them excessively in order to attain the climax of the feeling despite negative consequences. The top culprits are the youth that have a natural adventurous behaviour that draws them to pryingly venture into the unexpected and at times risky life experiences that involve experimenting with illicit hallucinogenic drugs (Tsujikawa et al., 2007; van Amsterdam et al., 2011).

A hallucinogen can be psychedelic, dissociative or deliriant depending on its subjective and behavioural effects. A psychedelic hallucinogen falsifies cognitive and perceptual aspects of the mind by provoking hidden but real aspects of the mind. It alters the brain's ability to filter certain sensory transmissions associated with perceptions and emotions from reaching the conscious mind. A psychedelic experience is often ecstatic followed by extra-ordinarily paresthetic feelings characterized by tremendous sensations like trance, euphoria and synaesthesia. However at elevated levels the sensations and feelings may result in panic attacks due to fear of losing control, paranoia and mania which may result in reckless and/or dangerous behaviour with the situation elevated for schizophrenics and other drug abusers. Examples include lysergic acid diethylamide (LSD), psilocybin and psilocin, methylenedioxymethamphetamine, mescaline and N,N-

dimethyltryptamine (Hasler et al., 2002; Nichols, 2004; Passie et al., 2002a; Wittmann et al., 2007).

Dissociatives result in depersonalization and derealization experiences where one's feelings become detached from the body and his surrounding, and the world becomes dream-like. The individual may either experience catalepsy or seize to actively take control of his actions and yet goes through them or has improper judgment of his mobility, a condition known as dysmetria. Deliriant induce symptoms similar to delirium, an acute confusional syndrome characterised by general instability, dysmetria and even severe disorientation, with potential aggressive behaviour. The neuropsychiatric experience due to muscimol and ibotenic acid is considered sedately hypnotic, depressant, dissociative and deliriant (Becker et al., 1999; Michelot and Melendez-Howell, 2003; Tsujikawa et al., 2007). The physical chronosymptomatology hallucinogenic influence includes vomiting, dryness of the lips and mydriasis (Michelot and Melendez-Howell, 2003).

Almost all hallucinogens contain nitrogen and are therefore classified as alkaloids with the exception of Tetrahydrocannabinol and salvinorin A. Psilocybin and psilocin are indolealkyltryptamine derivatives while ibotenic acid and muscimol are isoxazole alkaloids (Chen et al., 2011; Hasler et al., 2004; Manevski et al., 2010).

### **2.1.2 Mushrooms: history, uses and abuses**

A mushroom (or toadstool) is a fleshy, macroscopic spore-bearing fruiting fungal body that can either be hypogeous, epigeous or paratrophic (Miles and Chang, 2004). They belong to the *Basidiocota* phylum and fall under *Agaricomycetes* that are characterized by basidia on filamentous gills. The basidia are sexual structures that produce reproductive basidiospores. Typical mushrooms are of the order *Agaricales*. Mushrooms in the *Amanita* genus such as *Amanita muscaria* (Figure 1a), *Amanita pantheria* and *Amanita ibotengusske*, and *Psilocybe* genus like *Psilocybe cubensis* (Figure 1b) and *Psilocybe semilanceata* are known to have hallucinogenic properties while the *Agaricus* genus is considered edible. The *Amanita* mushrooms contain mainly muscimol, ibotenic acid, muscazone, and

muscarine. Muscimol is considered the principal psychoactive agent (Gennaro et al., 1997; Hasler et al., 2004, 2002; Michelot and Melendez-Howell, 2003). Hallucinogenic effects of *Psilocybe* mushrooms are mainly due to psychedelics psilocybin and psilocin with psilocin as the pharmacologically active agent.

*Agaricus bisporus* (Figure 1d) is commercially cultivated, harvested and marketed as the white button mushroom in popular supermarkets in South Africa and the world. The first mushroom to be intentionally cultivated for its delicacy was the paratrophic *Auricularia auricular* (Figure 1c) which is traced back to around 1400 years ago (about A.D 600) in China while *Agaricus bisporus* was first cultivated by the French in about the year 1600 (Miles and Chang, 2004). Most mushrooms are conditionally cosmedible in that the toxins are either leached out or destroyed by moderate heat when cooking (Rubel and Arora, 2008).



Figure 1 The hypnagogic *Amanita muscaria* (a), the psychedelic *Psilocybe cubensis* (b), the first ever cultivated paratrophic *Auricularia auricular* (c) and *Agaricus bisporus* at the shelves of a common supermarket in SA (d)

### 2.1.3 Pharmacokinetics and physiological effects of psilocin and muscimol

Psilocybin (O-phosphoryl-4-hydroxy-N,N-dimethyltryptamine) and psilocin (4-hydroxy-N,N-dimethyltryptamine) first isolated from *Psilocybe mexicana* by

Hoffman in 1957 are indolealkyltryptamine derivative and have a structural similarity to the excitatory neurotransmitter, serotonin (Figure 2) (Chen et al., 2011; Geyer and Vollenweider, 2008; Hasler et al., 2004; Kamata et al., 2010; Lindenblatt et al., 1998; Manevski et al., 2010; Nichols, 2004; Passie et al., 2002b). They act as serotonergic agonists at the serotonin receptors in the brain. Pharmacokinetically, psilocybin is a pro-drug that undergoes first pass metabolism in the liver into the pharmacologically active compound, psilocin by a dephosphorylation reaction in the presence of alkaline phosphatases (Anastos et al., 2006; Hasler et al., 2004, 2002; Passie et al., 2002b). Psilocin is then either glucuronated to be excreted in the urine, or further converted to other non-exhilarating metabolites that enter the systemic circulation. (Hasler et al., 2004, 2002; Manevski et al., 2010)

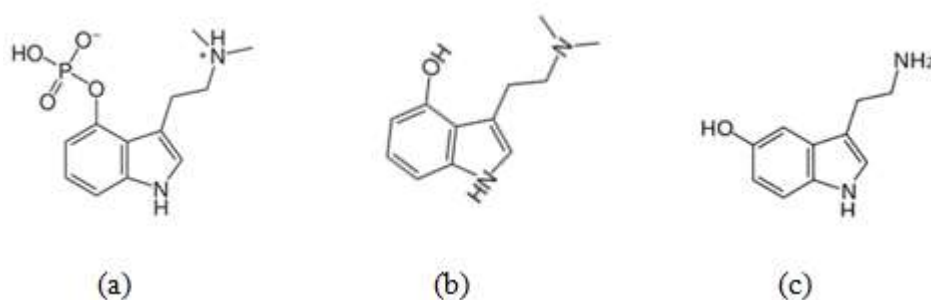


Figure 2 Psychedelics: psilocybin (a) and psilocin (b), and the neurotransmitter, serotonin (c)

Muscimol (5-(Aminomethyl)-isoxazol-3-ol) is an isoxazole alkaloid and has a structural similarity to the sensory inhibitory  $\gamma$ -aminobutyric acid (GABA) neurotransmitter (Figure 3). Produced naturally in the *Amanita* species, muscimol is also a decarboxylation product of ibotenic acid. Ibotenic acid is a glutamate neurotransmitter receptor agonist. Muscimol and ibotenic acid were discovered in 1964 from the fly-agaric mushrooms (Michelot and Melendez-Howell, 2003; Rogers, 2011).



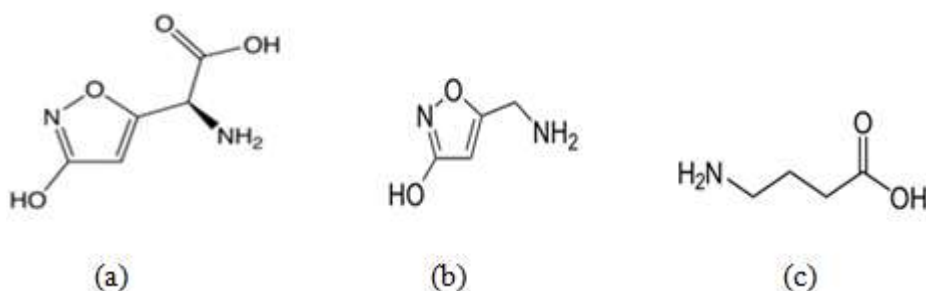


Figure 3 Psycho-sedatives: ibotenic acid (a) and muscimol (b), and gamma-aminobutyric acid (GABA), the neurotransmitter (c)

The mushrooms can be ingested as fresh or dried fruit bodies, in a tisane or combined with other foods to mask the bitter taste. For example in the Netherlands *Psilocybe cubensis* is ground and put as ingredients of chocolate bars while some users have injected mushroom extracts intravenously (van Amsterdam et al., 2011). Some poisoning is accidental in which the poisonous mushrooms are mistaken for edible ones (Tsujikawa et al., 2007). The pharmacokinetics and physiological effects of psilocin and muscimol are summarized in Table 1 (Becker et al., 1999; Berge, 1999; Hasler et al., 2004; Michelot and Melendez-Howell, 2003; Passie et al., 2002b; Tsujikawa et al., 2007; van Amsterdam et al., 2011).

The intensity and duration of the effects depend on species, dosage, brain chemistry, individual physiology, and whether the culprit is using other drugs (Becker et al., 1999; Berge, 1999; Passie et al., 2002b; van Amsterdam et al., 2011). The 4 – 10 mg dosage that induces psychedelic effects corresponds to about 50–300  $\mu\text{g kg}^{-1}$  of body weight. A 10 mg dosage corresponds roughly to at least 1 g of dried magic mushrooms with 1 %w/w hallucinogen content. However the accuracy of an effective dosage remains unresolved due to the potency variation factors discussed above and the presence of other active psychedelics like phenylethylamines in magic mushrooms.

Table 1 Pharmacokinetics and physiological effects of psilocin and muscimol

	Psilocin	Muscimol
Action	Agonist at serotonin neurotransmission receptors	Agonist at GABA neurotransmission receptors
Effect	Psychedelic: paresthetic feelings characterized by tremendous sensations like trance, euphoria and synesthesia	dissociative and deliriant: Depersonalization, derealization, sedately soporific, hypnagogic depressant
Onset	10 – 40 mins and lasts up to 8 h	2 – 3 h and lasts up to 8 h
Minimal dosage	4 – 10 mg	10 – 15 mg
Excretion	In urine as psilocin O-glucoronide	Excreted unchanged in urine
Toxicity	LD <sub>50</sub> of 280 mg kg <sup>-1</sup> in rats	LD <sub>50</sub> of 45 mg kg <sup>-1</sup> in rats

Even though the hallucinogenic effect has minimal intellectual impairment, low toxicity with LD<sub>50</sub> of 280 mg kg<sup>-1</sup> for psilocybin which is equivalent to about 17 kg of fresh mushrooms to be consumed to reach this rate in humans (Gable, 2004; Passie et al., 2002b; van Amsterdam et al., 2011) and absence of addiction (Nichols, 2004; Passie et al., 2002b), several case studies have declared that under elevated levels of psychoactive agents in the body, the individual becomes a risk to himself and his surroundings characterised by potentially fatal accidents, self-injury, and suicide attempts (Nichols, 2004; Sticht and Käferstein, 2000; van Amsterdam et al., 2011). The elevated sensations may result in reckless and/or dangerous behaviour with the situation elevated for schizophrenics and other drug abusers (Hasler et al., 2002; Nichols, 2004; Passie et al., 2002b; Wittmann et al., 2007). The tenacity of the hallucinogenic effect becomes detrimental especially to those with other ailments, driving, operating machines or walking the busy streets and roads. It is therefore essential to analyse body fluids from individuals suspected to be under the influence of hallucinogens so as to prospectively curb the possibility of unsocial behaviour. With reports of mushroom abuse and

casualties continuing to be published (Asselborn et al., 2000; Becker et al., 1999; Berge, 1999; Chen et al., 2011; Sticht and Käferstein, 2000; van Amsterdam et al., 2011), it is essential to scientifically evaluate and understand the recreational usage of hallucinogenic mushrooms. This starts with development of viable quantification methods.

#### **2.1.4 Hallucinogenic research: the past, the present and the future**

Although the use of hallucinogenic mushrooms especially for shamanic and consumption purposes is traced back to historic times as evidenced in rock art and ancient documents belonging to primitive societies like the soma of ancient India scientific studies only started in the early 20th century. The most ancient portrait of mushrooms on a rock is found in the desert town of Tassil in Algeria discovered by Samorini in 1992 dating back to about 7 000 – 9000 B.P that Guzman et al. 1998 predicts to be *Psilocybe mairei* (Akers et al., 2011; Gennaro et al., 1997; Guzmán et al., 1998; Nichols, 2004). However, Mexico (mainly *Psilocybe* species discovered by Heim in 1956) and Siberia (mainly *Amanita muscaria*) have been identified as the two major countries with the most documented historic shamanistic usage of mushrooms (Akers et al., 2011; Gennaro et al., 1997; Guzmán et al., 1998). The first publication on psychoactive plants was Louis Lewin's Phantastica in 1928 which was meant to describe the sensations associated with these mushrooms (Nichols, 2004). More research intensified with Weitlamer rediscovering the Mexican hallucinogenic mushrooms in 1936 while Albert Hoffman's discovery of the semi-synthetic LSD in 1938 is arguably responsible for the explosion of interest in the study of hallucinogens (Berge, 1999; Geyer and Vollenweider, 2008; Vollenweider et al., 1998). It was during this time that ethno-mycological explorations exploded provoking a hallucinogen naming frenzy as an attempt to describe the totality of the feeling. Psychedelic, psychotomimetic, psychogenic, schizophrenic, mysticomimetic and entheogenic were some of the terms proposed. Psychedelic was coined by Humphrey Osmond to describe the mysterious mind manifesting extent while Ruck C. A. proposed entheogen to describe spiritual enhancing abilities during religious rituals (Nichols, 2004; Ruck et al., 1979).

However experiments were prohibited in the late 1960s. Despite prohibition, the recreational, spiritual, and medical use of psychedelics continued illegally and still continues today. In October 27, 1970 both psilocybin and psilocin were officially labelled as hallucinogens and eventually classified under Schedule 1 drugs (Nichols, 2004). Schedule 1 drugs are illicit, high potential for abuse compounds with no known medical benefit and a lack of accepted safety. However the psychedelic-containing mushrooms were not included. Thus the techniques of growing psilocybin mushrooms continued to be published in several books, like the *Psilocybin: Magic Mushroom Grower's Guide* of 1981, with the end of the 20th century seeing the mushrooming in production of psilocybin as an entheogen of choice.

The turn of the century has seen some organizations like the Heffter Research Institute and Center for Cognitive Liberty and Ethics, and proponents including Albert Hoffman calling for legalizing research into the safety and efficacy of hallucinogens. Thus during the last decade there has been a resurgence of authorized interest in hallucinogen therapeutic and recreational applications (Johnson et al., 2008; Nichols, 2004). With loopholes in legislation leading to legal availability of the magic mushrooms in smart shops and online in European countries (Chen et al., 2011; Hasler et al., 2002; Tsujikawa et al., 2007; van Amsterdam et al., 2011), there was a need to reconsider a broader and prospective approach through legalized scientific research. Many western countries have now started to legally approve studies to test the physiological effects and therapeutic possibilities of hallucinogens. In 2008, Johnson and colleagues together with the Johns Hopkins research team published guidelines and recommendations for screening potential study volunteers when performing hallucinogen clinical trials in humans (Johnson et al., 2008).

## **2.2 HF-LPME sample preparation**

### **2.2.1 Principle of the HF-LPME**

The HF-LPME technique involves transfer of an analyte from a DP where it exists in its neutral form across a liquid membrane on the pores of a hollow fibre (HF). The analyte is accepted by a phase placed inside the lumen of the fiber through ionization and diffusion processes (Chimuka et al., 2011, 2010; Ebrahimpour et al., 2011b). The HF-LPME technique can be classified as either a two-phase or three-phase HF-LPME based on the number of phases involved. In the two-phase approach, the same solvent embedded on the HF pores is used as the AP. In the three phase extraction, the DP, the SLM and the AP solvents are all different. The organic solvent impregnated into the supporting pores of the HF in the three-phase system must always be immiscible in the other phases to ensure that the DP and the AP are not in direct contact (Asensio-Ramos et al., 2011; Chimuka et al., 2011; Ebrahimpour et al., 2011b). Either way, the AP now containing the analyte is directly injected into the analytical instruments for identification and quantification.

### **2.2.2 Advantages of the HF-LPME**

The HF-LPME technique is simple and rapid, inexpensive, convenient, sensitive and has good precision and accuracy. Besides improvement in efficiency, the HF-LPME could be done without any sample pre-treatment or further clean-up. This greatly reduces the number of steps involved. During extraction, the phases do not mix thus minimal volumes of solvents are required usually in the micro scale. The sample-to-acceptor volume ratio is elevated with the DP volume ranging in the 50  $\mu\text{L}$  – 1 L while the AP is usually less than 30  $\mu\text{L}$ , typically 20  $\mu\text{L}$ . This is essential for improvements in enrichment factors. The low volumes used also make HF-LPME a green extraction technique (Abadi et al., 2012; Bello-López et al., 2012; Dadfarnia and Shabani, 2010; Dziarkowska et al., 2008; Ghambarian et al., 2012; Han and Row, 2012; Lin et al., 2013; Pedersen-Bjergaard et al., 2002; Pena-Pereira et al., 2010a; Poliwoda et al., 2010).

The tubular geometry of the hollow fiber provides a high packing density that offers a higher surface area per unit of volume. This coupled with the small thickness of the membrane (and hence small SLM volume) allows for effective mass transfer. Non-mixing of the phases eliminates possibilities of emulsion formation. However the sample, the extractant and the acceptor are in contact continuously. This provides a basis for a continuous, real-time process that can easily be automated and connected on-line to instruments (Abadi et al., 2012; Bello-López et al., 2012; Chimuka et al., 2010; Dadfarnia and Shabani, 2010; Ghambarian et al., 2012).

The sample solution may be stirred, shaken or sonicated without any loss of the extracting liquid because it is mechanically protected and is immiscible with the DP and the AP. The small pore size of the HF becomes a clean-up barrier that prevents high molecular mass compounds from passing the liquid phase membrane during extraction (Pena-Pereira et al., 2010a; Tahmasebi et al., 2009). The HF-LPME technique is also suitable for analysis of a wide variety of inorganic and organic analytes over a wide range of polarity and pH with successful applications in environmental, forensic, food and pharmaceutical trace analysis and can be combined with almost any analytical technique (Abadi et al., 2012; Al Azzam et al., 2010; Dziarkowska et al., 2008; Ghambarian et al., 2012; Han and Row, 2012; Lee et al., 2008; Lin et al., 2013; Poliwoda et al., 2010). The membrane is used once and then discarded to eliminate possibility of carryover problems and cross contaminations. The suitability of the HF-LPME as a sample preparation approach has been reported in several applications with publications reporting high sensitivity and selectivity (Al Azzam et al., 2010; Bello-López et al., 2012; Dadfarnia and Shabani, 2010; Ebrahimpour et al., 2011b; Ebrahimzadeh et al., 2011; Poliwoda et al., 2010; Quintana et al., 2004).

The disadvantage of HF-LPME against traditional methods is that the rate of mass transfer is slower. It is only applicable in acidic or basic analytes with functional groups that are ionizable (Ebrahimzadeh et al., 2011; Lin et al., 2013; Tahmasebi et al., 2009).

### 2.2.3 Critical parameters in HF-LPME

Since sample preparation is dependent on analyte and matrix effects, a suitable optimization procedure on preparation parameters is essential. A proper understanding of the desired extraction sequence during an HF-LPME process allows one to focus on optimizing essential parameters that lead to a successful extraction. Chimuka et al. 2010 clearly dissects the parameters that are deemed critical and need to be optimized when analysing ionizable compounds using an SLM extraction technique. The parameters are derived from the mass transfer kinetics associated with HF-LPME (Chimuka et al., 2010; Jönsson and Mathiasson, 2000).

The aqueous phase pH needs to be optimized so that the analyte maintains electrical neutrality in the DP and exists as an ionized compound in the AP to prevent back-extraction (Chimuka et al., 2010; Dadfarnia and Shabani, 2010; Ghambarian et al., 2012; Pena-Pereira et al., 2010a). A basic compound will ionize under low pH. To maintain the neutrality and thus reduce its solubility within the DP, the DP pH should be adjusted to basic conditions. The AP should be acidified in order to ionize and promote the dissolution of the basic analyte as a way of preventing back extraction. For an acidic compound the DP has to be acidic while the AP is basic.

If the pKa value of the analyte is known, the pH value of the AP that maximizes extraction can be estimated. Likewise the pH value of the DP that enhances transfer to the AP can be predicted. For an acidic analyte, the pH of the AP should be higher than the pKa value by at least 3.3 units while for a basic analyte the AP pH is at least 3.3 units lower than the pKa value. The pH of the DP containing an acidic analyte must be 2 units less than the analyte pKa value. For a basic analyte the pH is at least 2 units more than the pKa value. These predictions allow for a focussed optimization merely meant to formally verify the best pH of the DP and AP. For example, Azzam et al., 2010 analysed ROSI, a basic drug with pKa values of 6.1 and 6.8 and optimized the DP pH at 9.5 by concentrating within pH 6.5 – 11.5 (Al Azzam et al., 2010).

The type of supported liquid phase is also essential in HF-LPME depending on the polarity of the analyte and thinness of the supporting membrane. For optimum extraction, the embedded solvent must have low solubility in water, be immiscible in the DP and the AP and be easily immobilized in the HF pores. Several studies have used dihexyl ether as an SLM of choice following studies by Chimuka et al., 2000 that identified dihexyl ether (DHE) and n-decane as transferring agents that give optimum extraction efficiencies (Chimuka et al., 2000).

Agitation of the aqueous solution has shown to increase the extraction efficiency and reduce the extraction time by continuously exposing the extraction and diffusion surfaces of the membrane to fresh aqueous sample in the DP and the small volume of the AP respectively. Increase is attributed to diffusion as the limiting factor in mass transfer of the analyte. When solvent dissolution into the membrane becomes limiting, the efficiency becomes non-linear and finally plateaus. Plateauing is also attained when the system reaches equilibrium and/or when almost all the analyte has been transferred into the AP. However excess vigorous shaking can lower extraction efficiencies because of loss of the SLM, solvent evaporation or creation of air bubbles that accumulate on fiber surface (Al Azzam et al., 2010; Chimuka et al., 2010; Pena-Pereira et al., 2010a).

Other factors that might affect the extraction efficiency include extraction temperature, presence of humic acids and salting out effect (Bello-López et al., 2012; Chimuka et al., 2010; Saaïd et al., 2009). However these factors are not so important and are mainly influenced by other factors like the module and experimental design (for temperature), amount of trapped analyte (for humic substances) and amount of un-ionized analyte in the AP observed for longer extractions (for salt addition).

#### **2.2.4 Carrier-mediated three phase HF-LPME for polar compounds**

A carrier-mediated microextraction is essential for analytes that are too polar to freely dissolve into the hydrophobic supported liquid membrane, have multiple functional chargeable groups that can exist in different charged states at the same pH level and/or exist in their charged state in the entire pH range (Dziarkowska et al., 2008; Poliwoda et al., 2010; Romero et al., 2002). The purpose of a carrier



molecule is therefore to create a neutral moiety by binding to the analyte at the charged functional group. The carrier molecule must be hydrophobic so that it remains impregnated in the supported liquid membrane. The type of carrier molecule used depends on the charge of targeted functional group of the analyte. The quaternary ammonium salt, N-Methyl-N,N,N-trioctylammonium chloride (Aliquat 336) is preferred for combining with anionic functional groups while bis(2-ethylhexyl) hydrogen phosphate (DEHPA) is common in extracting positively charged analytes (Dziarkowska et al., 2008; Poliwoda et al., 2010; Shariati et al., 2009; Yamini et al., 2006). Other carriers that have been used include tris(2-ethylhexyl)phosphate (TEHP), Trioctylphosphine oxide (TOPO) and sodium octanoate (Fotouhi et al., 2011; Ghaffarzadegan et al., 2014; Ho et al., 2005, 2003; Li et al., 2014). The anionic DEHPA in Figure 4 was used in this research.

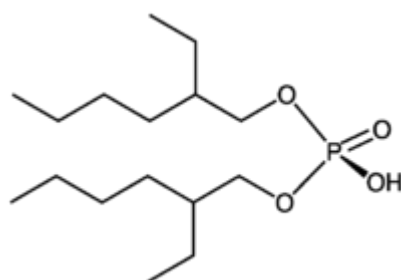


Figure 4 Structure of DEHPA

The mechanism of extraction is summarized in Figure 5. At the donor phase-SLM interface, the cationic analyte is picked up by the negatively charged carrier molecule. The neutralized and hydrophobic analyte-carrier moiety then migrates to the SLM-acceptor phase interface where it exchanges the analyte for a proton from the acceptor phase (Ho et al., 2003; Lin and Chen, 2006). Migration of the analyte from the donor phase into the acceptor phase depends on the availability of the counter protons. A high proton gradient between the donor phase and the acceptor phase is therefore crucial for effective extraction of the analyte.

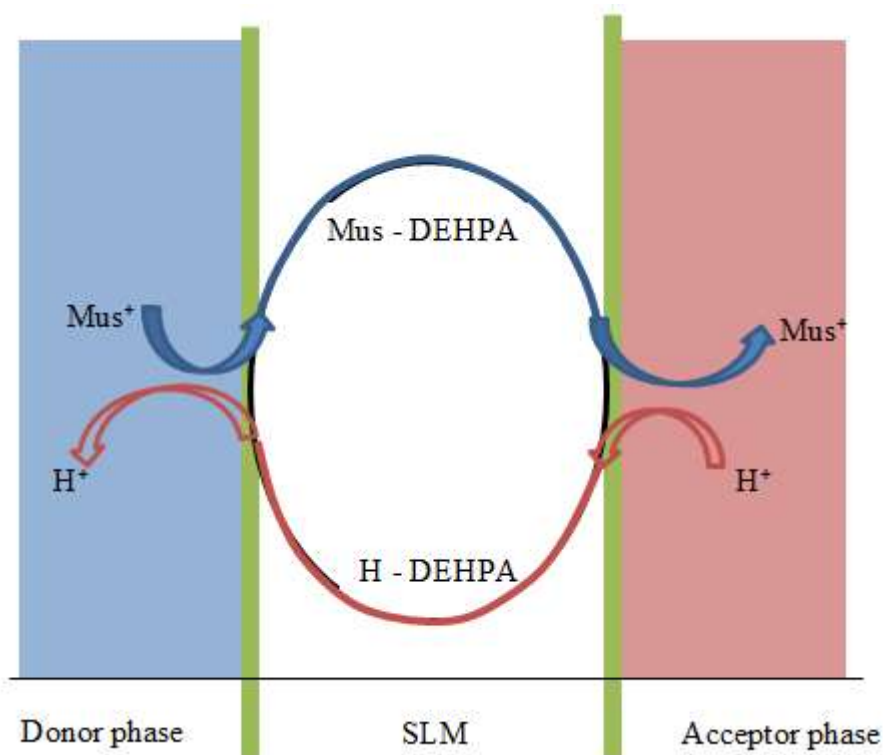


Figure 5 The carrier-mediated extraction of MUS from an acidic donor sample to a more acidic acceptor phase

### 2.3 Quantification of muscimol in urine samples

Development of analytical methods for quantification of hallucinogenic compounds in urine samples of individuals suspected to have consumed hallucinogenic mushrooms whether intentionally or by mistake is essential in mushroom toxicology. The reliability of results for legal investigation of culprits or victims depends solely on the validity and the accuracy of the method used for quantification. MUS is excreted unchanged in urine and its quantification in urine can be used to prove prior exposure to *Amanita* mushrooms. Very few publications have reported quantifying MUS in human body fluids. Hasegawa et al., (2013) has reported solid phase extraction coupled to LC-MS to extract MUS from blood serum (Hasegawa et al., 2013). NMR-NOESY spectroscopy, capillary electrophoresis coupled with electrospray tandem mass spectrometry and cation exchanger with GC-MS with derivatization have also been reported (Deja et al., 2014; Ginterová et al., 2014; Stříbrný et al., 2012). The present work targeted

extraction of muscimol and its two precursors, tryptophan and tryptamine using the HF-LPME approach in conjunction with HPLC-UV technique. The premise of this study was to contribute towards finding alternative quantification methods for hallucinogenic compounds in human body fluids that are simple, inexpensive and environmentally friendly.

## **2.4 Multivariate approaches to design of experiments**

### **2.4.1 Multivariate design of experiments**

A design of experiment (DOE) is the process whereby a researcher makes decisions about how to answer their research questions through experimentation. A multivariate DOE is a research study that enables designers to predict interdependence of several variables that might affect a process output. It helps in turning any standard design into a robust one by providing a full insight of interaction between design elements that could cause problems in output if not monitored (Condra, 2001; Guo et al., 2007). Designers are then able to fix these problems and produce robust and higher yield designs prior to going into production.

Use of multivariate approaches instead of the one-factor-at-a-time (OFAT) method or an expert trial-and-error helps to evaluate the effects and possible interactions of several factors. An OFAT approach varies one factor at a time while keeping all other factors constant (Czitrom, 1999; Mursyid and Saberi, 2010). This approach disregards the possible impact of effects from interaction between factors. This becomes a disadvantage considering that one factor cannot produce the same response in the entire range of another factor.

A multivariate experimental strategy involves two major steps; an initial screening process followed by an optimization stage. A factor screening design is meant to literally screen the parameters to determine the most important factors affecting a response among a selection of potential factors. When the vital-few have been selected, a further optimization step is done to maximize output.

### **2.4.2 Multivariate Data Analysis Software**

Several Windows compatible statistical packages that support a wide spectrum of multivariate data manipulation in offline mode are available. These include High-D, the JMP (statistical software), MiniTab, R, Calc, PLS\_Toolbox / Solo (Eigenvector Research), PSPP, SAS (software) SciPy for Python, SPSS., Stata, STATISTICA, The Unscrambler, SmartPLS - Next Generation Path Modeling, MATLAB, EvIEWS, Prosensus ProMV, Umetrics SIMCA, OpenStat, DOE++ among others. Most of these packages are generally comparable with regard to functionality. The choice of use would mainly be based on the researcher's scope of the experimental design expectations and the availability for free downloading. Some of these can be downloaded freely and can work offline in their full functional mode with no need for updates while some are limited in some way and may need updates every now and then.

In this research Minitab 16 was used for experimental design and analysis. Minitab is a general purpose statistical software developed at the Pennsylvania State University by researchers Barbara F. Ryan, Thomas A. Ryan, Jr., and Brian L. Joiner in 1972. It can be freely downloaded for use in offline mode. Although the performance of the free version is limited in some way, it remains powerful enough for use in analysis of most experimental designs. Its user-friendly and simplified visual plots of results help identify patterns making interpretation of data an easy task. Minitab has Factorial designs and Taguchi designs available for screening purposes while optimization of the main effects is achieved using central composite approaches.

### **2.4.3 Factorial Designs**

The most common factor screening design in experimental research is the factorial approach where there are multiple factors and the researcher is interested in their combined effect on the response output and need to be investigated simultaneously during the test (Atkinson et al., 2007; Cox and Reid, 2000; Franceschini and Macchietto, 2008). The objective of these designs is to identify

factors that have a significant effect on the response among factors that have been predicted to have an impact on an experimental response.

The factors included in the design can be identified based on related publications. The levels of each factor for investigation can then be predicted based on the extraction method being developed, properties of the target analyte, the matrix and the chemicals to be used as well as the instrument response. A predictive first-degree polynomial model is then used to sufficiently identify the important factors that have an impact on the response. A two level design involves identifying two points of a factor, one a lower value denoted by a negative (-) and the other the upper level denoted by a positive (+) sign. A three level will have three value points, a lower (-), a central (0) and an upper (+) value. For example, a two level design for temperature can be 30 and 60 while a three level design will involve investigation effect of temperature at 30, 45 and 60 value points. The choice of these limits can also be determined during preliminary studies where general OFAT studies are done. A factorial design can be classified as a full factorial or a fractional factorial.

### ***Full Factorial Designs***

As implied in its name, a full factorial experiment considers the predicted factors and all their interactions possible for the design. The entire treatment combinations of the factors and their selected level limits are investigated. They look at the effects that the predicted factors and all the interactions between factors have on the measured responses.

The number of treatments is given by  $l^k$  where  $l$  is the number of factor levels and  $k$  is the number of factors. For example, if in our case, six (6) factors at three levels each are to be used it will require 729 different treatments ( $3^6 = 729$ ). It is obvious that the number of the levels of factors has a great effect on the size of the investigation. If two levels are used for each factor, only 64 experiments are needed to complete the screening process ( $2^6 = 64$ ). For this reason, most of the designs involve only 2 levels of each factor compared to a general full factorial experiment with 3 or more levels. The main disadvantage with two level designs is that it only models a linear response ignoring any possibility of curvature.

Full Factorial designs are not desirable mainly because of the number of the experimental treatments that have to be done and the expense associated with it. An alternative is the use of fractional factorial designs.

### ***Fractional Factorial Designs***

During a fractional factorial design only a certain carefully chosen subset of the expected treatment combinations is investigated. A fractional factorial approach exploits the sparsity-of-effects principle to extract information about the most relevant features of the problem studied, while using a fraction of the effort of a full factorial design in terms of experimental runs and resources. The sparsity-of-effects principle predicts that main effects and low order interactions (usually two-factor interactions) are of most interest, and are usually more significant than high order interaction terms. This principle is based on Vildredo Pareto's probability distribution which predicts that about 80% of the observed phenomena are caused by about 20% of the factors. It is thus also referred to as the Pareto principle and refers to the idea that only a few effects in a factorial experiment will be statistically significant. The major assumption is that higher order interactions (those between three or more factors) are not significant and a compromise is taken when looking into interaction effects (Box and Hunter, 1961; Cochran and Cox, 1957; Gunst and Mason, 2009; Hinkelmann and Kempthorne, n.d.; Montgomery et al., 2009). This compromise is called confounding and involves aliasing main effects with high order interactions. If the effects are confounded, they cannot be estimated as single entities but are combined and predicted as effects due to interactions.

### ***The fractional factorial design equation***

Fractional designs are expressed in the form  $2^{k-p}$  and allow for analysing k factors with only  $2^{k-p}$  experiments where 2 refers to the factor levels, k is the number of factors investigated and p describes the size of the fraction of the full factorial used. Formally, p is the number of confounded effects and is used to describe the fractional design. A design with p such generators, is a fraction of the full factorial design and is described as a  $\frac{1}{2^p}$  fractional factorial design. When p

= 1, the design is a half fractional factorial implying that only half of the full factorial experiments is needed or half of the treatment have been confounded. A  $2^{k-1}$  design requires only half as many experiments while a  $2^{k-2}$  design requires only one quarter of the experiments. Where there is six factors to be investigated using a half fractional factorial design, 32 treatments are conducted ( $2^{k-p} = 2^{6-1} = 32$ ). This is half of the 64 experiments that would have been required if a full factorial was used ( $2^k = 2^6 = 64$ ). If a three level approach was used, it would require 243 experiments ( $3^{6-1} = 243$ ).

In identifying a best fractional factorial, a design's resolution is used. The resolution of a design describes the extent of aliasing of effects in a fractional factorial design. A design's resolution is therefore its ability to separate main effects and/or low-order interactions from one another. A design with higher resolution is considered better.

### ***The resolution of a fractional factorial design***

A resolution of the design relates to the minimum number of factor interactions that can be effectively predicted. The most important fractional designs are those of resolution III, IV, and V. Resolutions below III are not useful and resolutions above V are wasteful in that the expanded experimentation has no practical benefit in most cases and the bulk of the additional effort goes into the estimation of very high-order interactions which rarely occur in practice. Table 2 summarizes the possible resolutions and their acceptability in predicting interactions.

When creating a factorial design in Minitab 16, the available designs with resolutions from III to VIII are displayed as shown in Figure 6. The green-coded resolutions represent the best fractional factorial for a specific number of factors. A full resolution occurs when all the possible interaction effects are investigated and no effect is confounded with another effect. A yellow-coded resolution is acceptable but not recommended while a red-coded one implies that the number of runs for that particular number of factors is unreliable because important information has been lost in confounded effects. The target is therefore to do the number of runs that give a green-coded resolution. For example, when

investigating effects of six factors a full resolution and resolution VI will give reliable predictions. A full resolution is due to a full factorial where all the 64 possible runs ( $2^6 = 64$ ) are conducted. A half-fractional factorial which requires 32 experiments ( $2^{6-1} = 32$ ) has a resolution of VI.

Other multivariate screening designs include the Plackett-Burman Designs and the Taguchis Orthogonal Arrays (Atkinson et al., 2007; Cox and Reid, 2000; Miller and Miller, 2005; Ziegel, 2004). The Plackett-Burman approach was proposed by R. L. Plackett and J. P. Burman in the 1940s where only a few specifically chosen runs from two level fractional factorial designs are performed to investigate just the main effects. The interaction effects are not considered. Taguchis orthogonal arrays are highly fractional designs, used to estimate main effects using only a few experimental runs. Their minimized experimental runs are essential where main effects are predicted from three or more factor levels. Their main disadvantage is the presumption that interactions are non-significant.

#### **2.4.4 Response surface designs for main factor optimization**

Once the main effects have been identified, optimization of the factor values is achieved through a response surface design. A response surface approach predicts the main factor relationships that maximize response by fitting a second-order quadratic model within a specific factor value range (Bezerra et al., 2008; Carley et al., 2004; Khuri and Mukhopadhyay, 2010; Myers and Montgomery, 2003). A quadratic model is essential in predicting the optimum response output if the surface response has curvature. Unlike in DOE where the lower and upper values only are investigated, at least three values (or levels) of a factor are included in response surface designs. The two common approaches in response surface designs are the central composite design (CCD) and the Box-Behnken design while Doehlert designs for different factors studied at different levels and Mixture designs for mixture (or ingredient) proportions have been used for specific purposes (Atkinson et al., 2007; Chiao and Hamada, 2001; Cox and Reid, 2000; Ferreira et al., 2007; Miller and Miller, 2005).



The number of levels per factor depends on an alpha ( $\alpha$ ) value. The alpha value represents positions of some star (or axial) points on both axis of the design as represented in Figure 7.

Table 2 Resolutions and their acceptability in predicting interactions

Resolution	Ability
I	Not useful: only one run (or value) is used to test the effect of a single factor and hence can't even distinguish between the high and low levels of that factor.
II	Not useful: serious confounding of vital effects.
III	Ability to estimate major effects. However these may be confounded with two-factor interactions.
IV	Ability to estimate major effects and two-factor interactions. The major effects may be confounded with three-factor (or more) interactions while the two-factor interactions may be confounded with other two-factor interactions.
V	Ability to estimate major effects, two factor interactions and three factor interactions. Major effects may be confounded by four-factor (or more) interactions while the two-factor interaction effects may be with confounded with three-factor (or more) interactions. The three-factor interaction effects may be confounded with other two-factor interactions.
VI	Ability to estimate major effects not confounded with four-factor (or less) interactions. The two-factor interaction effects may be confounded with four-factor (or more) interactions while the estimated three-factor interaction effects may be confounded with other three-factor interactions.

Available Factorial Designs (with Resolution)

	Factors														
Run	2	3	4	5	6	7	8	9	10	11	12	13	14	15	
4	Full	III													
8		Full	IV	III	III	III									
16			Full	V	IV	IV	IV	III	III	III	III	III	III	III	
32				Full	VI	IV	IV	IV	IV	IV	IV	IV	IV	IV	
64					Full	VII	V	IV	IV	IV	IV	IV	IV	IV	
128						Full	VIII	VI	V	V	IV	IV	IV	IV	

Available Resolution III Plackett-Burman Designs

Factors	Runs	Factors	Runs	Factors	Runs
2-7	12, 20, 24, 28, ..., 48	20-23	24, 28, 32, 36, ..., 48	36-39	40, 44, 48
8-11	12, 20, 24, 28, ..., 48	24-27	28, 32, 36, 40, 44, 48	40-43	44, 48
12-15	20, 24, 28, 36, ..., 48	28-31	32, 36, 40, 44, 48	44-47	48
16-19	20, 24, 28, 32, ..., 48	32-35	36, 40, 44, 48		

Figure 6 Available factorial designs as displayed on Minitab 16

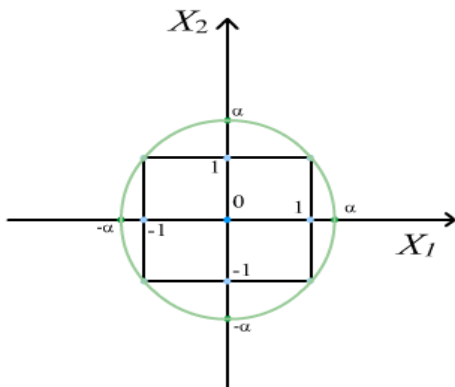


Figure 7 Star points for a  $2^2$  factorial as given by  $\pm\alpha$  on the axial lines. Modified from <https://onlinecourses.science.psu.edu/stat503/node/59>

The CCD is the most popular mainly because it can have up to five levels per factor. A CCD needs to be spherical and rotatable. This is essential because if the level points are equidistant from the center of the design and so are the axial points then the variance (rotatability) of the responses from levels or axial points (positive or negative) is constant. Rotatability requires that  $\alpha > 1$  while sphericity is defined by  $\alpha = \sqrt{k}$  where  $k$  is the number of vital factors (Atkinson et al., 2007; Ferreira et al., 2007).

Where there are 4 vital factors,  $\alpha = \sqrt{4} = \pm 2$ . The levels of each factor will therefore be investigated at -2, -1, 0, 1 and 2 representing five levels per factor where 0 represents the mid-range value. For example, if the lower and upper temperatures of a CCD are set at 40 and 80, then the levels will be 20, 40, 60, 80 and 100. A pH 4 – 6 range would be investigated at pH 3, 4, 5, 6 and 7.

Analysis of a CCD is built on the foundation of the analysis of variance and a collection of models that partition the observed variance into components according to what factors the experiment must estimate or test. The F-test analysis is the basis for model evaluation of both single factor and multi-factor experiments. This analysis is commonly output as an ANOVA table.

Once the CCD has been created it is then investigated experimentally. This allows for pairing of the main factors according to their extent of effect. The interaction effects of the paired factors are then investigated using response surface models. An empirical quadratic response surface model given by equation 1 is used to visualize the response surface through contour plots, surface plots and optimization plots of response.

$$y = b_0 + \sum_{i=1}^k b_i x_i + \sum_{1 \leq i < j} b_{ij} x_i x_j + \sum_{i=1}^k b_{ii} x_i^2 + \varepsilon \quad (1)$$

Where y is the average peak area, k is the number of factors,  $b_0$  the intercept parameter,  $b_i$  are the regression parameters for linear factor effects,  $b_{ij}$  are the regression parameters for interaction factor effects, and  $b_{ii}$  are the regression parameters for quadratic factor effects. For a k-number of factors, this model would have  $(k+1)(k+2)/2$  number of parameters. For example, for two factors, there would be six parameters.

The optimum value of the response occurs at the point of curvature and can be considered as a stationary point where the partial derivatives  $\delta y_1 / \delta x_1 = 0, \delta y_2 / \delta x_2 = 0, \dots, \delta y_i / \delta x_i = 0$ . The optimum response can be a saddle point, a minimum point or a maximum point as shown in Figure 8 below.

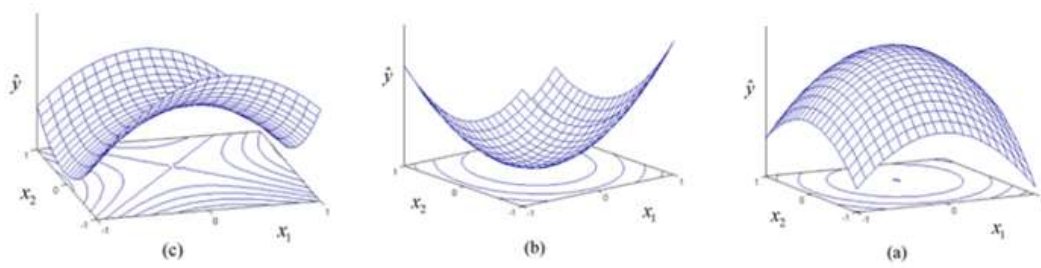


Figure 8 Mesh contour plots showing a saddle point (a), a minimum point (b) and a maximum point (c). Modified from <http://reliawiki.org/index.php/>

### 2.4.5 Desirability functions

A desirability function is a model designed to measure how the optimized factor value satisfies the targeted response. The idea is that if a response output is dependent on various vital variables, then the effect of all the optimized values must fall within a desired limit otherwise such settings would be unacceptable (Del Castillo et al., 1996; Rueda et al., 2003; Wu et al., 2000). In desirability studies, a response output is assigned a desirability function denoted by  $d_i y_i$  where  $y_i$  is the  $i^{th}$  response. The  $d_i y_i$  values range from zero to one. A  $d_i y_i$  value of one denotes an ideal situation while zero implies unacceptable settings. This range is dependent on setting a lower limit and a target value, or a target value and an upper limit, or both for the  $i^{th}$  response depending on the goal of the method as shown Figure 9.

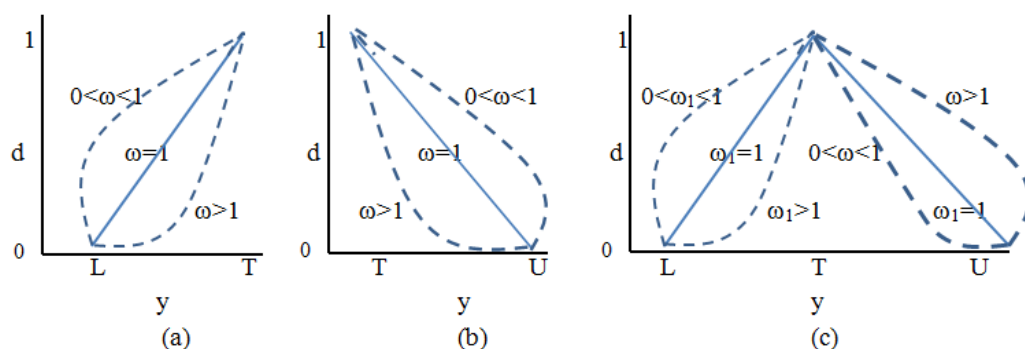


Figure 9 Plots of desirability functions when the goal is to maximize the set response value (a), the goal is to minimize the set response value (b) or the goal is to set a target value for the response.

Each plot has its own mathematical definition. In this research, the goal was to maximize the response and the desirability was defined as equation 2.

$$d_i y_i = \begin{cases} 0 & y_i < L \\ ((y_i - L)/(T - L))^\omega & L \leq y_i \leq T \\ 1 & y_i > T \end{cases} \quad (2)$$

T is the target value, L the set lower limit,  $y_i$  the  $i^{th}$  response and  $\omega$  the weight of the factor. For a vital factor,  $\omega$  is set to one and the  $d_i y_i$  function is linear. Almost all optimizations follow the  $\omega < 1$  route where emphasis is on getting a value close to the optimum. The  $\omega > 1$  approach requires that the target be achieved at all costs. When  $d_i y_i = 0$ , the response  $y_i$  is below the set limit. Most desirability values are acceptable when  $d_i y_i > 0.5$ .

A desirability function in which the effectiveness of an optimum point of two vital points is evaluated is called an individual desirability function because a single response is affected. A problem arises where the effect of several factors and factor levels on multiple responses are to be investigated.

Each response output will have its own optimum factor values different from the optimum values for the other responses. This creates a practical concern because what is optimum for extraction of one compound cannot be optimum for the other compounds. This leads to a conflict of optimum settings considering that the aim of this research was to simultaneously optimize extraction of three compounds with different physicochemical properties. A balanced setting has to be found that would give the most appropriate response values for all the analytes. The composite desirability approach is used to compromise the factor values in order to satisfy an optimized response output.

### ***Composite desirability function***

A composite desirability function, D(Y) evaluates how the overall universal settings affect a set of responses. It gives an estimate of having a single factor value on multiple responses. It is therefore a function of the responses under a

single compromised value and can be summarized as equation 3. It is calculated as a geometric mean of individual desirabilities as given by equation 4 where  $m$  is the number of responses and,  $\omega$  the weight of each factor. If all the factors are regarded as vital, then  $\omega$  is set to 1. The composite desirability then simplifies to equation 5. The choice of universal main factor levels is dependent on the importance of each response and the purpose of the design experiment.

$$D(Y) = f(y_1, y_2, \dots, y_m) \quad (3)$$

$$D(Y) = (d_1^{\omega_1} y_1 \cdot d_2^{\omega_2} y_2 \dots d_m^{\omega_m} y_m)^{1/(\omega_1 + \omega_2 + \dots + \omega_m)} \quad (4)$$

$$D(Y) = (d_1 y_1 \cdot d_2 y_2 \dots d_m y_m)^{1/m} \quad (5)$$

## 2.5 Method application to human body fluids

### 2.5.1 Urine samples

An ideal urine specimen for method development must be adequately concentrated to ensure that matrix effects are catered for during detection of analytes of interest (Brunzel, 2013). The quality of the urine as given by its visual appearance depends on the person's state of hydration and the length of time the urine is held in the bladder. Urination in the morning is mainly due to the body's involuntary desire to discharge urine that accumulated in the bladder overnight. Such a specimen would have been returned in the bladder for at least 6 hrs and is ideal for testing matrix effects during method development for urinalysis. An early morning urine specimen will therefore have maximum matrix effects. Such a specimen is ideal for testing the performance of a method.

## 2.6 Matrix-based calibration curves

Total analyte discrimination during extraction from biological samples is impossible. The profound effect of the matrix on the quality of an HPLC-based analysis requires that certain strategies be taken during method development as a way of accounting for matrix effects. The most accepted approach that

approximates the matrix effects is to construct a calibration curve for your analytes by spiking the sample matrix with analyte standards at different concentration levels and extracting the analytes back out. The instrument response over a specific range of spiking concentrations is then plotted against the spiking concentrations giving a matrix-based calibration curve. Other calibration approaches that have been introduced in urinalysis include the kinetic calibration approach and the desorption kinetic calibration approach initially developed for solid phase micro-extractions (Chen and Pawliszyn, 2004; Cui et al., 2012; Xu et al., 2015).

## **2.7 Method validation parameters**

Various approaches that include linearity, repeatability and reproducibility, limit of detection (LOD) and limit of quantification (LOQ) are used to validate the suitability of a method for its intended application.

### **2.7.1 Linearity**

Linearity is tested as a linear regression model between the instrument's response to the extracted analyte and the spiking concentration. The coefficient of determination denoted by  $R^2$  ( $r^2$  if the point of y intersection of the calibration curve is specified) is used to evaluate how the regression line fits the data set or how close the residual data are to the fitted regression line. The  $R^2$  values range from 0 to 1 and are an indication of the degree of certainty when predicting a dependent variable using the linear regression equation. An  $R^2$  value of 0 implies that the dependent variable cannot be predicted using the linear regression line from the independent variable. An  $R^2$  value of 1 indicates that the regression line passes through all residual points and hence the prediction is without error (Miller and Miller, 2005).

### 2.7.2 Limits of detection and quantification

A limit of detection (LOD) is generally the minimum amount of an analyte that can be reliably distinguished from a blank sample but not necessarily quantifiable under specific experimental conditions. An LOD can be instrument-based or method-based depending on why the minimum amounts of the analyte need to be determined. An instrument-based LOD is meant to evaluate the instrument's sensitivity towards an analyte in the absence of interference (or using standard solutions) while a method-based approach is used to test the detection capabilities of a method by taking into consideration the presence of interferences. The method-based LOD is a sample specific approach dependent on both the instrument's minimal response and the sample preparation techniques used. Determination of the LOD can be empirical through visual evaluation of the peak responses or statistical through calculations that use the standard deviation (SD) of the response. There are three common methods used in estimation of analyte detection limits (Box et al., 2005; Guideline, 1995; Shrivastava and Gupta, 2011; US Food and Drug Administration, 1996).

Common in chromatographic responses that exhibit baseline noise is the signal to noise (S:N) method. The highest peak-to-peak noise around the retention time of the analyte is measured and the concentration of the analyte that would give three times the peak height of the noise is estimated using the calibration curve regression equation. The predicted concentration is then injected and the true S:N ratio calculated using equation 6.

$$LOD = 2H / h \quad (6)$$

Where  $H$  is the peak height of the prescribed analyte concentration and  $h$  is the peak-to-peak background noise

The S:N approach is limited to instrument detection limits where the instrument background noise is of main concern rather than the presence of interfering compounds. This approach was not applicable in our method development considering that percentage matrix effects were profound.



Another approach is the linear regression method. It estimates the LOD from the linear regression equation. For a calibration curve with linear regression equation  $y = bx + c$ , equation 8 is used.

$$LOD = 3SD_{response} / b \quad (8)$$

Where  $SD_{response}$  represents the standard deviation of  $y$ , and  $b$  the slope of the calibration curve. These values can be obtained using the LINEST function in Excel.

This approach is only applicable where there is no background noise or interference, a situation that is impossible in a typical analytical procedure.

Finally is the blank determination procedure which estimates the LOD and LOQ from the mean of the blank and the standard deviation of the blank. This approach expresses the LOD as the sum of the average blank response and its three fold standard deviation. This is mathematically expressed as equation 9.

$$LOD = mean_{blank} + 3SD_{blank} \quad (9)$$

This is a method-based approach in which both the baseline noise and the interference are taken into account. The blank determination became our detection limit determination method considering the enhancing effect of the matrix experienced in our developed method. The limit of quantification (LOQ) was then calculated using equation 10.

$$LOQ = mean_{blank} + 10SD_{blank} \quad (10)$$

The LOQ is the minimum amount that can be confidently ascertained with a degree of precision and accuracy using a linear regression model if the analyte were existent in the sample.

### **2.7.3 Other method validation parameters**

Repeatability and reproducibility of a method are essential precision and accuracy parameters and are determined comparatively as intra-day and inter-day repetitions of the response output. Other parameters that are considered when

attempting to demonstrate the applicability of a developed method include specificity, selectivity, accuracy, robustness, extraction range and system suitability (Miller and Miller, 2005; Shrivastava and Gupta, 2011; Ziegel, 2004).

### **3 RESEARCH OBJECTIVES**

#### **3.1 General objectives**

The main objective of this research was to develop a hollow fibre-based liquid phase microextraction of hallucinogenic compounds from human urine followed by chromatographic quantification.

#### **3.2 Specific objectives**

- (1) To extract and quantify muscimol and its precursors, tryptamine and tryptophan from urine samples using HF-LPME coupled to HPLC-UV
- (2) To select chromatographic conditions for the separation of hallucinogenic alkaloids
- (3) To use multivariate factorial designs in identifying essential HF-LPME parameters
- (4) To use central composite designs to optimize levels of essential parameters that would maximize enrichments of analytes during HF-LPME
- (5) To test the developed method on spiked human urine

#### **3.3 Justification**

Even though the hallucinogenic effect has low toxicity and is non-addictive, the potential risk and potential fatality at elevated levels coupled with documented evidence on the continued abuse and in some cases poisoning by hallucinogenic is a cause for concern (TsujiKawa et al., 2007; van Amsterdam et al., 2011). Very few publications have been reported on quantification of MUS in urine samples.

Development of quantification methods that are simple, inexpensive yet effective and environmental friendly is a necessity. The high extraction efficiencies and selectivity and sensitivity of the follow fibre-based liquid phase microextraction reported in literature offers a good starting point for considering its applicability in the extraction of polar hallucinogens from biological matrices. The target compounds have never been analysed using this approach. The results of the study can offer better alternatives for analysis of hallucinogenic alkaloids in the fields of forensics and food toxicology.

## **4 RESEARCH METHODOLOGY**

### **4.1 Chemicals and reagents**

All compounds except Psilocin (PSI) were purchased from Sigma-Aldrich (Johannesburg, South Africa). PSI in powder form was obtained via the Department of Forensic Sciences, Johannesburg, South Africa. Muscimol (MUS), Tryptophan (TRP), Tryptamine (TA) and 3,4- Dimethoxyphenethylamine (DMPE) were all purchased in powder form while Phenethylamine (PEA) and Hordenine (HO) were in liquid form.

Ammonium acetate, di-(2-ethylhexyl)phosphoric acid (DEHPA), dihexylether (DHE), hydrochloric acid (HCl), ammonium formate, acetic acid, acetone and formic acid were also from Sigma-Aldrich (Johannesburg, South Africa). HPLC-grade acetonitrile (MeCN), methanol (MeOH) and tetrahydrofuran (THF) were obtained from Merck Chemicals (Pty) Ltd, Johannesburg, South Africa. Deionized water (d-H<sub>2</sub>O) used to prepare standard solutions and the mobile phase was purified from a Milli-Q-RO4 system (Millipore, Bedford, MA, USA).

### **4.2 Instrumentation**

A Bishoff LC-CaDI 22-14 system (Leonberg, Germany) with a Lambda 1010 UV detector set at 280 nm was used for quantification of the analytes. Elution was done isocratically with injection of the analyte solutions done using a Rheodyne Series 7725i manual injector with a 10 µL sample loop. Data acquisition and processing was done on McDAcq32 version 2.4.702 software. Separation of analytes was done on a Waters Ascentis Express HILIC with dimensions 10 cm x 2.1 mm x 2.7 µm using a mobile phase that had been buffered at pH 3 with formate. Prior to elution, the column was equilibrated with the mobile phase for at least 30 mins to allow for creation of a pseudo-stagnant aqua layer on the surface of the HILIC column. After investigation the column would then be washed with a MeCN: H<sub>2</sub>O mobile phase with a same organic component composition as the

last mobile phase used for elution and finally 100% MeCN for 10 mins. Degassing of the mobile phase was done using an online Degasys DG-1310 from Uniflows Co., Ltd, Tokyo, Japan. A Transsonic T460 D-78224 by Elma, Germany was used for all sonication. All pH recordings were done using an HQ430d benchtop flexi meter by Hach Company, Loveland Cc. USA. For stirring of the sample solution, a multi-point magnetic stirrer MS-MP8 by Daihan Scientific Co.,Ltd, Seoul, South Korea was used. A galvanized steel binding wire by Mac Indies Company, South Africa branded as NPS/BW-071-50 with 0.71 mm thickness was used for holding hollow fibres in samples solutions during extraction.

### **4.3 Preparation of standard solutions and buffered mobile phase**

Analyte stock solutions of  $1000 \mu\text{g mL}^{-1}$  were prepared separately in 100 ml methanol and kept in the refrigerator at  $4^{\circ}\text{C}$  when not used and brought to room temperature just before use. New stock solutions were prepared after every fourteen days.

For instrument calibration, separation was achieved when the analyte stock solutions were dissolved in THF and eluted at  $0.4 \text{ mL min}^{-1}$  with a pH 3-buffered mobile phase consisting of MeCN: Buffer 90:10% (v/v) 10 mM formate. This mobile phase-buffer composition was freshly prepared on a daily basis and when needed by mixing 4 mL of 500 mM ammonium formate with 16 mL of 500 mM formic acid and making up to 200 mL with MECN.

At pH 3, all our research compounds were positively charged on the basic N atom while the -OH group remained neutral except for TRP whose pKa (OH) value made it zwitterionic with however a zero global net charge. The acidic acceptor phase to be injected into HPLC-UV system was first diluted into MeCN as a modifier and finally into THF in order to achieve separation.

#### 4.4 Chromatographic conditions

Several columns and mobile phases were investigated in order to find suitable chromatographic conditions that could separate the analytes. The interest in selecting column(s) that can be used in chromatographic separation of hallucinogenic alkaloids was evoked by the failure of the reverse phase columns in separating our target analytes during preliminary studies. While most of the hallucinogen extractions have used liquid chromatographic separations in reverse phase mode (Becker et al., 1999; Berge, 1999; Bigwood and Beug, 1982; Björnstad et al., 2009; Brandt and Martins, 2010; Chen et al., 2011; Gennaro et al., 1997; Kamata et al., 2010; Lindenblatt et al., 1998; Manevski et al., 2010; Marcano et al., 1994; Martin et al., 2014; Pichini et al., 2014; Saito et al., 2005; Tsujikawa et al., 2007; Wurst et al., 1992), it was observed that there has never been an attempt to simultaneously quantify muscimol and psilocin despite being identified as the active agents responsible for the hallucinogenic effects of mushrooms. The extent of separation of seven polar hallucinogenic tryptamine and phenethylamine derived alkaloids containing a basic N atom that becomes protonated at low pH values was investigated on two alkyl reverse phase (RP-alkyl) columns, a reverse phase amide (RP-amide), two phenyl-based reverse phase columns and a HILIC column.

The physicochemical properties of the compounds and the columns used are given in Figure 10 and Table 3 respectively. The choice of the alkyl RP columns was based on the fact that most liquid chromatographic separations of hallucinogens are based on this type of columns. Active phase-analyte interactions are exclusively hydrophobic. The RP-Amide was chosen for the presence of the embedded polar amide group that is expected to improve retention of polar analytes and also because it has always been viewed as one of the first definite alternative to C<sub>18</sub> columns for analysis of polar compounds.

The phenyl-based columns were targeted for the phenyl group that might interact through  $\tau$ - $\tau$  interactions available through the phenyl ring with the cyclic groups of the target compounds. The negatively charged fused-core silica Ascentis

Express HILIC choice was based on studies by Chirita et al. 2010 (Chirita et al., 2010) and recommendations by McCalley 2010 (McCalley, 2010) considering that our model compounds have positively charged N atoms at low pH values.

#### **4.5 Calibration of the HPLC-UV**

Six calibration standards between  $0.5 \mu\text{g mL}^{-1}$  and  $10 \mu\text{g mL}^{-1}$  were used in construction of external calibration curves for muscimol, psilocin, tryptophan and tryptamine. Each calibration standard was injected in triplicate as part of quality assurance. Standard deviations were calculated and used for error bars in constructing calibration curves. The coefficient of determination ( $R^2$ ), limits of detection (LOD) and the limits of quantitation (LOQ) were also determined and reported.

#### **4.6 Hollow fibre preparation**

Q 3/2 Accurel 200/600 Accurel® PP polypropylene hollow fibre tubings having a wall thickness of  $200 \mu\text{m}$ ,  $600 \mu\text{m}$  inner diameter and a pore size of  $0.2 \mu\text{m}$  supplied by Membrana GmbH (Wuppertal, Germany) were used. 8 cm long strips of the fibre were cut using a scalpel with a detachable size 10 Swann-Morton surgical blade. An 8 cm long fibre has an internal volume of  $22.6 \mu\text{L}$ . The fibre would then be heat sealed on one end.



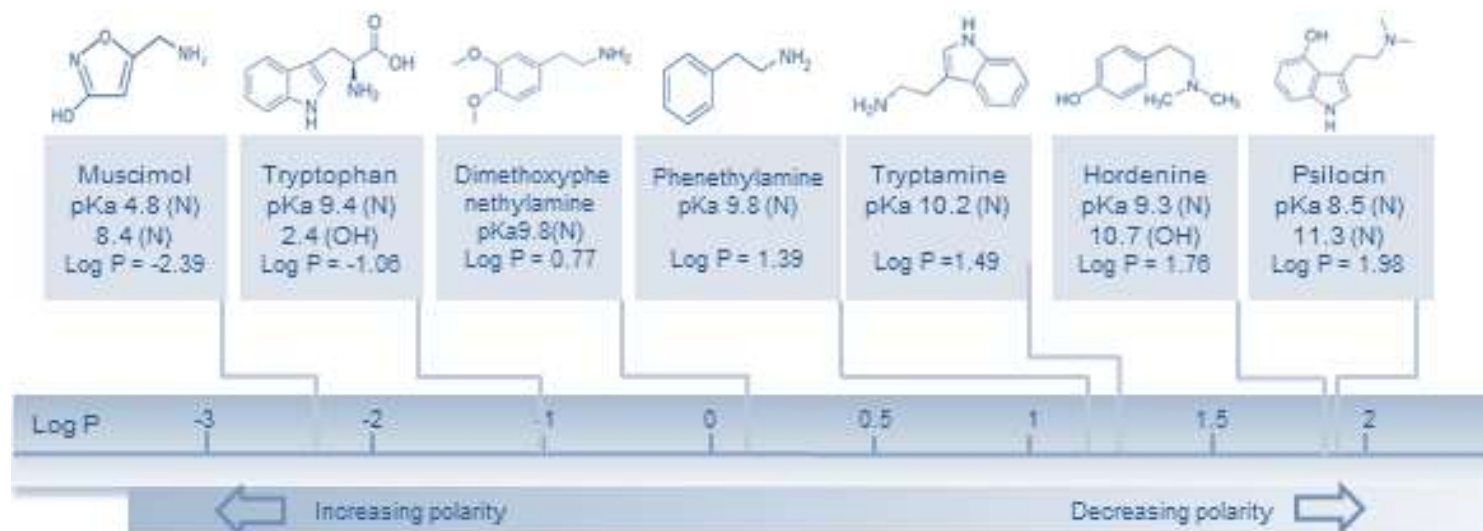


Figure 10 Chemical structures of the model compounds and their relevant physical properties

Table 3 Properties of the six columns used

	Discovery C <sub>18</sub>	Discovery HS C <sub>18</sub>	Gemini Hexyl Phenyl	Waters Spherisorb Phenyl	Ascentis RP-Amide C <sub>16</sub>	Waters Ascentis Express HILIC
Mode of chromatography	Reversed phase (RP)	Reversed phase (RP)	Reversed phase (RP)	Reversed phase (RP)	Reversed phase (RP)	Hydrophilic interaction
Mode of interaction	Hydrophobic	Hydrophobic	$\pi$ - $\pi$ interactions and hydrophobic	$\pi$ - $\pi$ interactions and hydrophilic	H-bonding	Hydrophilic
Particle platform	Silica	Silica	Silica	Silica	Silica	Fused-Core
Active group	C <sub>18</sub> (octadecyl)	C <sub>18</sub> (octadecyl)	Phenyl-hexyl	Phenyl ring with short butyl spacer	Amide, alkyl	Bare silica with silanols
Feature	Endcapped	Endcapped	Endcapped	Endcapped	Endcapped	Not endcapped
L × I.D.	25 cm × 4.6 mm	15 cm × 2.1 mm	25 cm × 4.6 mm	25 cm × 4.6 mm	25 cm × 4.6 mm	10 cm × 2.1 mm
Particle size(μm)	5	5	5	5	5	2.7

All information was obtained from Sigma-Aldrich, South Africa

#### 4.7 HF-LPME procedure

The HF-LPME procedure included adding 10 mL of the sample solution into a 15 mL sample vial. The sample solution was adjusted to the appropriate pH value using dilute NaOH or HCl. The 8 cm long hollow fibers were ultra-sonicated in acetone for 60 mins to remove any contaminants. Thereafter, they were removed and dried by evaporation at room temperature on clean paper towels. About 30  $\mu\text{L}$  of AP of appropriate composition was withdrawn using a 50  $\mu\text{L}$  syringe. The syringe needle was inserted into the unsealed end of the HF segment. The AP was transferred into the HF until bubbles of the solvent appeared on the walls of the HF. The bubbles were wiped off using paper towel to remove excess AP solvent on the outside. The syringe needle was then replaced with a wire acting as hook for hanging the fiber into solution. The fiber containing the AP was then dipped into the organic phase with appropriate composition for 10 seconds to embed the pores of the HF with DEHPA impregnated in a DHE solution. Care was taken not to lose any AP solution due to small back pressure once fibre was dipped into the impregnated organic phase. The SLM-embedded fibre was then taken out and dipped in de-ionized water for 5 seconds in order to wash away the extra organic solvent from the surface of the HF.

The HF containing the AP and the embedded solvent membrane was finally placed in the vial containing the sample solution. The cap of each of the sample vials was pierced to allow the supporting wire to be tightly held in order to support the HF. The complete extraction setup was agitated using a magnetic stirrer. After a specific time of extraction, the stirrer was switched off, the HF removed from the sample solution and the wire carefully replaced by another 50  $\mu\text{L}$  HPLC syringe with the piston pushed down.

With slight pulling of the piston to prevent any loss of the AP, the sealed end of the hollow fiber was cut and the AP drawn back into the syringe by pulling up the piston. Only 20  $\mu\text{L}$  of the AP would be collected and what remained was discarded with the HF. The collected AP solution would then be divided into two aliquots each 10  $\mu\text{L}$  and diluted accordingly for injection into the HPLC-UV

system. Volumes of diluents used were depended on the extent of enrichment of the analyte into the HCl acceptor phase. Thus one portion of the acceptor phase was prepared and analyzed for MUS and TRP while the other was for analysis of TA and PSI whose enrichments were very high compared to those of MUS and TRP and needed to be diluted more. Table 4 summarizes the amounts of diluents used. The schematic diagram in Figure 11 summarizes the general procedure.

Table 4 Dilution of acceptor phases for injection into the HPLC system

Target analytes	Volume of AP ( $\mu\text{L}$ )	Volume of MeCN ( $\mu\text{L}$ )	Volume of THF ( $\mu\text{L}$ )	Dilution factor
Mus & TRP	10	10	40	6
TA & PSI	10	20	500	53

#### 4.8 Efficiency of the method

Method efficiency was calculated as the extent of enrichment of the analytes from the donor phase to the acceptor phase. Poliwoda et al. 2010 declares that for analytical purposes, the enrichment factor (EF) is more important than the extraction efficiency (Poliwoda et al., 2010). The sole purpose of this research was quantification of MUS and its precursors. The EF values were calculated using equation 11.

$$EF = \frac{\text{concentration of analyte in the acceptor phase after extraction}}{\text{concentration of analyte in the donor phase before extraction}} \quad (11)$$

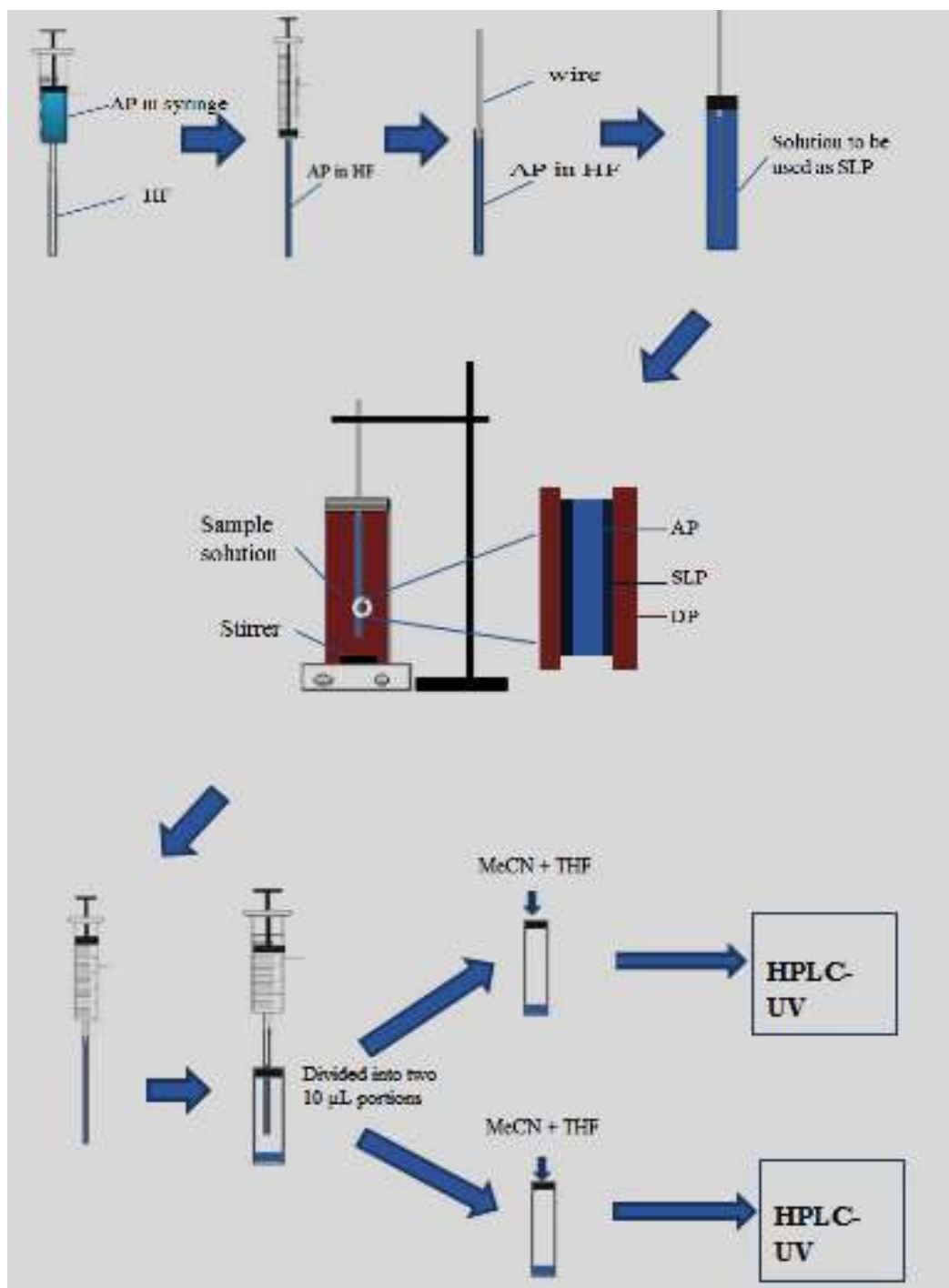


Figure 11 Schematic diagram for the HF-LPME procedure

## 4.9 Multivariate optimization of the HF-LPME parameters

### 4.9.1 Screening experiments using a half fractional factorial design

A two-level half fractional factorial design denoted by  $2^{k-1}$  was created in Minitab 16 in which the number of factors (k) was set to six. The six factors identified from related studies and publications that are involved in carrier-mediated HF-LPME were donor phase pH, acceptor phase concentration, supported liquid membrane composition, NaCl content, stirring rate and extraction time. The half fractional factorial had a green-coded resolution of VI. This design needed thirty two experiments to be run. The parameters of the design are summarized in Table 5.

Table 5 Summary of a fractional factorial design used

Design	Runs	Resolution	$2^{k-p}$
$\frac{1}{2}$ fraction	32	VI	$2^{6-1}$

The donor phase pH, acceptor phase concentration, SLM composition, extraction time, stirring rate and %NaCl were coded as A, B, C, D, E and F respectively. Table 6 shows the lower and upper limits set for each factor. The choice of DP pH limits was based on properties of the carrier molecule and the target analytes. The carrier embedded on the SLM is anionic so the analytes are expected to exist in their cationic state in the donor phase for effective transportation by the carrier. Our analytes were basic at the peripheral N atom and were expected to be cationic in acidic conditions. The carrier used, DEHPA is itself acidic and if the donor phase was to be basic ( $\text{pH} > 7$ ), the carrier would be lost due to neutralization. The choices of SLM composition levels were based on publications while the levels of the other four factors were based on the researchers' preliminary studies. The designs were then investigated for TA (and PSI) and MUS (and TRP).

Table 6 Lower and upper levels for the six factors

	Lower level	Upper level
DP pH	3	7
AP concentration (mM HCl)	10	100
SLM composition (% w/w)	5	20
Extraction time (mins)	10	30
Stirring rate (rpm)	600	800
NaCl content (% w/v)	0.001	0.01

An unfolded design with randomized runs was created in Minitab. The coded design was summarized in form of Table A1 while Table 7 shows the resolution VI types of confounding for the six factors. Table 7 shows that the chosen design could estimate main factors that were only confounded with at least five-factor interaction effects. The estimated two-factor interactions were free from confounding with three-factor (or less) interactions. However the three-factor interactions estimated by this design had been aliased with other three-factor interactions. The uncoded levels of each factor were specified and the signs represented in Table A1 were enumerated as shown in Table 8.

Once the design had been constructed using two levels (a lower value and an upper value) of each factor, triplicate experiments were carried out for the 32 runs and the peak areas statistically analyzed using ANOVA.

The extent of the factor effects on the EF values was then analyzed using Pareto charts of effects, normal plots of effects and the main effects plots for averages. The three different plots of effects were used to identify those parameters having a huge impact on the enrichment factor for the extraction of each analyte from spiked samples. Only thirty largest factor effects were represented in the three plots.

Table 7 Alias structure of the  $2^{6-1}$  fractional factorial design for six factors

Factor interactions	Minimum number of confounding factor combinations
I	ABCDEF
A	BCDEF
B	ACDEF
C	ABDEF
D	ABCEF
E	ABCDF
F	ABCDE
AB	CDEF
AC	BDEF
AD	BCEF
AE	BCDF
AF	BCDE
BC	ADEF
BD	ACEF
BE	ACDF
BF	ACDE
CD	ABEF
CE	ABDF
CF	ABDE
DE	ABCF
DF	ABCE
EF	ABCD
ABC	DEF
ABD	CEF
ABE	CDF
ABF	CDE
ACD	BEF
ACE	BDF
ACF	BDE
ADE	BCF
ADF	BCE
AEF	BCD



Table 8 Design of experiment summary showing uncoded randomized runs when a  $2^{6-1}$  fractional factorial was designed with each factor having two levels; a lower level and an upper level

Run Order	DP pH	AP concentration (mM HCl)	SLM composition (% w/v)	Extraction time (mins)	Stirring rate (rpm)	NaCl content (% w/v)
1	3	100	5	10	600	0.01
2	7	10	5	10	800	0.001
3	3	10	20	30	600	0.001
4	7	100	20	30	800	0.01
5	3	100	5	30	800	0.01
6	7	100	5	10	600	0.001
7	3	10	20	30	800	0.01
8	3	10	20	10	800	0.001
9	7	10	5	30	800	0.01
10	7	10	20	10	800	0.01
11	3	10	5	10	600	0.001
12	7	10	20	30	800	0.001
13	3	10	5	30	600	0.01
14	3	10	20	10	600	0.01
15	7	10	20	30	600	0.01
16	3	100	5	10	800	0.001
17	3	100	20	30	800	0.001
18	7	10	5	30	600	0.001

19	7	10	5	10	600	0.01
20	7	100	5	10	800	0.01
21	3	10	5	30	800	0.001
22	7	100	5	30	600	0.01
23	7	100	5	30	800	0.001
24	3	100	20	10	600	0.001
25	3	100	20	30	600	0.01
26	3	100	5	30	600	0.001
27	7	10	20	10	600	0.001
28	3	10	5	10	800	0.01
29	7	100	20	30	600	0.001
30	3	100	20	10	800	0.01
31	7	100	20	10	600	0.01
32	7	100	20	10	800	0.001

#### 4.9.2 Optimization experiments using central composite designs

After identifying four factors as essential for the HF-LPME of the analytes, a spherical and rotatable CCD was created by setting  $\alpha = \sqrt{4} = 2$  as shown in Figure 12.

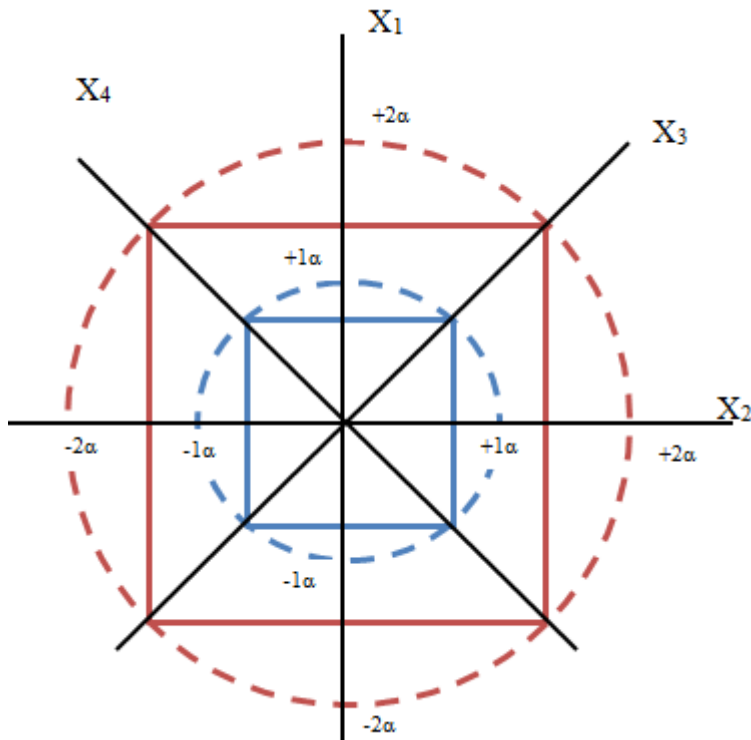


Figure 12 Designing a spherical rotatable central composite approach.  $X_{1-4}$  refers to the four vital factors identified from fractional factorial design.

From the design in Figure 12, it could be shown that there were eight star (axial) points represented by either  $\pm 1\alpha$  or  $\pm 2\alpha$ . There were sixteen factorial points that existed where the four factor lines ( $X_1$ ,  $X_2$ ,  $X_3$  and  $X_4$ ) touched the sides and the vertices of the small square and the big square. Only one centre point could be seen but if Fig 12 had been observed from two or three dimensional, a total of six centre points would have been observed. The overall number of points was therefore thirty (16 factorial points, 8 star points and 6 centre points). This design was simplified mathematically using equation 12 below in which  $2^k$  represented the factorial points,  $2k$  the star points and  $C$  the centre points.  $N$  represents the total number of points.

$$N = 2^k + 2k + C \quad (12)$$

Thus thirty runs were carried out for each compound in order to classify the extent of each of the four vital factors. The levels of each factor were code-set using  $\alpha = \pm 2$  giving a 5-factor level design represented as -2, -1, 0, 1 and 2 where 0

represented the mid-range value and  $\pm 1$  were factor levels chosen by the researcher.

***Central composite design for main factors for MUS (and TRP)***

The chosen factor levels that were entered into Minitab in order to create the design are given in Table 9 while Table 10 shows the actual levels used for each factor. The randomized coded design was represented as shown in Table A2. The uncoded central composite design for the four essential factors for the extraction of MUS is represented in Table 11.

Table 9 Factor levels that were entered into Minitab when creating the CCD for the main factors

	DP pH	AP concentration (mM HCl)	SLM composition (% w/w)	Stirring rate (rpm)
Set lower level	4	50	10	600
Set upper level	6	100	20	800

Table 10 Actual factor levels of the main factors that were experimentally investigated

Alpha ( $\alpha$ ) value	-2	-1	0	1	2
DP pH	3	4	5	6	7
AP concentration (mM HCl)	25	50	75	100	125
SLM composition (% w/w)	5	10	15	20	25
Stirring rate (rpm)	500	600	700	800	900

Table 11 Randomized central composite design for the essential factors at  $\alpha = 2$

Run	DP pH	AP concentration (mM HCl)	SLM composition (% w/w)	Stirring rate (rpm)
1	3	75	15	700
2	5	125	15	700
3	5	75	15	500
4	5	25	15	700
5	5	75	5	700
6	5	75	25	700
7	5	75	15	900
8	5	75	15	700
9	5	75	15	700
10	7	75	15	700
11	4	100	10	800
12	5	75	15	700
13	5	75	15	700
14	6	50	10	600
15	6	50	20	600
16	4	100	20	800
17	6	100	20	600
18	4	50	20	600
19	4	50	20	800
20	6	100	10	800
21	6	50	20	800
22	4	50	10	800
23	5	75	15	700
24	4	50	10	600
25	6	50	10	800
26	6	100	20	800
27	4	100	10	600
28	6	100	10	600
29	5	75	15	700
30	4	100	20	600

*Central composite design for main factors for TA (and PSI)*

For the extraction of TA, extraction time replaced stirring rate in the four main factors. Its values that were set on Minitab were 40 and 80 mins. This resulted in five levels of 20, 40, 60, 80 and 100 mins. The coded and uncoded central composite designs for the optimization of the vital factors for the extraction of TA are represented in Table A3 and Table 12 respectively.

The response from varying each factor was standardized and Pareto charts of standardized effects and normal plots of standardized effects were plotted in order to visualize the extent of effect of each of the four vital factors. The factors were then grouped into pairs accordingly.

The combined effect for each of the paired factors for the extraction of each analyte was then investigated over a specific range of factor values. The number of values in the specified range of each factor was decided by the researcher. The paired factors and the factor levels investigated for the individual extraction of analytes are shown in Table 13 – 19. Only one pair could be investigated for PSI.

Table 12 Randomized uncoded central composite design for the essential factors for TA

Run	DP pH	AP concentration (mM HCl)	SLM composition (% w/w)	Extraction time (mins)
1	5	75	15	100
2	7	75	15	60
3	5	75	5	60
4	5	75	15	20
5	5	75	15	60
6	5	25	15	60
7	3	75	15	60
8	5	75	25	60
9	5	75	15	60
10	5	125	15	60
11	4	100	10	40
12	6	100	10	40
13	6	100	20	80
14	5	75	15	60
15	4	100	20	80
16	6	50	10	80
17	6	100	10	80
18	4	100	10	80
19	4	50	20	40
20	4	50	20	80
21	4	100	20	40
22	4	50	10	40
23	6	100	20	40
24	5	75	15	60
25	6	50	10	40
26	5	75	15	60
27	6	50	20	80
28	4	50	10	80
29	6	50	20	40
30	5	75	15	60

Table 13 Factor levels for the investigation of the combined effect of DP pH and stirring rate in the extraction of MUS

DP pH	Stirring rate (rpm)				
3	500	600	700	800	900
4	500	600	700	800	900
5	500	600	700	800	900
6	500	600	700	800	900

Table 14 Factor levels for the investigation of the combined effect of AP concentration and SLM composition in the extraction of MUS

AP concentration					
(mM HCl)	SLM composition (% w/w)				
30	5	10	15	20	
50	5	10	15	20	
75	5	10	15	20	
100	5	10	15	20	

Table 15 Factor levels for the investigation of the combined effect of DP pH and AP concentration in the extraction of TA

DP pH	AP concentration (mM HCl)				
3	50	100	150	200	
4	50	100	150	200	
5	50	100	150	200	
7	50	100	150	200	



Table 16 Factor levels for the investigation of the combined effect of SLM composition and extraction time in the extraction of TA

SLM composition				
(% w/w)	Extraction time (mins)			
5	30	40	60	80
10	30	40	60	80
15	30	40	60	80
20	30	40	60	80

Table 17 Factor levels for the investigation of the combined effect of donor phase pH and stirring rate in the extraction of TRP

DP pH	Stirring rate (rpm)				
3	500	600	700	800	900
4	500	600	700	800	900
5	500	600	700	800	900
6	500	600	700	800	900
7	500	600	700	800	900

Table 18 Factor levels for the investigation of the combined effect of AP concentration and SLM composition in the extraction of TRP

AP concentration				
(mM HCl)	SLM composition (% w/w)			
30	5	10	15	20
50	5	10	15	20
75	5	10	15	20
100	5	10	15	20

Table 19 Factor levels for the investigation of the combined effect of SLM composition and extraction time in the extraction of PSI

SLM composition				
(% w/w)	Extraction time (mins)			
5	30	40	60	80
10	30	40	60	80
15	30	40	60	80
20	30	40	60	80

The response results were then transferred into Minitab. An empirical second order response surface model was used in which the response was plotted against the combined effect of simultaneously varying the paired factor levels. The quadratic response surface model was estimated by setting the k number of factors in equation 4 to two. Thus the quadratic response models for each paired factors for each analyte were obtained by simplifying the parameters of equation 1 to six as represented in equation 13. Regression coefficients for response estimated from Minitab using data in uncoded units were used as  $b_i$  and  $b_{ij}$  values.

$$y = b_0 + b_1x_1 + b_2x_2 + b_{11}x_1^2 + b_{22}x_2^2 + b_{12}x_1x_2 \quad (13)$$

The resulting surface was visualized using contour plots and surface plots of response. Optimization plots which showed points of curvature for each model were also created. The optimum factor values for each pair were identified as the points of curvature on the plots. Included in the optimization plots were the individual desirabilities of the predicted optimum values of each pair factor in maximizing the desired response output.

### 4.9.3 Applying optimized method to spiked water samples

#### *Individual analyte extraction from spiked water samples*

The optimum values for the four factors were then investigated practically by applying them for the extraction of individual analytes from spiked water samples.

The response output given as EF values was then compared with the EF values predicted in the optimization plots.

#### ***Simultaneous extraction of analytes from spiked water samples***

The purpose of this method development was to simultaneously quantify MUS, TA and TRP from samples. However, each main factor had its own optimum factor level for the extraction of each analyte using HF-LPME from samples. There was a need to assess the importance of each analyte response in order to assign appropriate values for the factors during simultaneous quantification. In this case, the enrichment factor for MUS was deemed important mainly because muscimol had the lowest EF and it was the project's main analyte because of its hallucinogenic properties. The target was therefore to maximize the EF value of MUS. The optimum parameters of MUS were then set as the composite factor values for simultaneous extraction. These compromised factor values were changed from optimization plots in Minitab. The extent of the effect of the overall universal settings on the three analyte response outputs was evaluated using a composite desirability function,  $D(Y)$  in which the geometric mean of individual desirabilities for each analyte response output was calculated using equation 5 where  $d_m$  represented the individual desirability for changing the optimized factor levels in a paired interaction to universal settings and  $m$  the total number of responses due to paired factors for all the three analytes.

These MUS-based factor values were then applied to extract the three compounds from spiked water samples and the experimental EF values compared to the predicted ones.

#### **4.10 Method application to human urine**

The method optimized by spiking water samples was then applied on urine samples. The purpose at this stage was to do a comparison study of the possibility of matrix effects on the EF values and if possible find ways of counteracting such effects. Thus matrix-based calibration curves were constructed to address these matrix effects.

#### **4.10.1 Urine collection**

A routine void collection technique was done in collecting an early morning specimen type of dark yellow urine from a healthy 24 year old male with no prior exposure to hallucinogens and/or hallucinogenic mushrooms. Age and sex of the choice of individual that supplied the urine sample was random with no particular criteria followed except that the individual must have never used or consumed hallucinogenic compounds. No incentive was offered and participation during this research was on voluntary basis.

A total of 406 mL of dark yellow urine was completely voided into a 500 mL glass container with a lid. The conductance of undiluted urine was  $27.95 \text{ mS cm}^{-1}$ . A 50% (v/v) diluted specimen had a conductance of  $15.01 \text{ mS cm}^{-1}$  while that for a 20% (v/v) urine solution was  $5.09 \text{ mS cm}^{-1}$ . Marickar et al. (2010) has recorded a maximum conductance of  $33.9 \text{ mS cm}^{-1}$  for early morning urine while Kovacs et al. (1999) recorded  $25 \text{ mS cm}^{-1}$  (Kovács et al., 1999; Marickar, 2010).

#### **4.10.2 Urine preparation, spiking and extraction of analytes**

After setting the extraction samples to pH 4, the conductance was  $231 \text{ mS cm}^{-1}$ . Two portions of the urine sample were diluted at 50% (v/v) and 20% (v/v) urine into 200 mL beakers using deionized water. Each diluted urine solution was then separated into two equal 100 mL volumes. One of the 100 mL 50% (v/v) urine solutions would then be spiked with 200  $\mu\text{L}$  of the  $1000 \mu\text{g mL}^{-1}$  stock solutions to produce  $2 \mu\text{g mL}^{-1}$  individual hallucinogen concentrations. Three 10 mL volumes of the spiked 50% (v/v) diluted urine sample were then extracted under optimized conditions and enrichment factors evaluated. Unspiked portions of the 50% (v/v) urine samples were also extracted simultaneously with the spiked dilution solutions under optimized conditions in order to investigate possibility of matrix effects. Like the spiked urine solution, three extractions were done for the unspiked. The procedure was repeated with the 20% (v/v) diluted urine sample. The potential use of 100 mM and 200 mM HCl as acceptor phases were also tested and compared during this stage. The idea was to help decide on risk versus efficiency considering that the pH of 200 mM HCl remained outside the column

working range even after dilution for injection. The unused diluted urine samples, both spiked and unspiked were immediately placed in the refrigerator at 4°C.

#### 4.10.3 Calculating matrix effects

The influence of matrix effects were expressed mathematically as a percentage ratio of total peak area of analyte extracted from spiked urine to peak area of analyte in the absence of matrix effects. The peak area due to analyte after extraction from urine was its peak area contribution to the total peak area and was obtained using equation 14.

$$\text{Analyte peak area} = \text{total peak area} - \text{peak area of interfering compound} \quad (14)$$

The peak area of the interfering compound was obtained from blank urine extractions. The percentage matrix effect was calculated as an average of three analyte extractions from spiked diluted urine solutions in comparison to the average peak area of analyte in absence of matrix. Formula 15 was used.

% matrix effect

$$= \frac{100 \times \text{average total peak area from spiked urine sample}}{\text{average peak area of analyte}} - 100 \quad (15)$$

A negative value should indicate matrix suppression, while matrix enhancement is represented by a positive value. An absence of matrix effects is ideally given by zero, a value seldom obtained when extraction is done from biological samples.

#### 4.10.4 Constructing matrix-based calibration curves

A matrix-based calibration approach was used in which diluted urine samples were spiked with the analytes at different concentration levels and extracting the analytes back out. The general matrix-based calibration procedure involved preparing six 20% (v/v) diluted urine samples that were spiked in the 0.1 – 10 µg mL<sup>-1</sup> range with TA, MUS and TRP. The six spiked urine solutions had analyte concentrations of 0.1 µg mL<sup>-1</sup>, 0.5 µg mL<sup>-1</sup>, 1 µg mL<sup>-1</sup>, 2 µg mL<sup>-1</sup>, 5 µg mL<sup>-1</sup> and 10 µg mL<sup>-1</sup>. Each spiked concentration was then extracted using the MUS-based universal extraction conditions. The EF values of each analyte over the specific

range of spiking concentrations were then plotted against the spiking concentrations giving matrix-based calibration curves. The overall enrichment factor for each analyte was estimated as an average of EF values at each calibrator spiking concentration level.

#### **4.10.5 Method validation**

Various approaches that include linearity, repeatability and reproducibility, limit of detection (LOD) and limit of quantification (LOQ) were used to validate the suitability of our developed method for its potential use in quantifying MUS and its precursors from urine samples. These characteristics were investigated when the method was applied in spiked urine samples. These method validation measures were used as a way of determining the method's ability to maintain the extraction process at equilibrium over a wide range of analyte concentrations over a period of analyte existence in a sample.

Linearity was tested as the relationship between the instrument's response to the extracted analyte and the spiking concentration. A blank determination procedure was used to estimate the LOD and LOQ for each analyte from the mean of the blank and the standard deviation of the blank using equation 9 and equation 10 respectively.

The intra-day precisions were investigated by performing three repeat extractions simultaneously for every spiked analyte concentration. Standard deviations were used for error bars. Reproducibility was assessed by means of inter-day extractions. The 2  $\mu\text{g mL}^{-1}$  spiked diluted urine preserved at 4<sup>0</sup>C were extracted after a day and results compared statistically with those from the fresh urine extractions done the previous day using RSD values. The method was again tested on the preserved 2  $\mu\text{g mL}^{-1}$  spiked urine sample after five days.

Other validation parameters that were considered include selectivity and accuracy, robustness, extraction range and system suitability. Since it was impossible to completely discriminate our analytes from urine matrices, calculation of matrix effects was used to compensate for lack of specificity or selectivity. Accuracy of the developed method was reported as the reproducibility of EF values over six

spiking concentrations used in constructing matrix-based calibration curves. System suitability was limited to an HPLC-UV approach. Method suitability was addressed through a comparative summary in which the LOD, LOQ and  $r^2$  values for the developed method were compared to other methods that have been used to extract MUS from urine samples. The relevance or acceptability of the EF values obtained for the extraction of the three analytes was achieved by comparison with EF values of other compounds of similar polarity that have been extracted from urine samples using carrier-mediated HF-LPME.

## 5 RESULTS AND DISCUSSION

### 5.1 Selection of chromatographic conditions

Of the seven columns investigated, only the reverse phase phenyl and the HILIC were recommended for use in LC separation of tryptamine and phenethylamine derived polar alkaloids. Figure 13 shows the chromatograms obtained when the reverse phase phenyl, amide and hexylphenyl columns were used for separation of six alkaloids.

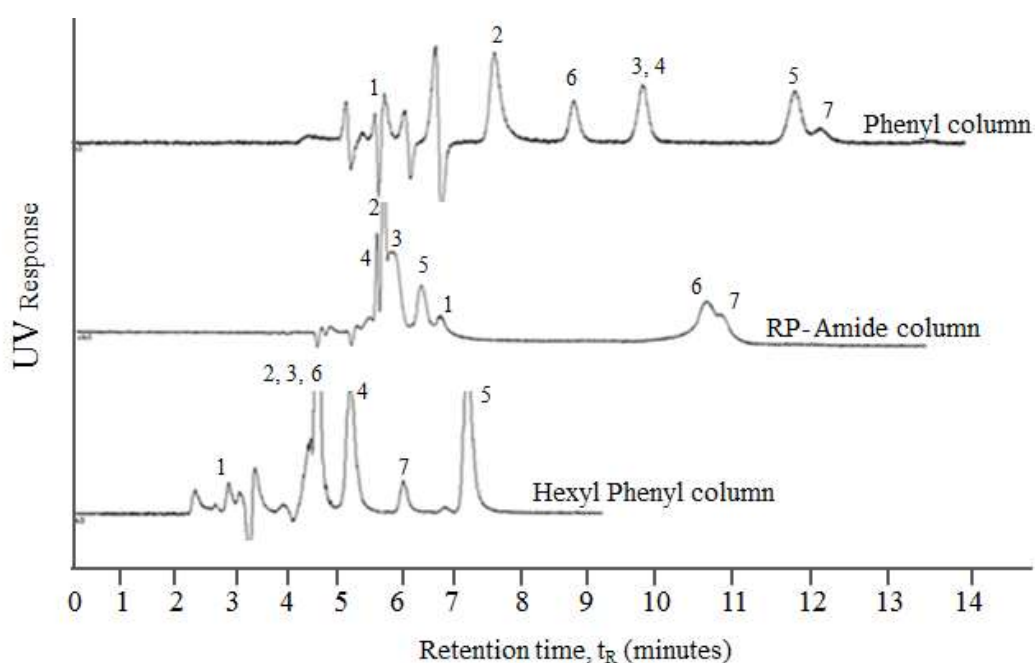


Figure 13 Retention and separation on three RP-columns at optimized conditions. Compounds: (1) Muscimol; (2) Tryptophan; (3) 3,4- Dimethoxyphenethylamine; (4) Phenethylamine; (5) Tryptamine; (6) Hordenine; (7) Psilocin. Compound numbering was based on descending polarity

In addition to the investigation parameters considered of greater effect in HILIC separations and the recommendations for analyte diluents that are considerably close to the mobile phase composition (Buszewski and Noga, 2012; Cheng et al., 2007; Guo and Gaiki, 2011; Hemström and Irgum, 2006; McCalley, 2010), the results of this research showed that better separations can be achieved if the



analytes extracted using polar protic extraction solvents are diluted with moderately polar aprotic solvents for injection. Water, methanol, acetonitrile and tetrahydrofuran were investigated as potential analyte diluents for injection into the HPLC system. A comparison of MeCN and THF in Figure 14 showed the better separating ability of a buffered MeCN mobile phase on a HILIC column when THF was used as the diluent. Decreasing the polarity of an injection solvent in HILIC separations was predicted to enhance separation by focussing the analytes onto the pseudo-stagnant water layer formed on the surface of the HILIC column. Thus, tetrahydrofuran (THF) was recommended where methanol is used as an extracting solvent of polar hallucinogenic analytes from biological matrices.

A HILIC column, its mobile phase composition and THF as an injection diluent were adopted for further experiments with muscimol, psilocin, tryptamine and tryptophan. Flow rate was set at  $0.4 \text{ mL min}^{-1}$  using a mobile phase composition of MeCN: Buffer 90:10% (v/v) 10 mM formate. The mechanism of analyte separation is the extent of partitioning of the analyte between the pseudo-stagnant aqua layer that forms at the surface of the stationary phase and the mobile phase as confirmed by McCalley and Neue (2008) and Dinh et al. (2013) (Dinh et al., 2013; McCalley and Neue, 2008). The result is that retention favours the more hydrophilic analytes as confirmed by the elution order in Fig 14. General peak broadening was observed for those compounds that retained more as shown by the peak for tryptophan, a situation that has been reported before (Chirita et al., 2010; McCalley and Neue, 2008).

## 5.2 Instrument calibration

The response results for calibrating the HPLC-UV instrument using analyte standard solutions in the  $0.5 - 10 \text{ } \mu\text{g mL}^{-1}$  are presented in Table 20. The actual calibration curves are presented in Fig A1 – A4. The linearity represented by coefficient of determination,  $R^2$  was good and ranged from 0.9929 to 0.9999. The high LOD value for TRP might be related to the observed broadening of its peak.

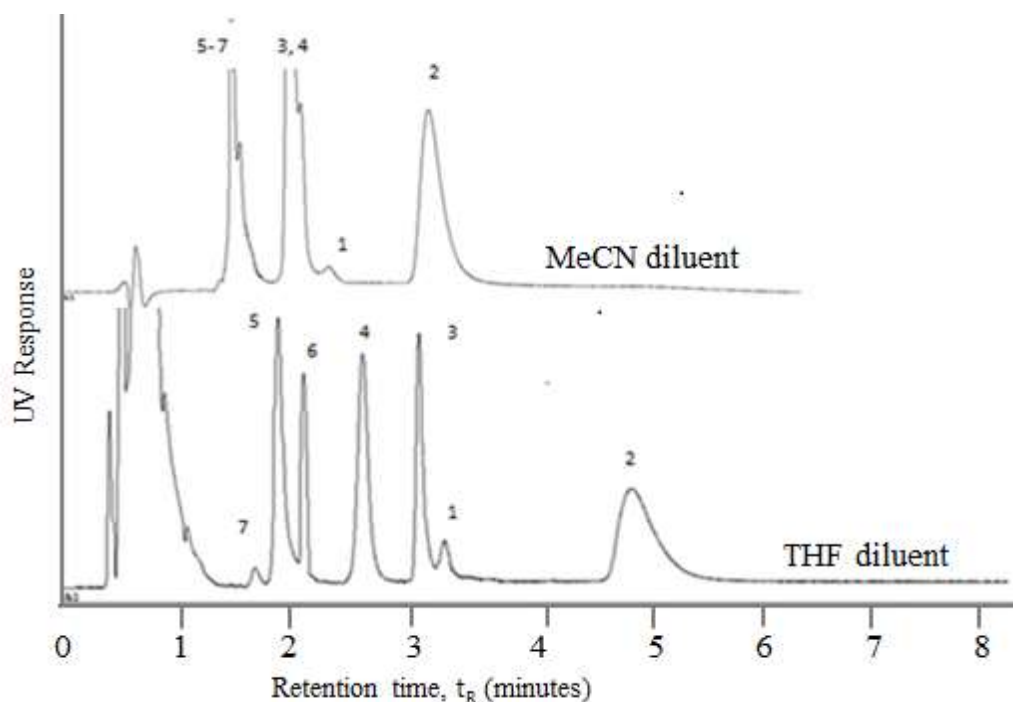


Figure 14 Chromatograms when THF and MeCN were used to dilute the MeOH stock solutions for analyte injection. Compounds: (7) Psilocin; (6) Hordenine; (5) Tryptamine; (4) Phenethylamine; (3) 3,4-Dimethoxyphenethylamine; (2) Tryptophan; (1) Muscimol. Muscimol and psilocin were injected at  $1 \mu\text{g mL}^{-1}$  and at  $0.5 \mu\text{g mL}^{-1}$  respectively

Table 20 Summary of instrument calibration results for the four analytes

Analyte	Calibration equation	$R^2$	LOD ( $\mu\text{g mL}^{-1}$ )	LOQ ( $\mu\text{g mL}^{-1}$ )
MUS	$y = 2.0162x + 0.1052$	0.9929	0.0237	0.0344
TRP	$y = 3.106x - 4.2568$	0.9976	0.1655	0.1671
TA	$y = 24.176x + 4.0073$	0.9999	0.0269	0.0401
PSI	$y = 9.8933x - 2.116$	0.9977	0.1007	0.1419

$y$  is the peak area and  $x$  the spiking concentration

### 5.3 Screening results

#### 5.3.1 Half fractional factorial design for tryptamine

The peak areas obtained from the half fractional factorial design experimental results for TA are shown in Table A4. The one way ANOVA results done on peak

areas in order to determine if the 32 runs gave similar output results is presented in Table A6 and Table 21. The F-observed value in the one-way ANOVA results was much greater than the F-critical value and the P-value was less than the set 0.05 implying that two or more of the peak areas of the 32 runs were different.

Table 21 One-way ANOVA results for extraction of TA (n=3)

<i>Source of Variation</i>	<i>SS</i>	<i>df</i>	<i>MS</i>	<i>F</i>	<i>P-value</i>	<i>F crit</i>
Between						
Groups	1348860.305	31	43511.623	4492.911	6.52E-96	1.631
Within						
Groups	619.808	64	9.685			
Total	1349480.113	95				

The experimental peak areas were then converted to EF values for TA and the results are summarized in Table A5. A Pareto chart of effects, normal plot of effects and the main effects plot for averages used to identify those parameters having a huge impact on the enrichment factor are shown in Figure 15, Figure 16 and Figure 17 respectively. The Pareto chart average value for the thirty largest factor effects was 29.8. All the factors and factor interaction with histograms higher than the average value were considered vital. In the normal plot of effects, the significant factors and factor interactions were marked in red. For the main effects plot, an average response value was represented as a horizontal line and the responses with highest deviation from the average were used to visualize the effects.

All the plots agreed on the enhanced effects due to change in SLM carrier composition, AP concentration, extraction time and DP pH. The extraction of analytes from the DP is carrier mediated hence the observed highest impact of SLM carrier composition. The driving force is also governed by the proton difference between the DP and the AP solvents. It is however the AP that provides counteracting H<sup>+</sup> ions. Thus SLM carrier composition, AP HCl concentration,

extraction time and DP pH were identified as the significant factors that could greatly affect the response output if not monitored. These four factors were then taken forward for optimization using response surface designs.

The Pareto chart and the normal plot of effects further identified the combined effects of SLM carrier composition and AP concentration as more vital than varying extraction time and DP pH. The AP composition-extraction time, the DP pH-SLM carrier composition combined effects were also effective. The combined effect of the DP pH and less effective stirring rate and presence of a salt appeared to be marginally effective.

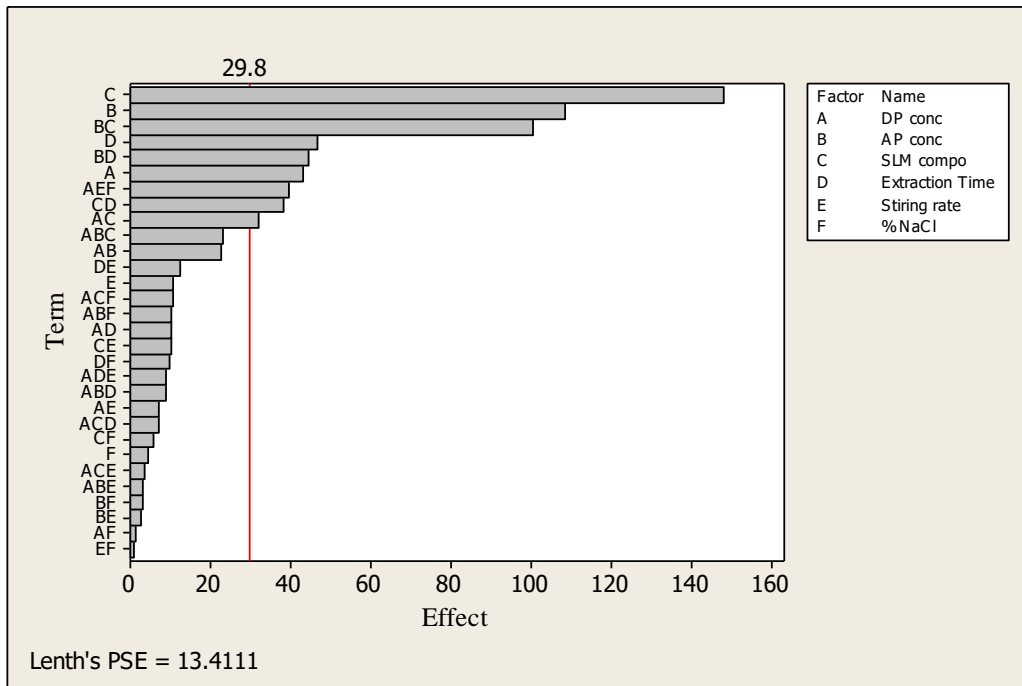


Figure 15 Pareto chart of factor effects for the extraction of TA (Alpha = 0.05, only 30 largest effects shown)

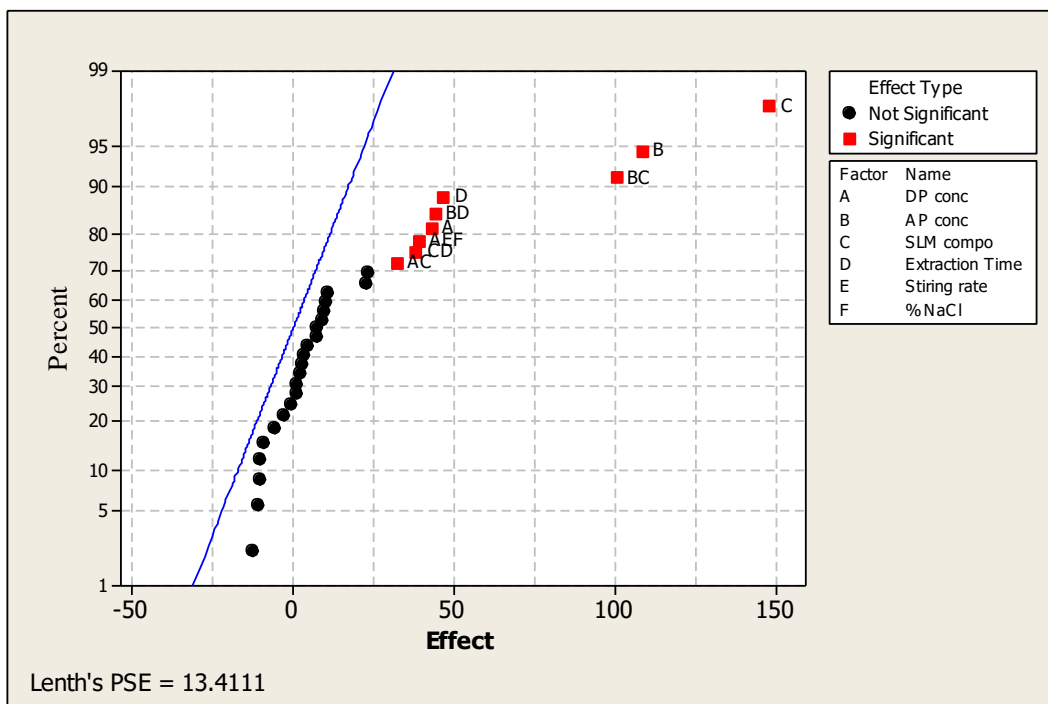


Figure 16 Normal plot of factor effects for extraction of TA (Alpha = 0.05, only 30 largest effects shown)

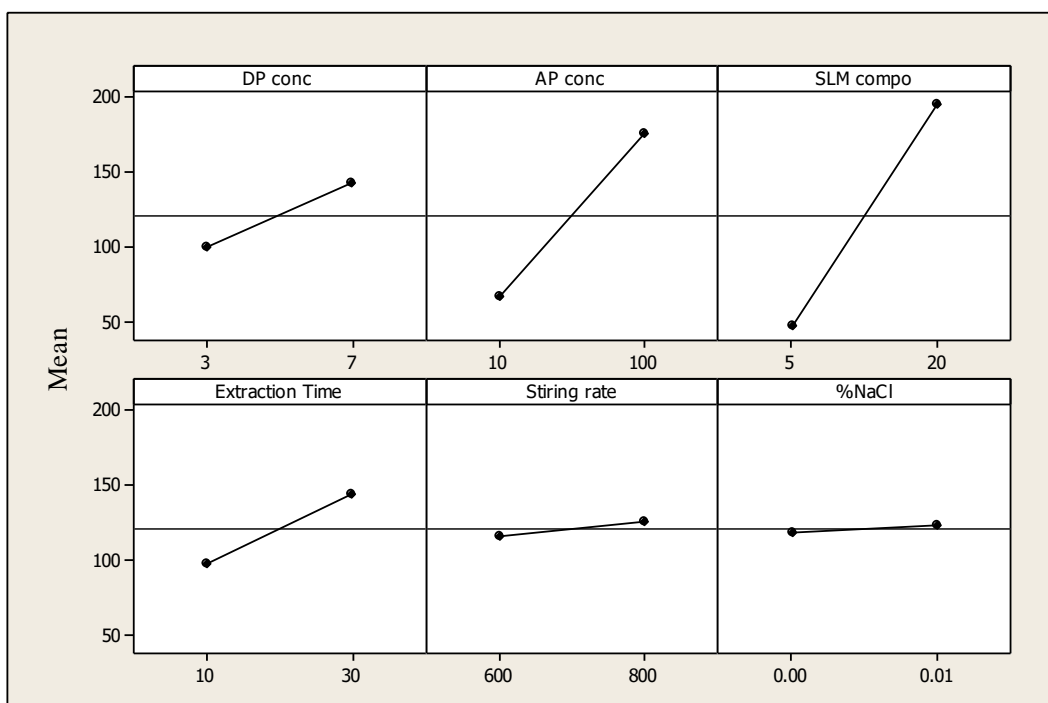


Figure 17 Main factor effects plot for response average during extraction of TA

### 5.3.2 Half fractional factorial design for muscimol

The procedure described in section 5.3.1 was repeated and the same analysis strategies were repeated for identification of essential factors when compounds of extreme polarity are to be extracted. The study compound was MUS. The peak areas and the variance results are given in Table A7 and Table A8. The single factor ANOVA results are summarized in Table 22.

Table 22 One-way ANOVA results for extraction of MUS (n=3)

<i>Source of Variation</i>	<i>SS</i>	<i>df</i>	<i>MS</i>	<i>F</i>	<i>P-value</i>	<i>F crit</i>
Between						
Groups	3953.554	31	127.534	32.794	2.16E-27	1.6423
Within Groups	233.339	60	3.889			
Total	4186.892	91				

The F-observed and the P-value confirmed that several of peak areas from 32 experiments were significantly different at 95% confidence interval. The average peak areas were then converted to EF values for MUS and the results are summarized in Table A9. The main effects were visually identified using the three plots of effects given in Figures 18, 19 and 20.

The Pareto chart of effects identified stirring rate as the only factor with a corrected effect value above average. This was also confirmed in the normal plot of effects and by a visual analysis of the main effects plot. The polarity of MUS is very high with an X log P3 value of -1.4 and water solubility of  $5.67 \times 10^5 \text{ mg L}^{-1}$ . This implied that MUS had a high tendency to remain in solution. Stirring increased its kinetic energy and its chances of being at the donor phase-SLM interface were increased. This might have explained the observed impact of stirring on the output compared to other factors.

The normal plot of effects identified the negative impact of the donor phase pH-extraction time interaction. The main effects plot further confirmed the negative

effect on the response when the donor phase pH was increased. The pKa value of the basic N on MUS is 4.8. This basic N can therefore only carry a positive charge as required for effective carrier-aided extraction at pH values below 4.8. Between pH 4.8 and pH 7 MUS is in its neutral state. In addition to stirring rate, three other factors deemed significant were SLM composition, AP concentration and DP pH. These factors were presumed to have the same impact on TRP because of polarity similarities between the two compounds. The main factor effects plot showed that salt content also had a negative impact on the extraction of MUS. This has also been observed by Saaid et al. 2009 (Saaid et al., 2009). The explanation lies on the increase in viscosity that restricts transfer of very polar compounds.

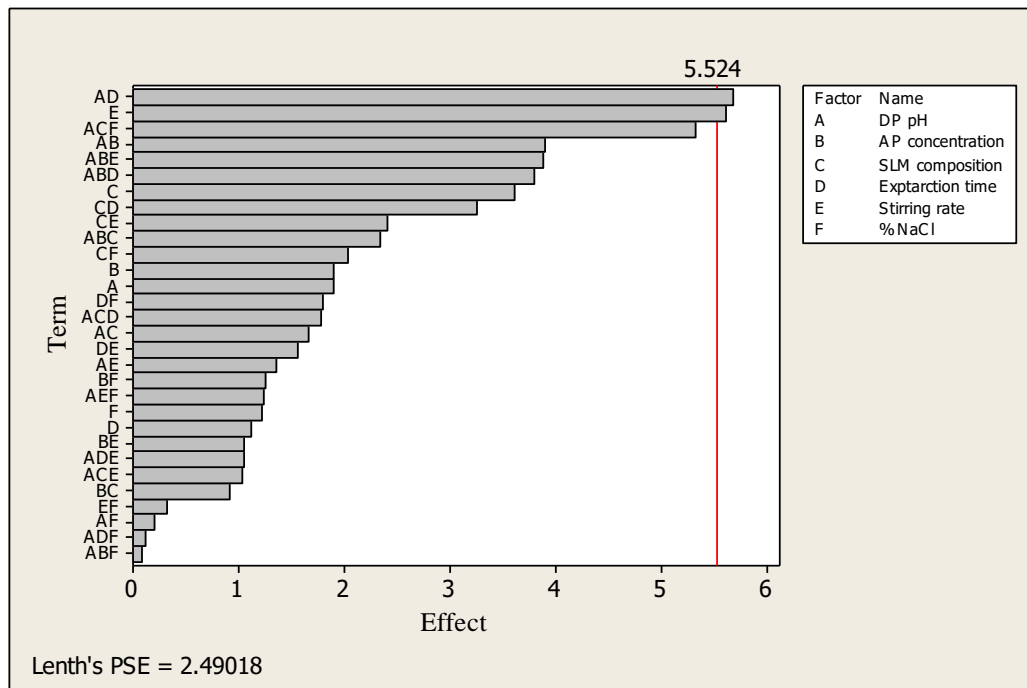


Figure 18 Pareto chart of factor effects for the extraction of MUS (Alpha = 0.05, only 30 largest effects shown)

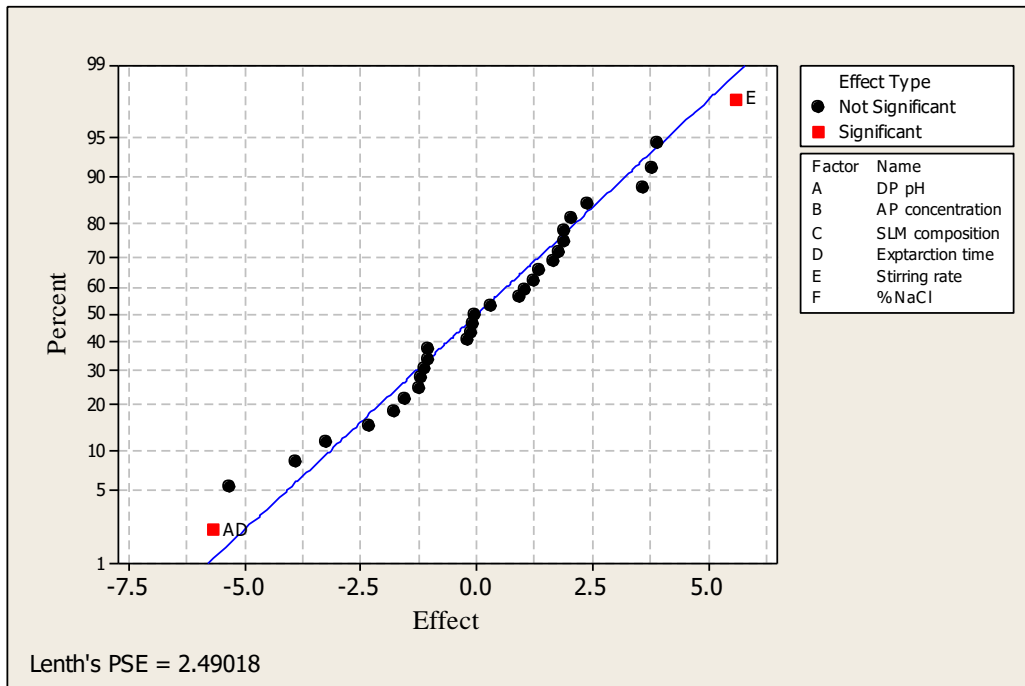


Figure 19 Normal plot of factor effects for the extraction of MUS (Alpha = 0.05, only 30 largest effects shown)

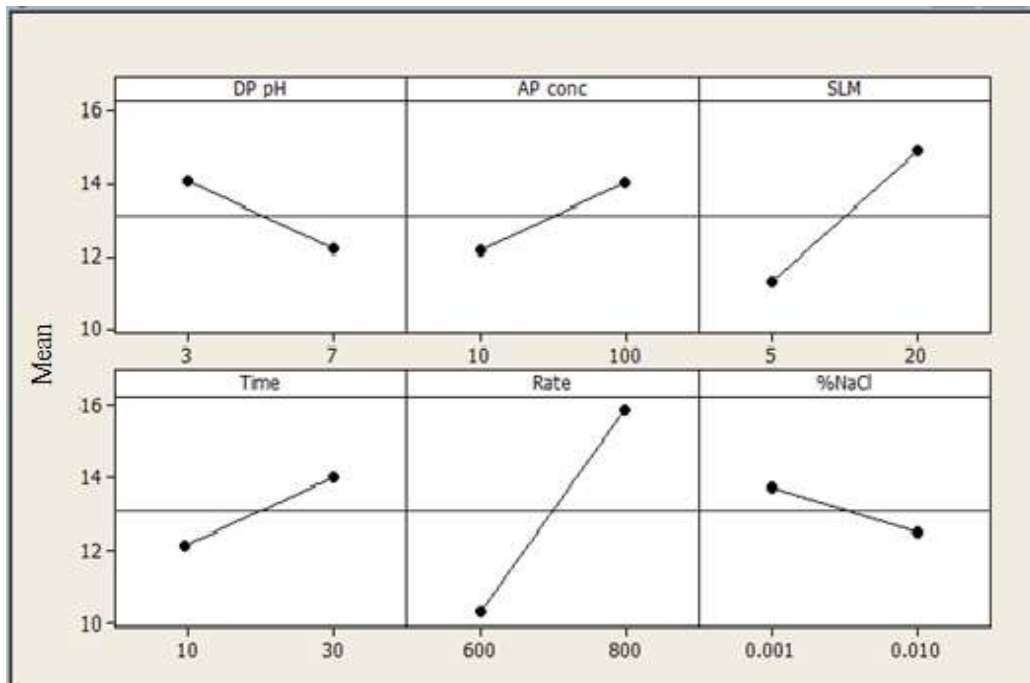


Figure 20 Main factor effects plot for response average during extraction of MUS



### **5.3.3 Comparing the current screening results to other related studies**

Table 23 shows that the screening results for the current study are comparable with fractional factorial screening results for other related compounds. Generally, very few studies on LPME have been conducted through multivariate approaches. In Table 23 it can be seen that the common factors that have been identified through fractional designs include the DP pH, AP concentration, extraction time. Some studies where a single analyte with a single pKa value, the DP pH and AP concentration were not considered for screening and their levels were set in relation to the pKa value. This approach has been used in the extraction of tramadol by Ghambarian et al. 2011 during which screening was done on extraction time, stirring rate, HF length and salt content only (Ghambarian et al., 2011) . Related to this approach were optimization experiments by Lezamiz and Jonsson, 2007 where only stirring rate, sample volume and fibre length were optimized using a Doehler matrix design (Lezamiz and Jönsson, 2007).

Table 23 Comparison of essential factors identified through fractional designs

Compounds (X log P3)	SLM composition	Factors selected as essential	Reference
MUS (-1.4) TRP (-1.1)	Carrier used	DP pH AP concentration SLM composition Stirring rate	Current study
TA (1.6) PSI (2.1)	Carrier used	DP pH AP concentration SLM composition Extraction time	Current study
Propylthiouracil (0.8)	Carrier used	DP pH AP concentration SLM composition Extraction time	(Ebrahimzadeh et al., 2011)
Fluoroquinolones (-1.1 - 2.9)	Carrier used	DP pH AP pH Extraction time	(Payán et al., 2011a)
Tramadol (-0.3)	No carrier	Extraction time Stirring rate HF length	(Ghambarian et al., 2011)
Dinitrophenols (1.4 – 3.6)	No carrier	Stirring rate DP volume Fibre length	(Lezamiz and Jönsson, 2007)
dextromethorphan (3.4) chloropheniramine (3.4) acidic pharmaceuticals	No carrier	DP pH AP concentration Extraction time Salt content	(Ebrahimzadeh et al., 2012)
Cannabinoids	No carrier	DP pH Extraction time Salt content DP pH Organic phase volume	(Emídio et al., 2010)

## 5.4 Central composite design results

### 5.4.1 Pairing of factors essential for muscimol

The Pareto chart and the normal plot of standardized effects in Figures 21 and 22 respectively showed that the DP pH and stirring rate had the greatest magnitude of effects effect on the EF values for the extraction of MUS. Thus DP pH and stirring rate were paired for further optimizations while AP concentration was interrelated with the less important SLM composition. The SLM composition standardized effect was lower than the critical standardized effect. Its inclusion in the vital factors was based on the researcher's discretion. DP pH and AP concentration are responsible for maintaining a high  $H^+$  gradient between the donor phase and the acceptor phase. A high proton gradient drives the carrier-aided extraction. Stirring rate is needed to enhance contact between the highly polar analyte and the carrier impregnated on the supported liquid membrane.

When compared to initial screening experiments, the following were further observed. A strong effect of AP concentration even though not as strong as DP pH and stirring rate and a change in the order of factor effects was observed. During screening experiments in which two levels of each factor were investigated, the order of effects was stirring rate followed by SLM composition then AP concentration and finally DP pH. This changed when five factor levels were investigated to DP pH, stirring rate, AP concentration and SLM composition in order of descending factor effect. This explains the need for an experimental-based pairing step before the factors can be optimized. As shown during screening designs, the DP pH had a pronounced negative effect. The pH values investigated were 3, 4, 5 and 6. The pKa value of MUS at the basic N is 4.8. Above pH 4.8, MUS exists in its neutral state. A neutral state of the analyte would result in a decrease in carrier mediated extractions.

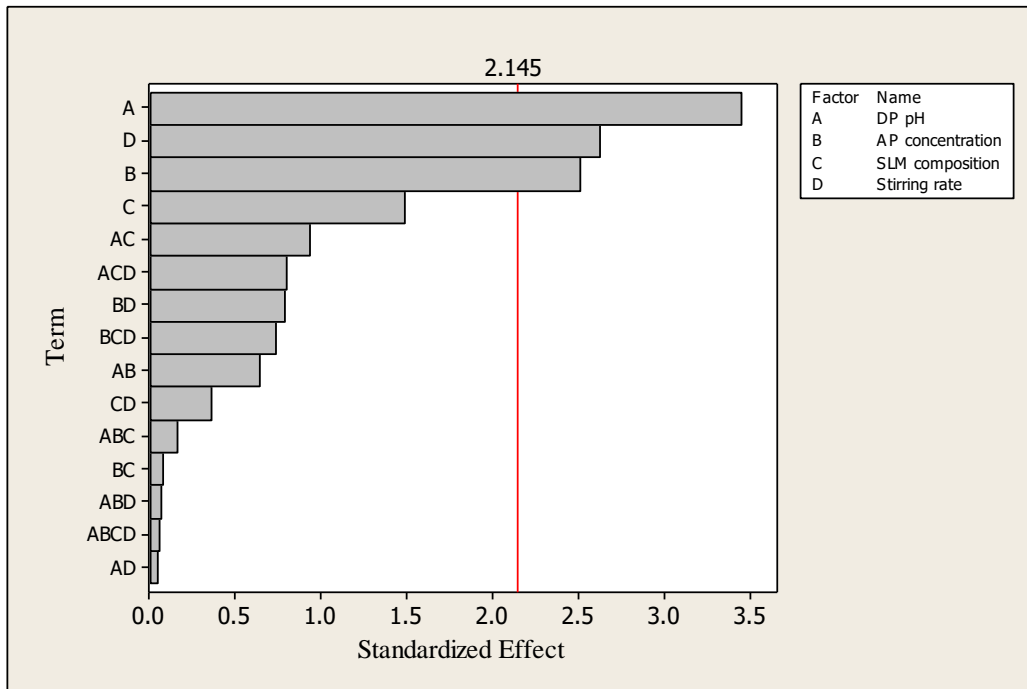


Figure 21 Pareto chart of standardized effects of the main factors of MUS (Alpha = 0.05)

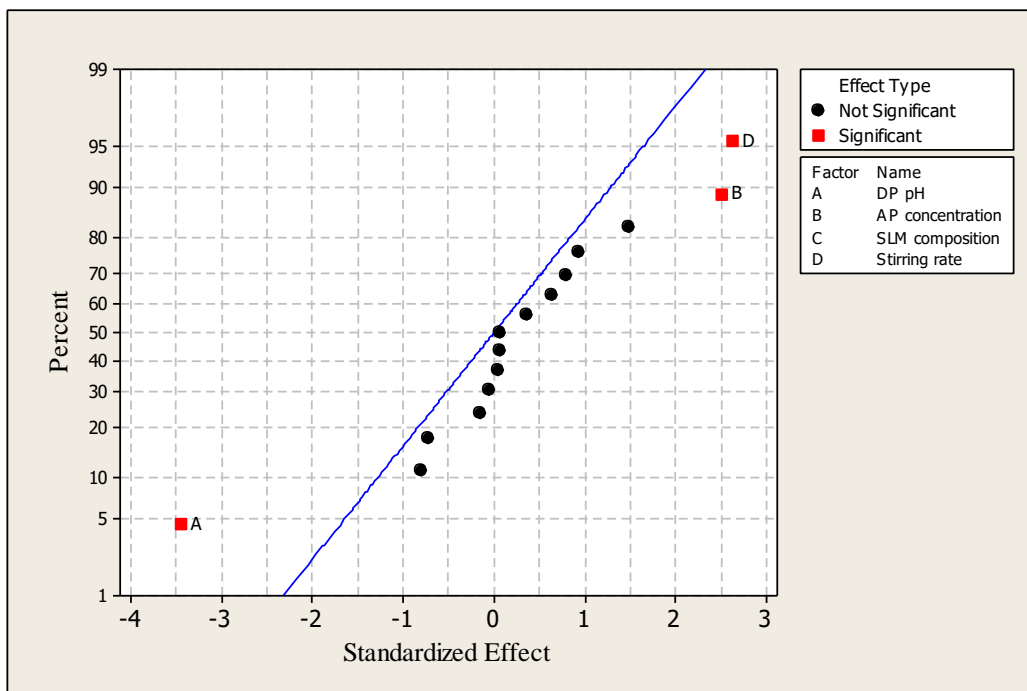


Figure 22 Normal plot of standardized effects of the main factors on MUS (Alpha = 0.05)

### 5.4.2 Pairing of factors essential for tryptamine

Based on visual analysis of the Pareto chart (Figure 23) and the normal plot (Figure 24) of standardized effects, the effects order was extraction time, AP concentration, DP pH and SLM composition. Keeping the analytes at the donor phase-SLM interface for a longer time enhances contact with the carrier molecule. Increasing the AP concentration helps maintain a higher proton gradient. These two factors were therefore observed to have standardized effects above the critical standardized value. The SLM composition had the lowest effect on the response output with several interaction effects having a greater impact than this factor. Also a change in the effect order was observed compared to screening design results.

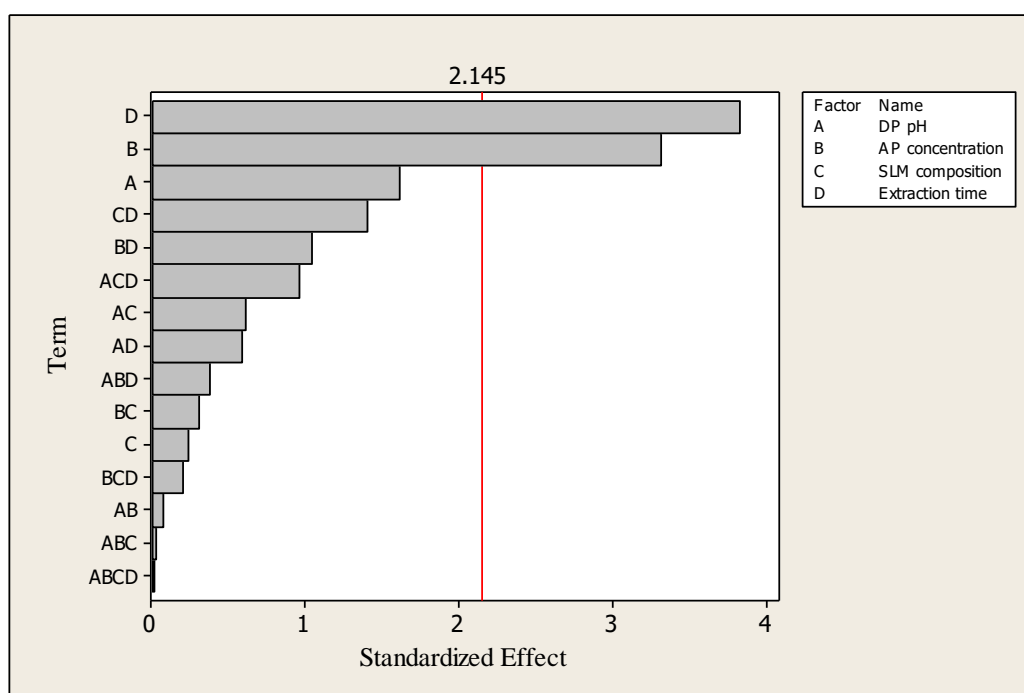


Figure 23 Pareto chart of standardized effects of TA (Alpha = 0.05)

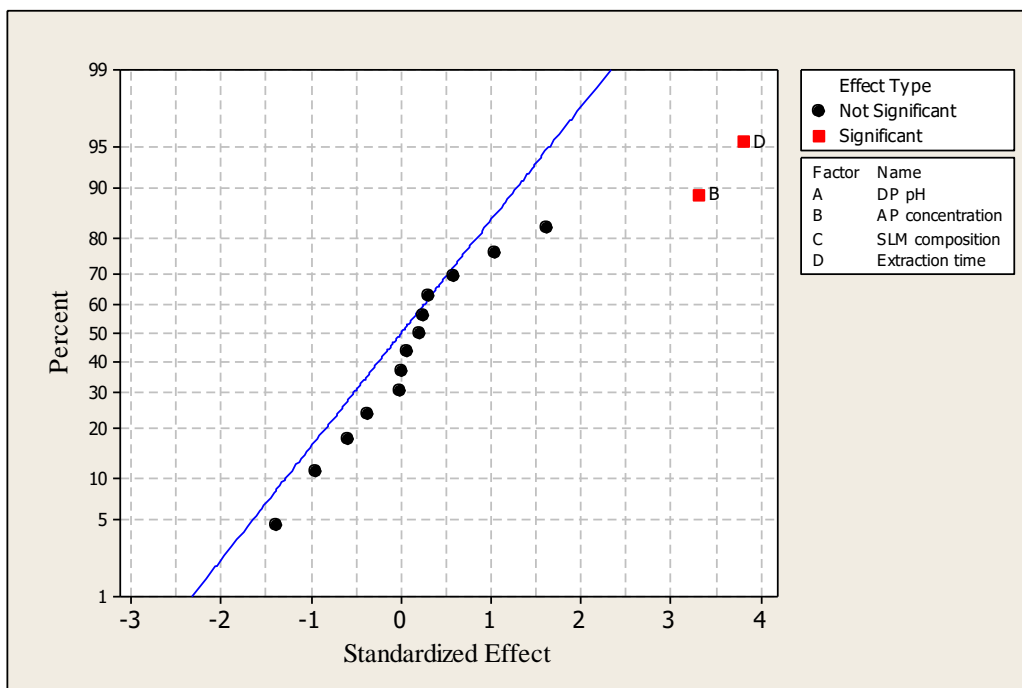


Figure 24 Normal plot of standardized effects of main factors on TA (Alpha = 0.05).

### 5.4.3 Paired factor optimization for muscimol

Unless specified, the conditions were DP pH 5, 100 mM HCl concentration, 15% (w/w) DEHPA in DHE and stirring at 800 rpm for 60 mins with no salt added.

#### *Donor phase pH and stirring rate optimization results for muscimol*

Figures 25 and 26 show a contour plot and a surface plot of effects versus a pairing of DP pH and stirring rate. A slightly negative rising ridge pattern was observed for both the contour plot and the normal plot. The darkening of the contour colours represented an increase in response while the brightening surface plot was used to represent increase. The rising ridge pattern implied that increase in response was achieved by increasing stirring rate while slightly reducing the DP pH. For a constant optimal stirring rate of 800 rpm, setting a pH value below 4 or towards 5 and above reduced the output response. This could be explained by the pKa value of MUS. Cationic MUS can only exist at pH 4.8 and below. Increasing stirring rate at pH values less than 4 resulted in a marked increase in the response compared to pH values above 5. Below pH 4 there were more cationic MUS. While the H<sup>+</sup> ion gradient between donor phase and acceptor phase

is minimal, increasing stirring rate increased the contact of the MUS cations and the carrier ions at the donor phase-SLM interface.

The optimum interrelated factor values were then estimated at the point of curvature and identified as DP pH 4 and stirring rate of 900 rpm. These were summarized as an optimization plot of factors as shown in Fig 27. Under these conditions the response, y which represented the EF value for the extraction of MUS from the spiked water into a 100 mM HCl acceptor phase was 11. The desirability of the two optimized factors in maximizing the response was an acceptable 0.797. Unlike the DP pH which maximized at pH 4, the stirring rate optimization rate showed that better responses could have been found if stirring had been done at higher rates. However the stirring rate was set by the researchers at 900 rpm. To confirm the predicted EF value, experimentation was done at DP pH 4 and 900 rpm stirring rate.

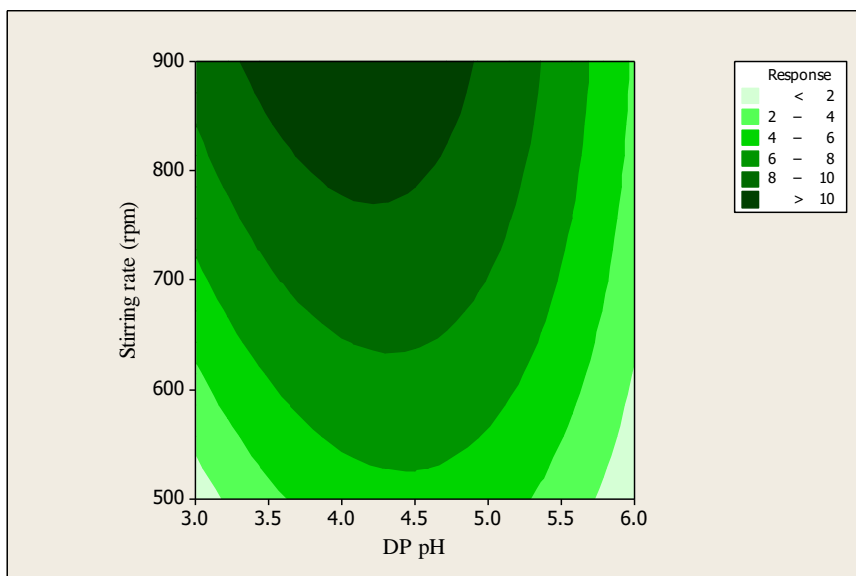


Figure 25 Contour plot of EF values of MUS versus the interrelated effect of stirring rate and DP pH

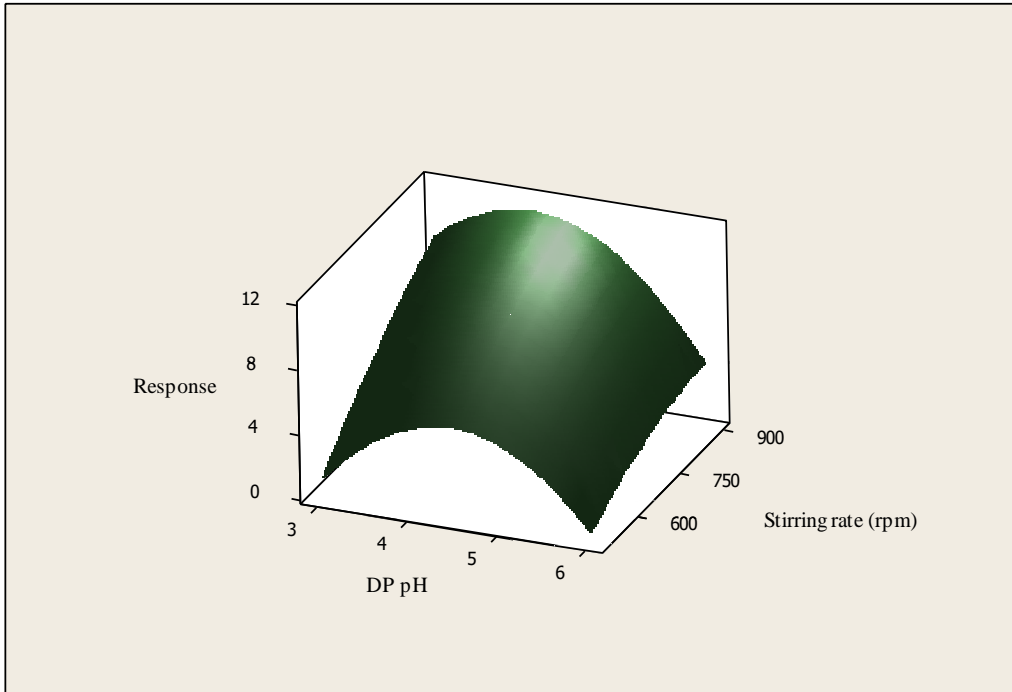


Figure 26 Surface plot of EF values of MUS versus the interrelated effect of stirring rate and DP pH

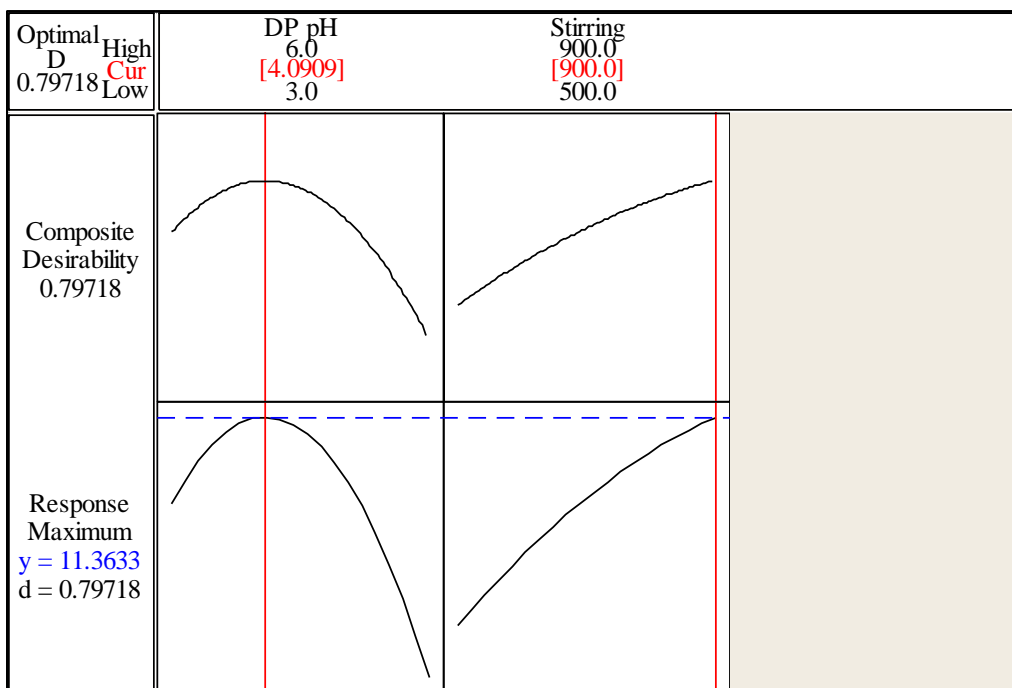


Figure 27 Optimization plot of effects of stirring rate and DP pH on enrichment of MUS



***Acceptor phase concentration and supported liquid membrane composition optimization results for muscimol***

The contour plot (Figure 28) and the normal plot (Figure 29) also showed a rising ridge pattern in the response output when the AP concentration and SLM composition were interrelated. The two factors had an almost linear correlation on the response output. The availability of the carrier molecule at a higher  $H^+$  ion gradient continuously increased the extraction of MUS from the donor phase into the acceptor phase. The AP concentration plateaued from 80 mM while the SLM composition minimal plateau value was 15% (w/w) DEHPA in DHE. The AP concentration upper limit was set at 100 mM HCl as an HPLC system protective approach.

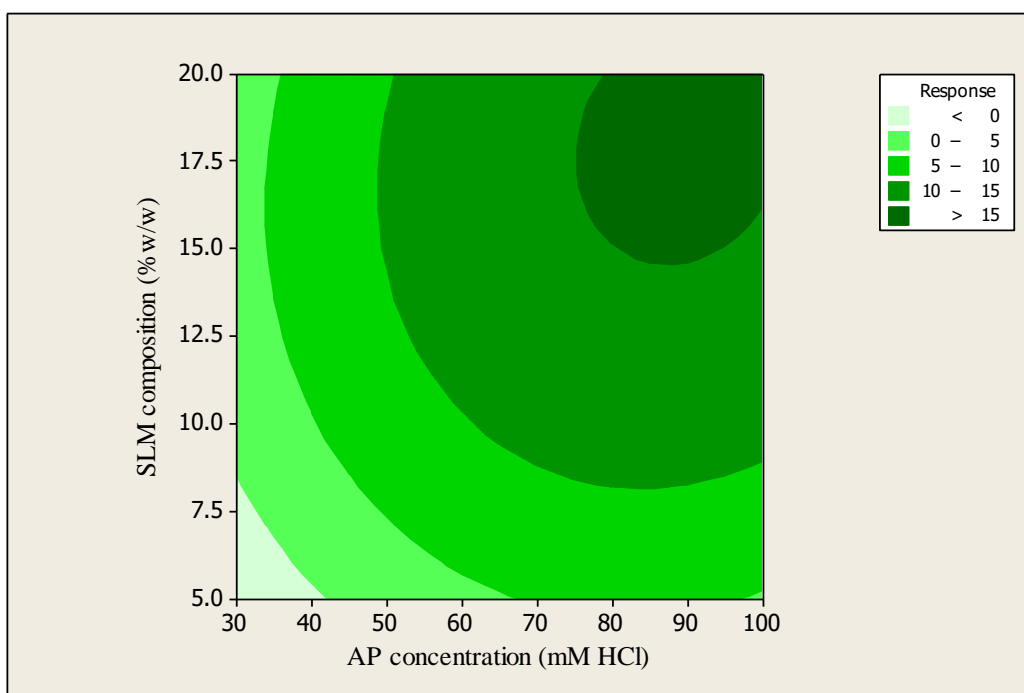


Figure 28 Contour plot of EF values of MUS versus the interrelated effect of SLM composition and AP concentration

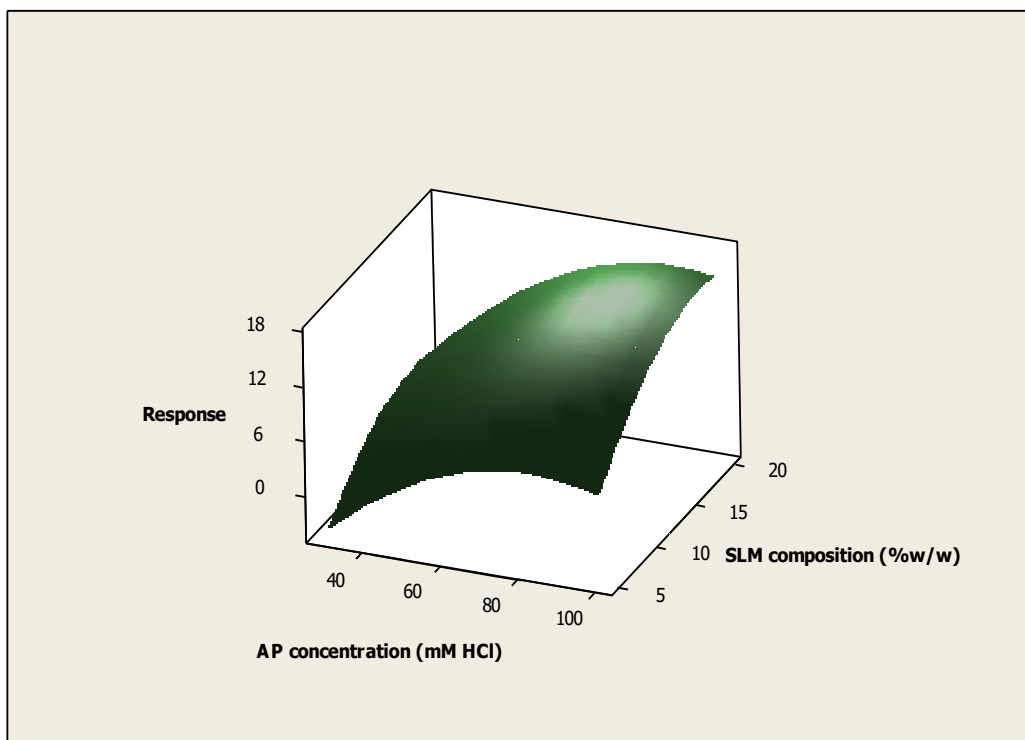


Figure 29 Surface plot of EF values of MUS versus the interrelated effect of SLM composition and AP concentration

The point of curvature values was identified from the optimization plot in Figure 30. The optimal AP concentration value was 89 mM HCl while SLM composition curved at 18% (w/w) DEHPA in DHE with a predicted EF value of 16. An individual desirability value of 0.918 was high enough to accept the optimized factor values. For experimental purposes, the AP concentration and SLM composition were set at 100 mM HCl and 20% (w/w) respectively.

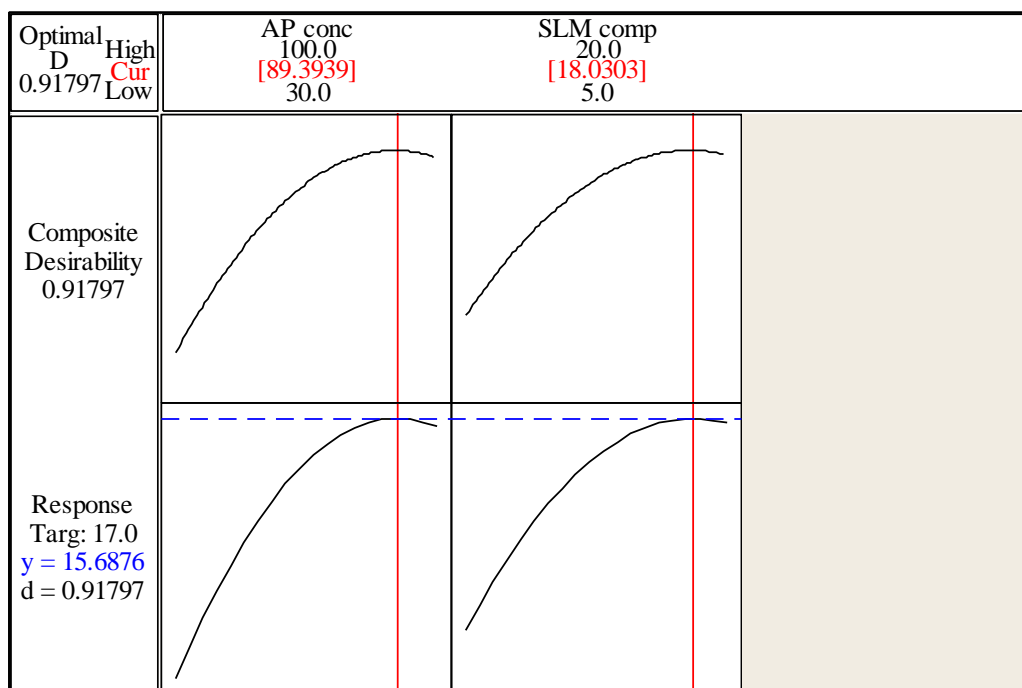


Figure 30 Optimization plot of effects of SLM composition and AP concentration on enrichment of MUS

#### 5.4.4 Paired factor optimization for tryptophan

TRP has polarity similar to MUS and the paired factors identified for MUS were used and optimized for the extraction of TRP. Unless specified, the conditions were DP pH 5, 100 mM HCl concentration, 15% (w/w) DEHPA in DHE and stirring at 800 rpm for 60 mins with no salt added.

##### *Donor phase pH and stirring rate optimization results for tryptophan*

The contour plot and the surface plot of the response due to the combined effect of stirring rate and DP pH showed a co-related response that is affected more by a change in DP pH. Increasing the DP pH at any constant stirring rate greatly affected the response as shown by the size of the contours across the pH value range in Figure 31 and the surface response in Figure 32. Increasing the stirring rate seemed less effective when a DP pH level was kept constant. For example, the response remained in the 28 – 32 region when stirring rate was increased from 600 to 900 rpm while DP pH was kept at 4. The response was greater than 36 for DP pH value of above 5 and stirring rate of 700 rpm. Also the graphs showed that when DP pH is increased above 5, a similar response can be obtained at lower

stirring rates. For example, at DP pH 7, the response remained higher than 36 with 600 rpm of stirring.

The optimum factor values were DP pH 7 and a stirring rate of 770 rpm as shown in the optimization plot in Figure 33. The stirring rate was identified as the point of curvature while the DP pH was limited by the set upper limit value. This value was set at pH 7 because of the acidic nature of the carrier molecule. During preliminary studies it was discovered that pH values in the basic region resulted in reduced response. The desirability value for the interrelated effect of DP pH and stirring rate was 0.746. The predicted EF value was 40. This value was tested experimentally by setting DP pH and stirring rate at 7 and 800 rpm respectively.

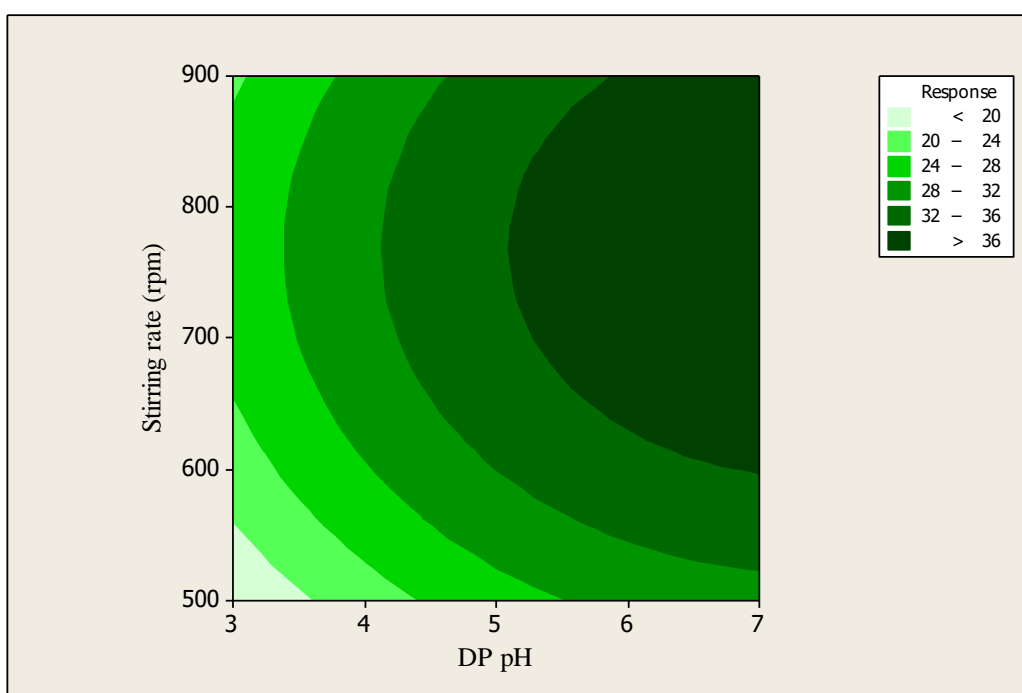


Figure 31 Contour plot of EF values of TRP versus the interrelated effect of stirring rate and DP pH

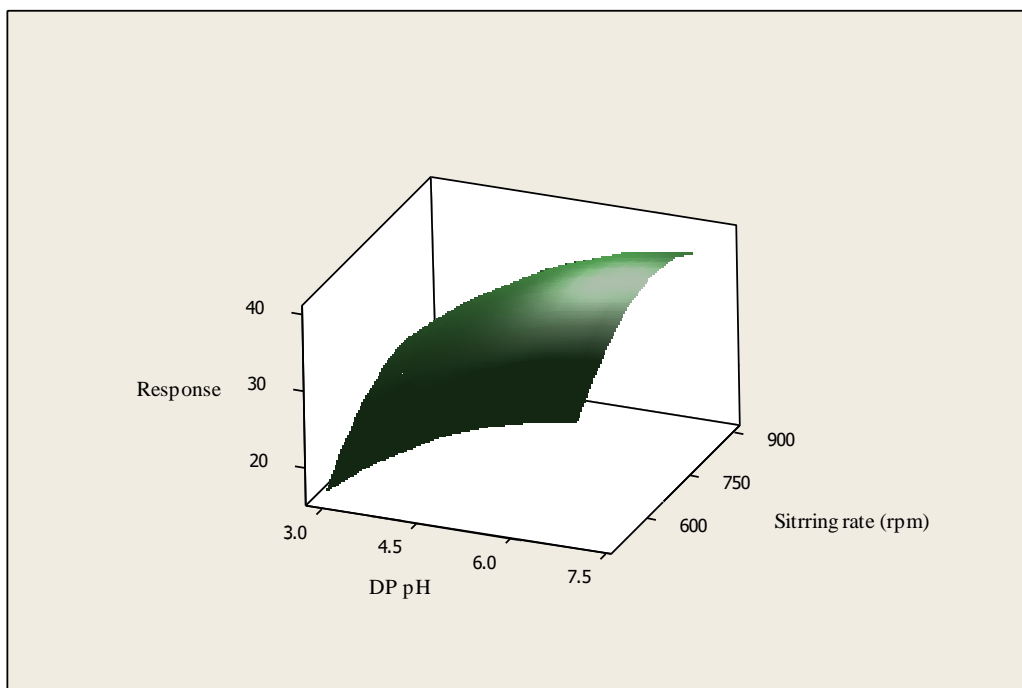


Figure 32 Surface plot of EF values of TRP versus the interrelated effect of stirring rate and DP pH

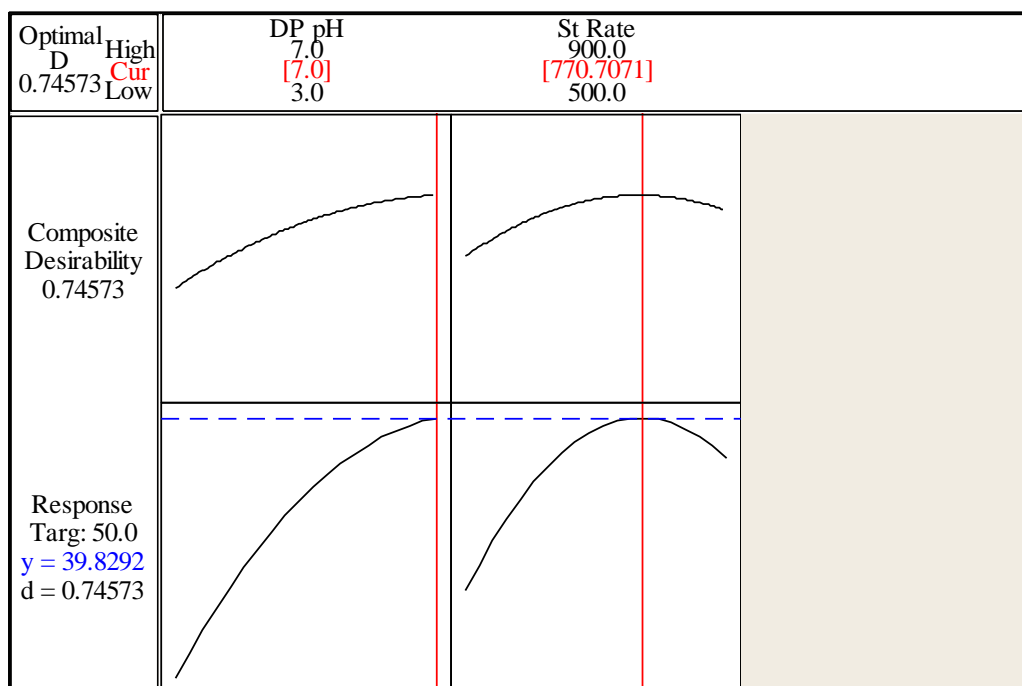


Figure 33 Contour plot of effects of stirring rate and DP pH on enrichment of TRP

***Acceptor phase concentration and supported liquid membrane composition optimization results for TRP***

Figure 34 shows a static ridge pattern in the 15 – 20% (w/w) SLM carrier composition range. Increasing the AP concentration in this region was more effective compared to SLM composition levels outside this ridge range. A change in the SLM composition in this region had minimal effect on the response output. While increasing SLM composition increases the amount of carrier available for extraction, it appeared that the AP concentration was more important in the vicinity of the optimum SLM composition. Figure 35 visualizes this observation as a surface plot.

The interrelated optimum conditions are summarised as an optimization plot in Figure 36. SLM composition polynomial showed curvature at 20% (w/w) DEHPA in DHE. For AP concentration, the set upper level value was identified as the optimum value. The optimum value could have been higher if a higher AP concentration was used. The desirability of the optimized values of the AP concentration-SLM composition paired effect was 0.776 with an expected enrichment response of 41. For experimentally, the AP concentration and SLM composition were set at 100 mM HCl and 20% (w/w) DEHPA in DHE respectively.

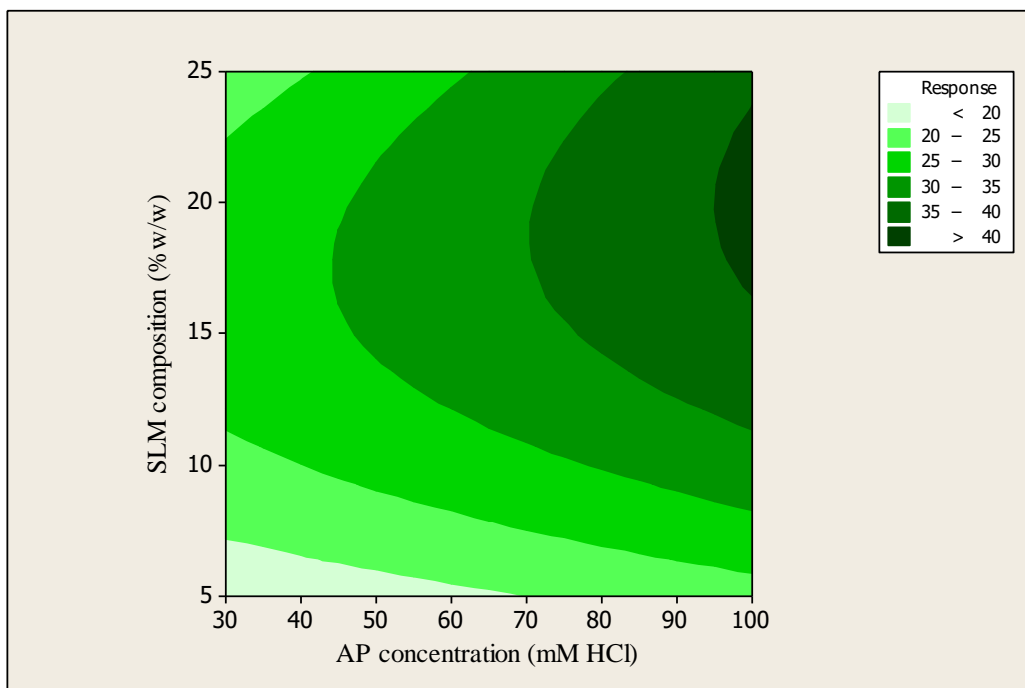


Figure 34 Contour plot of EF values of TRP versus the interrelated effect of SLM composition and AP concentration

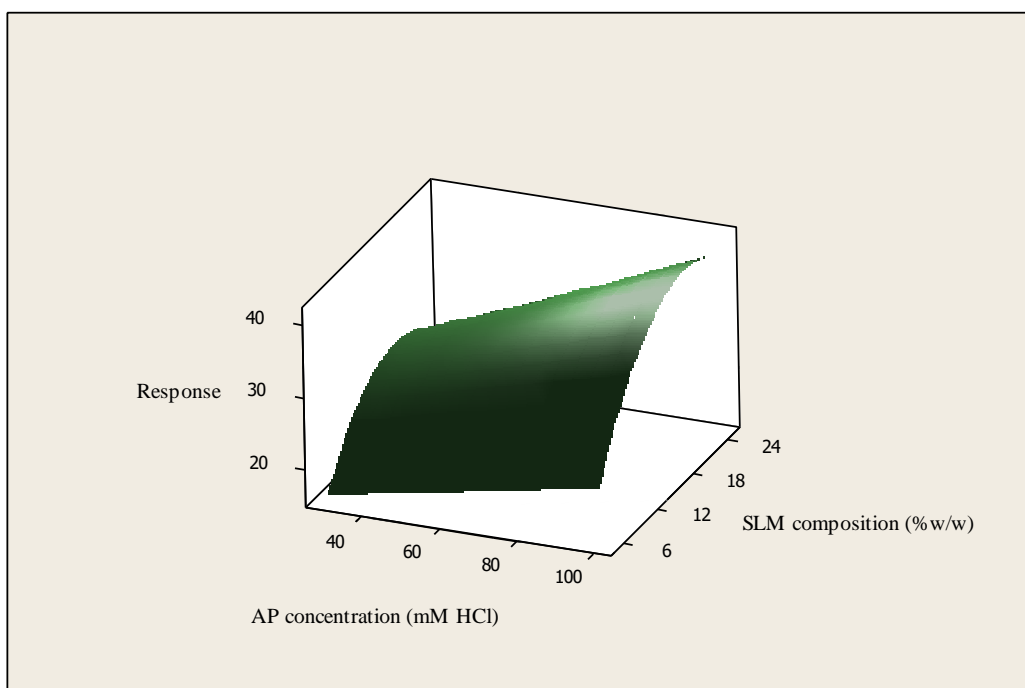


Figure 35 Surface plot of EF values of TRP versus the interrelated effect of SLM composition and AP concentration

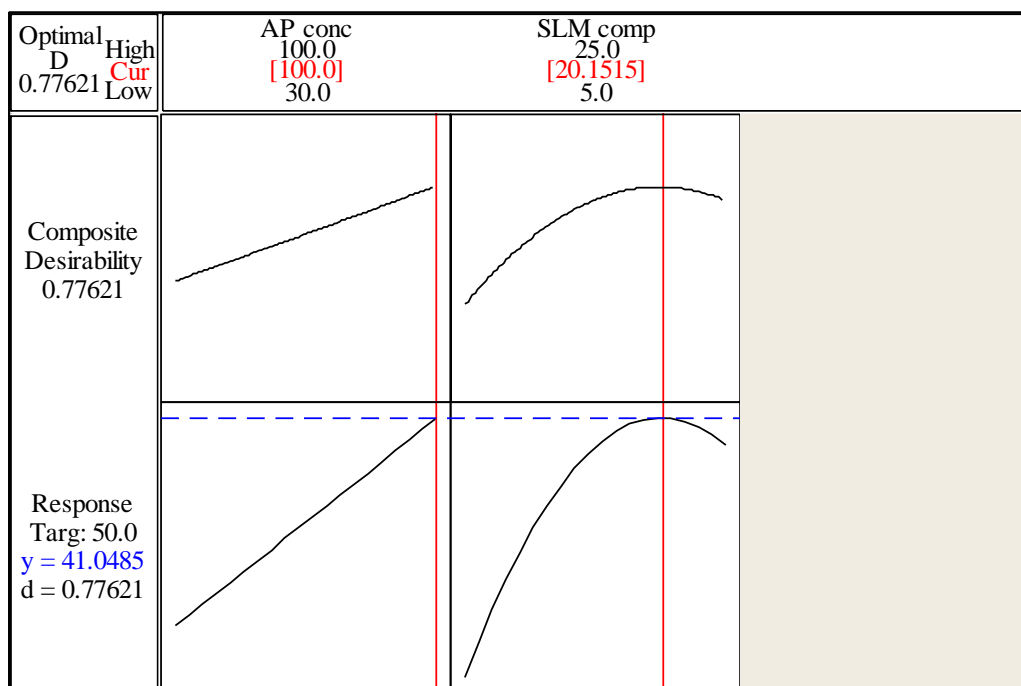


Figure 36 Contour plot of effects of SLM composition and AP concentration on enrichment of TRP

#### 5.4.5 Paired factor optimization for TA

Unless specified, the conditions were DP pH 5 with 0.001% (w/v) NaCl, 200 mM HCl AP, 15% (w/w) DEHPA in DHE at 800 rpm for 60 mins.

##### *Donor phase pH and acceptor phase concentration for tryptamine*

The contour plot and the surface plot of response versus the combined effect of DP pH and AP concentration were given in Figure 37 and Figure 38 respectively. A slightly rising ridge surface response pattern was observed at around DP pH 6. TA is completely cationic below pH 6.9. The response was affected less by a change in AP concentration compared to DP pH levels on either side of the slope of the ridge. In the vicinity of the ridge above pH 5, a further increase in the pH level had less impact on the response output. The interrelationship between AP concentration and DP pH seemed to be dependent on maintaining a high H<sup>+</sup> ion gradient. The ridge pattern showed that high responses were obtained at near neutral DP pH levels and higher AP concentration.



The optimum values were a DP pH of 6 and AP concentration of 200 mM HCl. Figure 39 below showed that the desirability of these two optimum values was 0.993 with an estimated enrichment of 298. As observed with other pairs that involved AP concentration, the optimum value for the AP concentration was limited by the set upper limit value. The DP pH value was obtained at the point of curvature of the quadratic polynomial. Adopted for extraction of TA was DP pH 6 and 200 mM HCl as the AP.

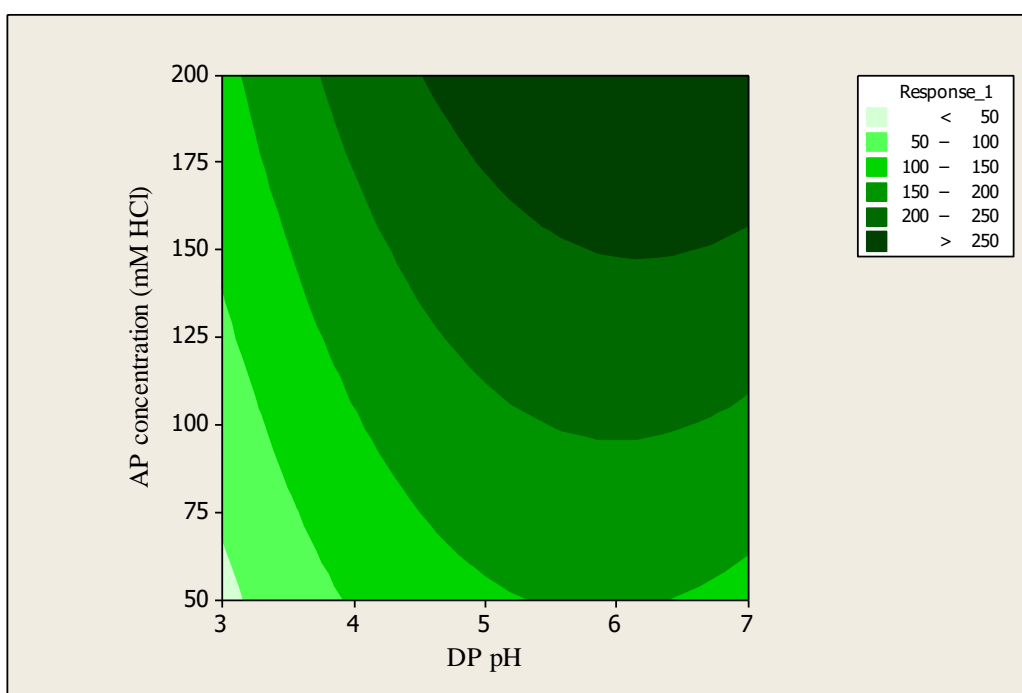


Figure 37 Contour plot of EF values of TA versus the interrelated effect of AP concentration and DP pH

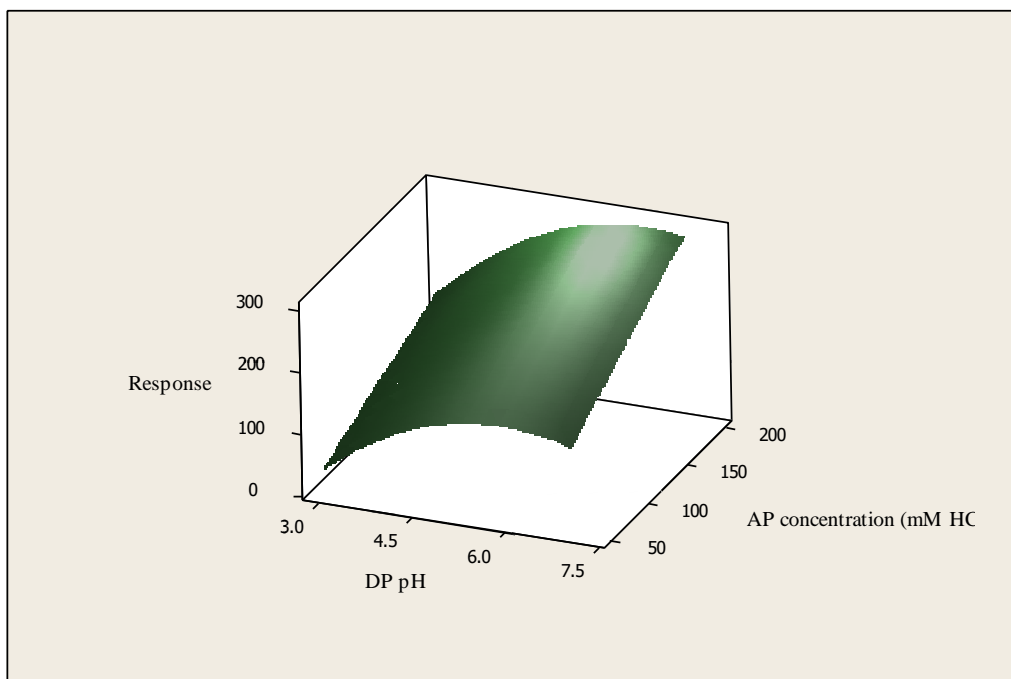


Figure 38 Surface plot of EF values of TA versus the interrelated effect of AP concentration and DP pH

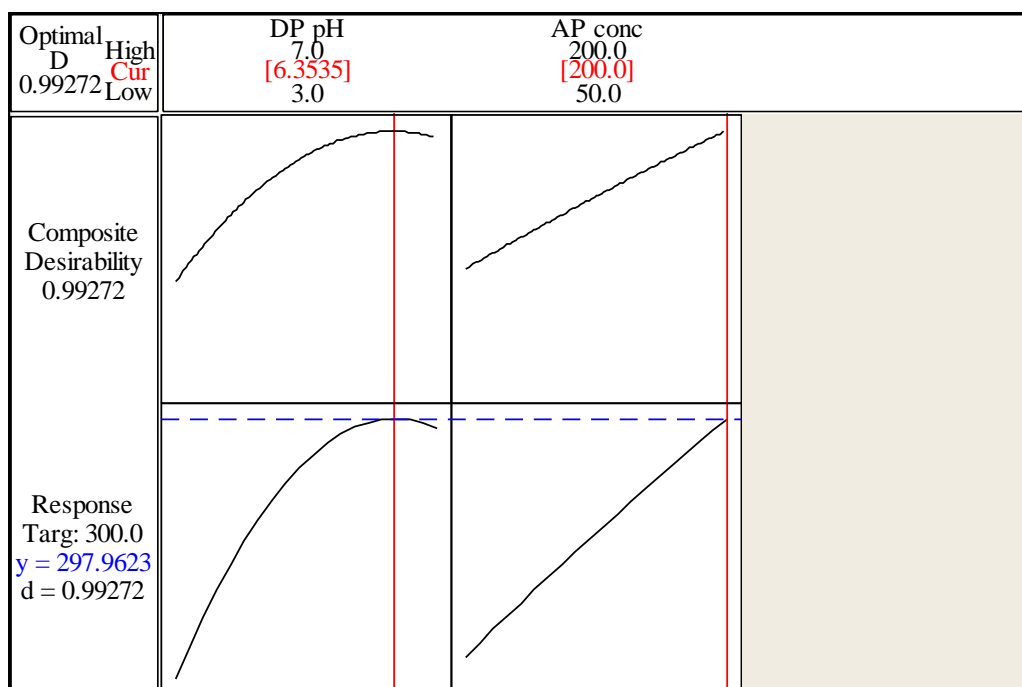


Figure 39 Optimization plot of effects of AP concentration and DP pH on enrichment of TA

### *Extraction time and supported liquid membrane composition for tryptamine*

A clearly defined maximum region of optimum response due to stirring rate-SLM composition interaction was observed as seen in Figures 40 and 41. This area was in the 55 – 75 mins extraction time and about 15% (w/w) DEHPA in DHE. On either side of the maximum spot, the response due to simultaneously changing the paired factor values was reducing. It was observed that at any SLM composition level, increasing extraction time was less important while the opposite was true for increasing SLM composition. This observation meant that the amount of carrier molecules in the supported liquid membrane in the pores of the hollow fibre was more important than the analyte-carrier contact time at the DP-SLM interface.

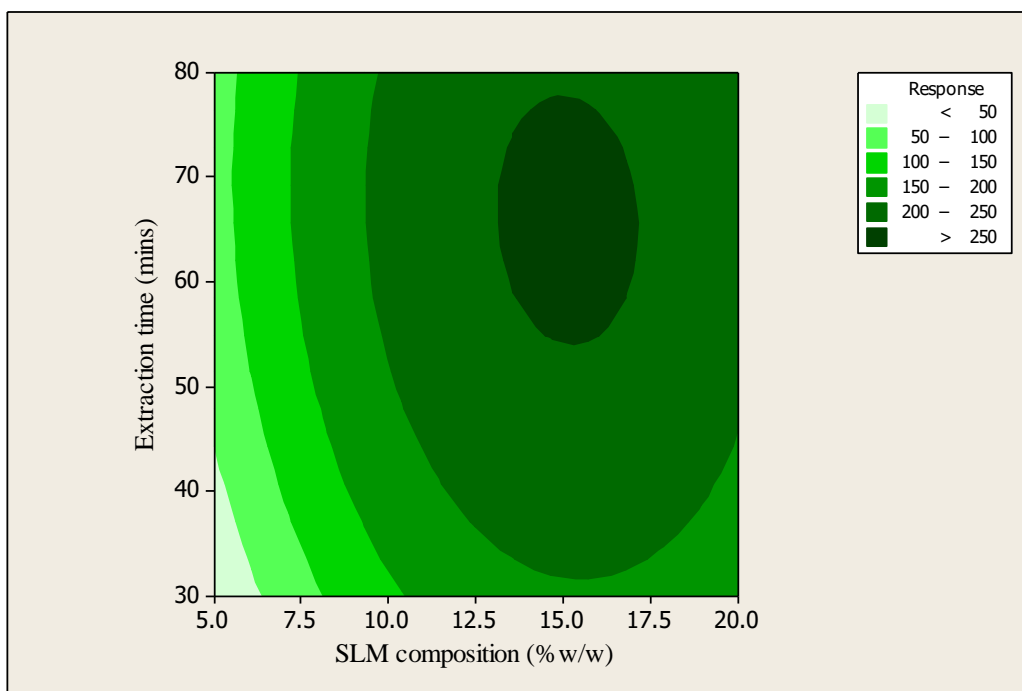


Figure 40 Contour plot of EF values of TA versus the interrelated effect of extraction time and SLM composition

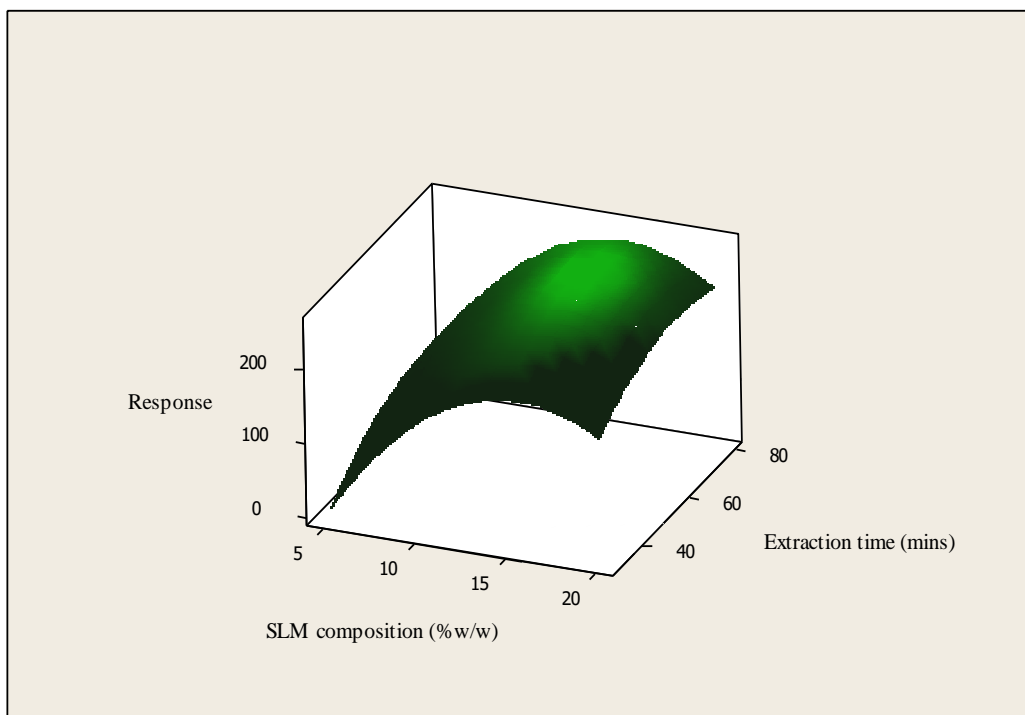


Figure 41 Surface plot of EF values of TA versus the interrelated effect of extraction time and SLM composition

Using a quadratic polynomial, the optimum factor values were 15% (w/w) DEHPA in DHE for SLM composition and 66 mins for extraction time. The polynomials for both factors had a point of curvature as shown in Fig 42 from which the optimum factor values were estimated. The dual desirability was 0.979 implying that an EF value of 257 achieved under these conditions was favourable for the enrichment of TRP.

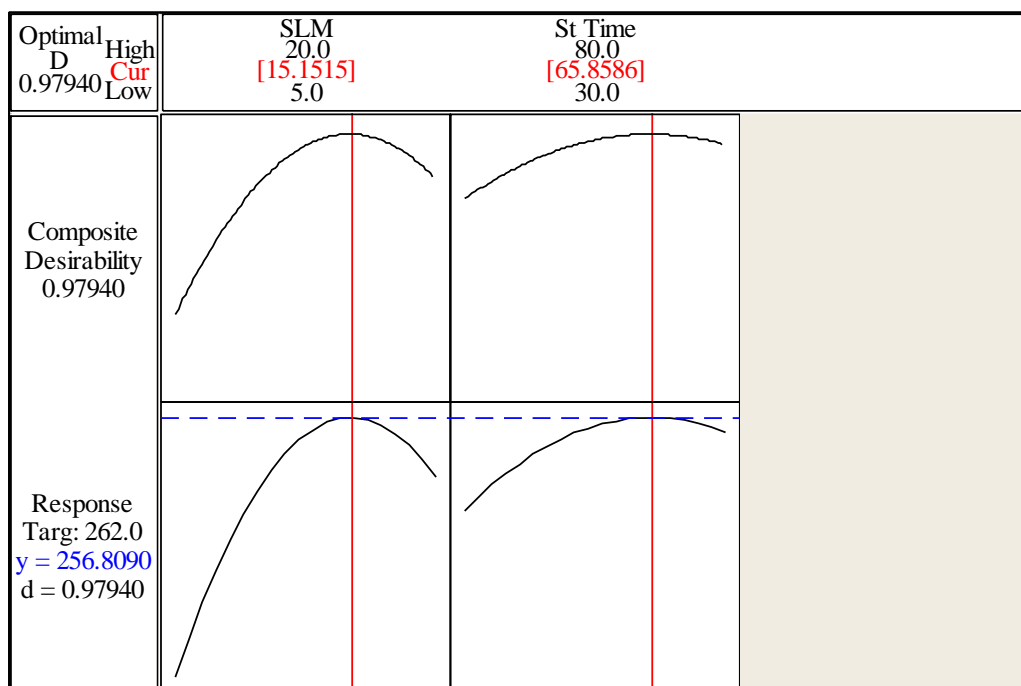


Figure 42 Optimization plot of effects of extraction time and SLM composition on enrichment of TA

#### 5.4.6 Paired factor optimization for psilocin

PSI has polarity similar to TA and the paired factors identified for TA were used and optimized for the extraction of TRP. Unless specified, the conditions were DP pH 5 with 0.001% (w/v) NaCl, 200 mM HCl AP, 15% (w/w) DEHPA in DHE at 800 rpm for 60 mins.

##### *Extraction time and supported liquid membrane composition for psilocin*

Figure 43 and Figure 44 show an apex region in the vicinity of 70 mins and 20% (w/w) DEHPA in DHE. The slope of its sides was non-static with a better enhancing response observed when the SLM composition was changed. This observation could have meant that the amount of DEHPA embedded on the SLM was more important than the extraction time. Increasing extraction time at any SLM composition level had very little impact on the response output.

The reduced slope of the contours in the vicinity of the optimum extraction time meant that around the optimum factor levels, the change in the response is minimal regardless of whether you are changing the SLM composition or the AP

concentration. These results meant that maintaining the amount of the carrier at optimal levels was more important than the time the carrier was in contact with the analyte. The optimization plot in Figure 45 showed optimum values of 20% (w/w) DEHPA in DHE and extracting the analyte for 67 mins. At this stage PSI got finished and no further optimization could be done. The dual desirability was 0.883 producing a predicted EF value of 311. Experimentally, SLM composition was set at 20% (w/w) DEHPA in DHE and extraction for 60 mins.

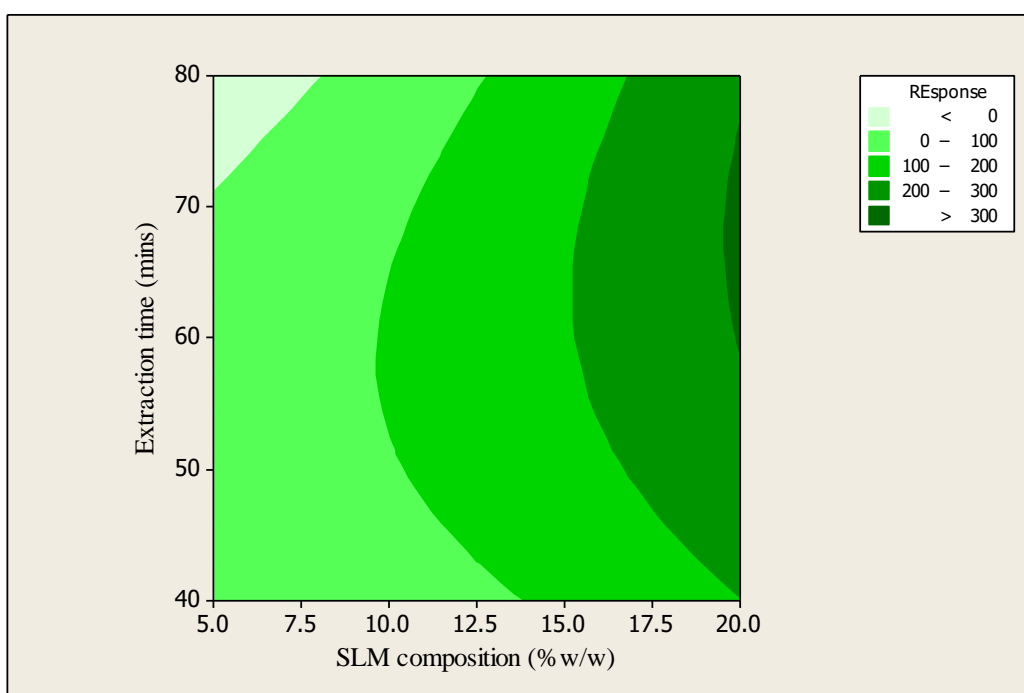


Figure 43 Contour plot of EF values of PSI versus the interrelated effect of extraction time and SLM composition

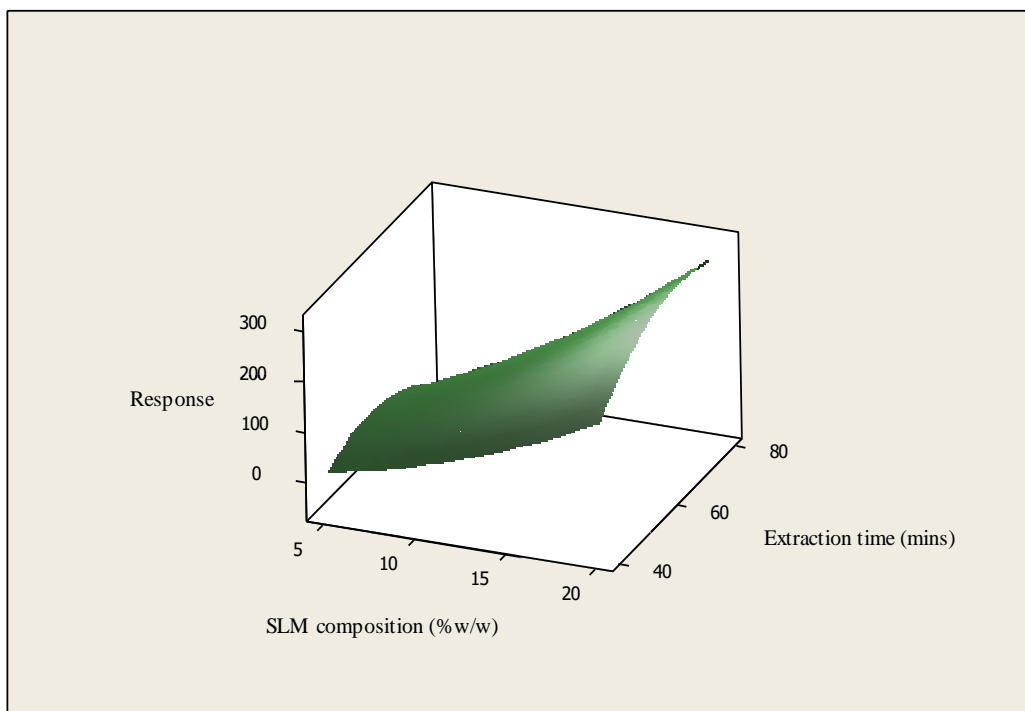


Figure 44 Surface plot of EF values of PSI versus the interrelated effect of extraction time and SLM composition

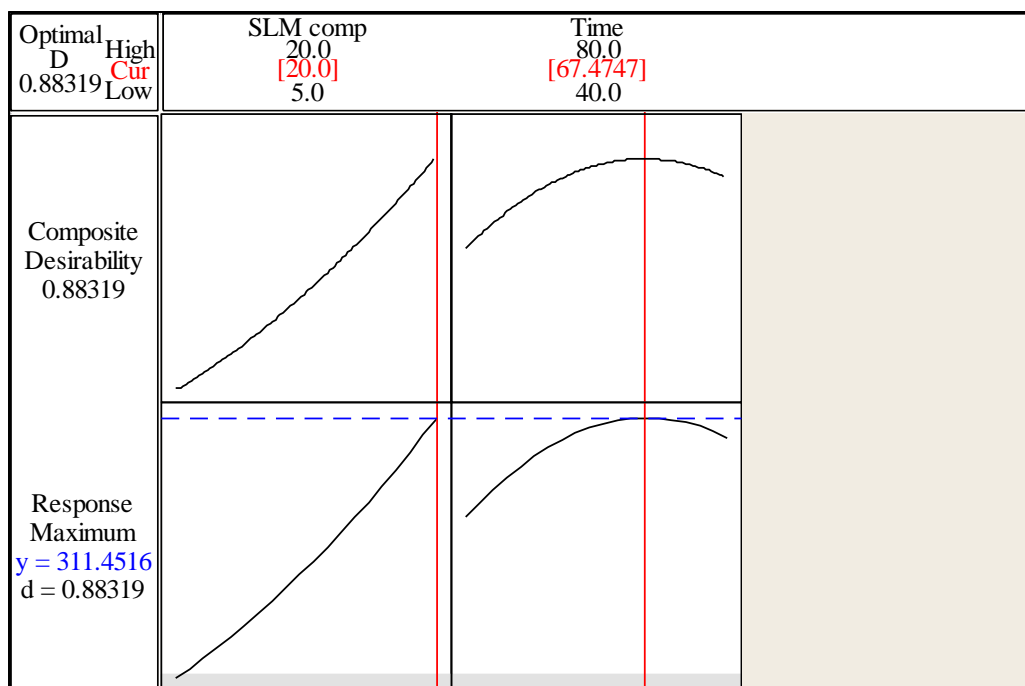


Figure 45 Optimization plot of effects of extraction time and SLM composition on enrichment of PSI

#### **5.4.7 Quadratic response surface models for paired factor optimizations**

All the prediction quadratic response surface models used to estimate optimum values in plots for each paired factor investigations are shown in Table 24. The models were estimated by quantifying equation 13. The regression coefficients for each response model were estimated using uncoded output data in Minitab.

#### **5.4.8 Comparison of optimized factor levels in different articles**

While the optimum values for DP pH and AP concentration are dependent on the physicochemical properties of the analytes under study, the SLM carrier composition, stirring rate and extraction time values are expected to be universal for a HF-LPME approach. A similar optimum value of 20% (w/w) DEHPA in DHE has been reported in other studies (Dziarkowska et al., 2008; Poliwoda et al., 2010). Romero et al. (2002) found a desirable optimum of 16.5% (w/w) DEHPA in DHE for extraction of eight analytes with individual optimum values ranging from 13% (w/w) DEHPA in DHE to 22% (w/w) DEHPA in DHE (Romero et al., 2002). Yamini et al. (2006) optimized the Aliquot 336 content in n-octanol at 20% (w/w) (Yamini et al., 2006). Table 25 shows factor values that are closely related to optimum values from this study. However some extreme factor values like 1600 rpm for 30 mins (Saaid et al., 2009), 2200 rpm for 2 h (Van Pinxteren et al., 2012), 300 rpm for 6 h (Payán et al., 2011b) and 900 rpm for 4 h (Hyder and Jönsson, 2012) have been reported.



Table 24 Summary of quadratic response surface models for two factor interactions using uncoded data.

	Paired factors	Predictive quadratic response models for paired factor optimizations during individual analyte extractions
	DP pH and stirring rate	$y = -65.565 + 21.200(DPpH) + 0.0585(Rate) - 2.129(DPpH)^2 - 1.732 \times 10^{-5}(Rate)^2 - 0.00375(DPpH)(Rate)$
MUS	AP concentration and SLM composition	$y = -25.875 + 0.564(APconc) + 1.821(SLMcompo) - 0.00354(APconc)^2 - 0.0599(SLMcompo)^2 + 0.00377(APconc)(SLMcompo)$
	DP pH and extraction rate	$y = -76.334 + 10.764(DPpH) + 0.1984(Rate) - 0.732(DPpH)^2 - 0.0001(Rate)^2 + 0.0001(DPpH)(Rate)$
TRP	AP concentration and SLM composition	$y = 3.177 + 0.0496(APconc) + 2.472(SLMcompo) + 8.022 \times 10^{-5}(APconc)^2 - 0.0796(SLMcompo)^2 + 0.00726(APconc)(SLMcompo)$
	DP pH and AP concentration	$y = -363.140 + 163.371(DPpH) + 0.524(APconc) - 14.360(DPpH)^2 - 5.840(APconc)^2 + 0.0955(DPpH)(APconc)$
TA	SLM composition and extraction time	$y = -387.551 + 54.556(SLMcompo) + 7.038(Time) - 1.716(SLMcompo)^2 - 0.0487(Time)^2 - 0.0409(SLMcompo)(Time)$
PSI	SLM composition and extraction time	$y = -360.116 - 8.528(SLMcompo) + 14.729(Time) + 0.411(SLMcompo)^2 - 0.148(Time)^2 + 0.265(SLMcompo)(Time)$

Table 25 Summary of optimum levels for non-analyte related factors

Stirring rate (rpm)	Extraction time (mins)	Reference
800	60	(Current study)
800	60	(Yang et al., 2010)
1000	80	(Hadjmohammadi and Ghambari, 2012)
600	60	(Han and Row, 2010)
660	90	(Lezamiz et al., 2008)
750	50	(Miraee et al., 2014)
900	60	(Xiao-Wang et al., 2012)
600	50	(Yamini et al., 2006)

### **5.5 Comparison of predicted EF values with experimental values for individual extractions under specific optimum values**

When each analyte was extracted individually, the experimental EF values were above the predicted EF range as shown in Table 26 except for MUS. The range for MUS was obtained in the absence of salt. The expected EF values were given as a range because each pair of factors gave its own response. The peak areas obtained through experimentation are shown in Table A5.

Table 26 Experimental versus Minitab 16-predicted EF values under optimum conditions for extracting TA, MUS and TRP individually.

	TA	MUS	TRP	PSI
SLM composition (% w/w)	15	20	20	20
DP pH	6	4	7	5
AP concentration (mM HCl)	200	100	100	200
Extraction time (mins)	60	60	60	60
Stirring Rate (rpm)	800	900	800	800
NaCl composition (% w/v)	0.001	0.001	0.001	0.001
Expected EF	257 - 298	11 - 16	40 - 41	311
Experimental EF values	316	11	45	-
%RSD	4.24	10.01	1.75	-

## 5.6 Comparison of predicted EF values versus experimental values for simultaneous extractions under conditions optimized for muscimol

### 5.6.1 Changes in predicted EF values and individual desirabilities

Figures 46 - 50 show the changes in individual desirabilities and predicted EF values when the optimized conditions for MUS were set for a simultaneous extraction of all the analytes. Only the stirring rate was changed to 800 rpm. A general decrease in EF values and individual desirabilities was observed. Most affected was extraction of TA especially the desirability of setting DP pH and AP concentration to 4 and 100 mM HCl respectively. A desirability of 0.448 was considered unsuitable but was accepted in this case because the developed method targeted maximizing the primary analyte, MUS. An individual desirability of 0.448 for TA still predicted an EF value of 145.

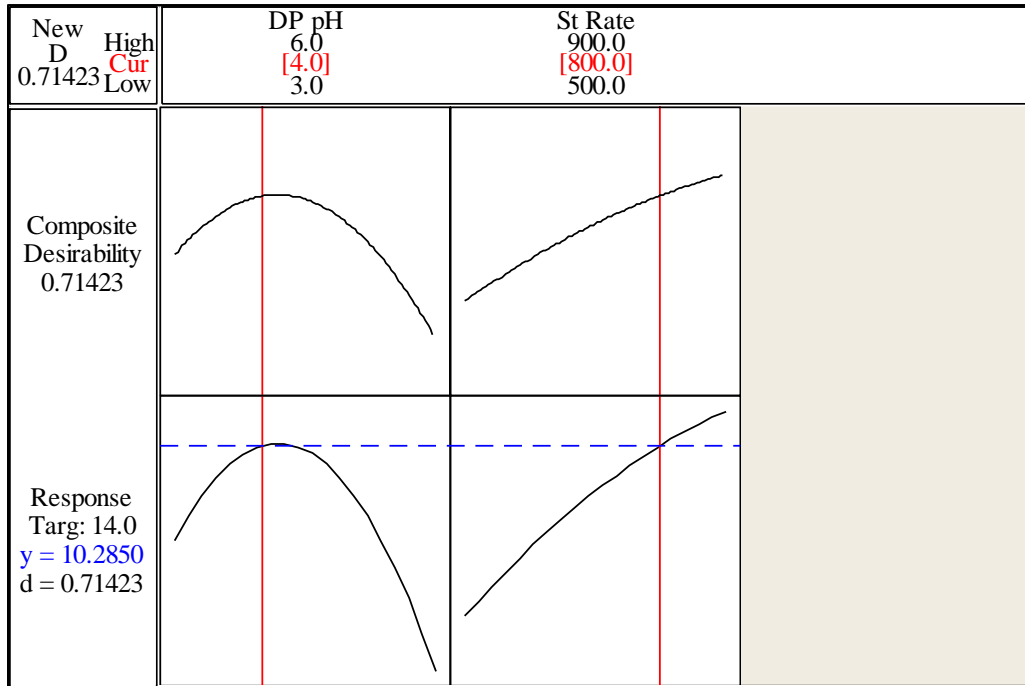


Figure 46 Effects of setting the stirring rate to 800 rpm on the desirability and response output for MUS

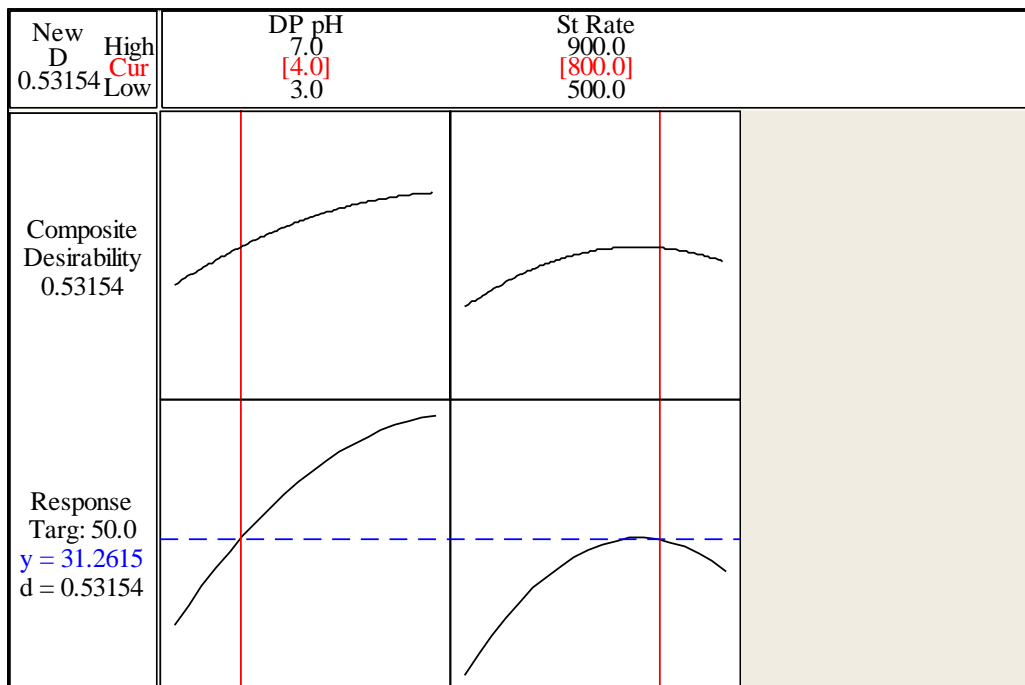


Figure 47 Effects of setting MUS-based levels of DP pH and stirring rate on the dual desirability and response output for TRP

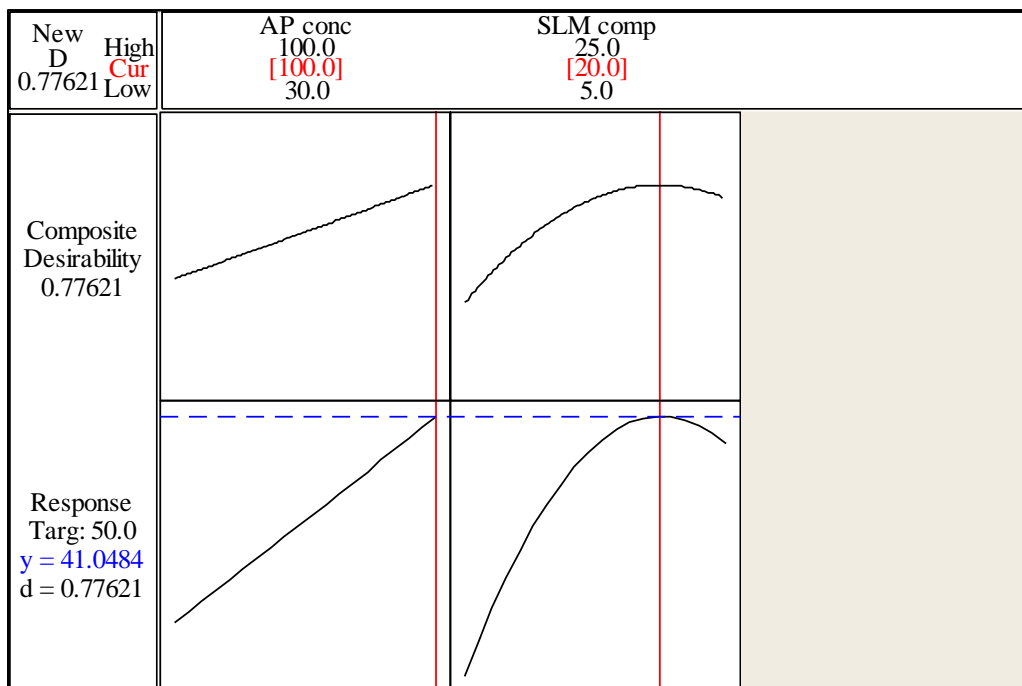


Figure 48 Effects of setting MUS-based levels of AP concentration and SLM composition on the dual desirability and response output for TRP

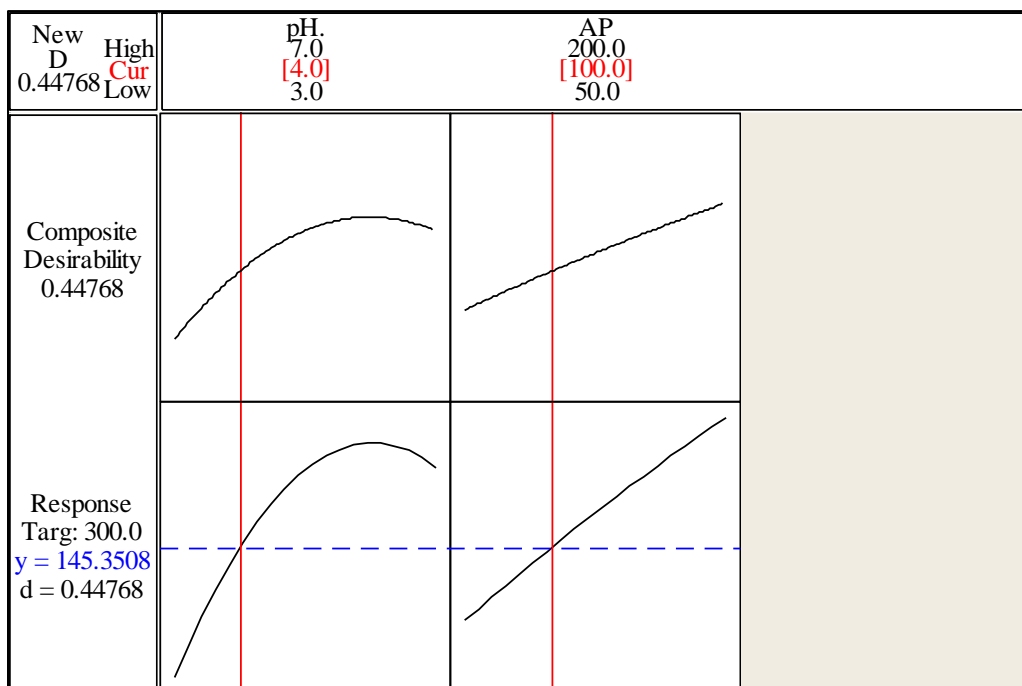


Figure 49 Effects of setting MUS-based levels of DP pH and AP concentration on the dual desirability and response output for TA

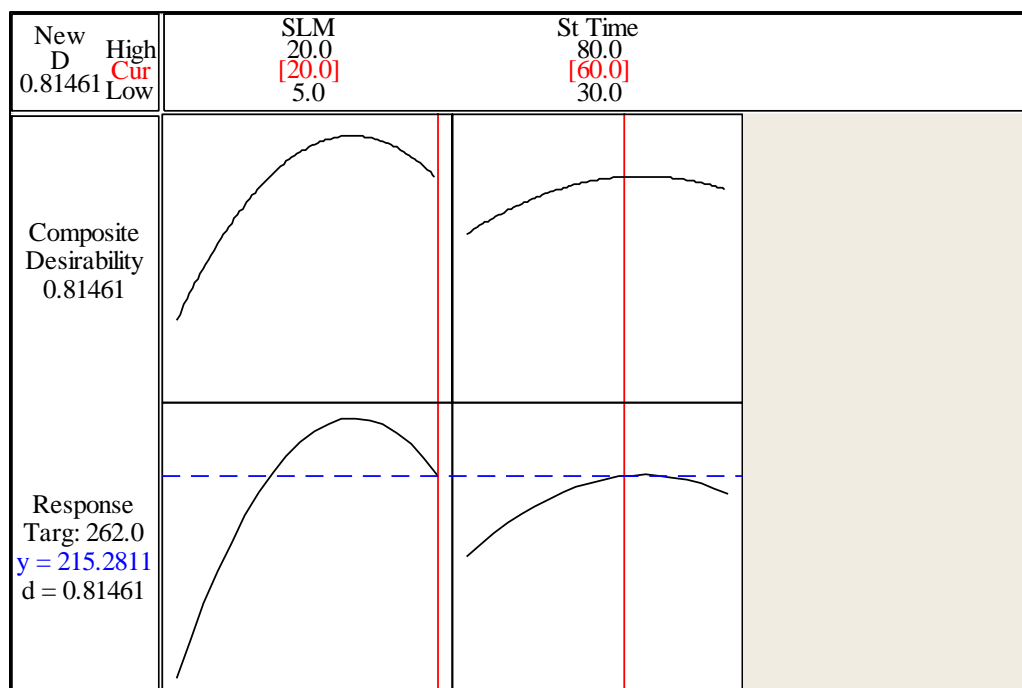


Figure 50 Effects of setting MUS-based levels of SLM composition and extraction time on the dual desirability and response output for TA

### 5.6.2 Compound desirability

The compound desirability,  $D$  of setting MUS optimum conditions as universal factor levels for a simultaneous extraction of MUS, TRP and TA was finally done by substituting for  $m$  in equation 5 to form equation 15.

$$\begin{aligned}
 D &= (d_1 y_1 \cdot d_2 y_2 \cdot d_3 y_3 \cdot d_4 y_4 \cdot d_5 y_5 \cdot d_6 y_6)^{1/6} & (15) \\
 &= (0.71423 \times 0.88268 \times 0.53154 \times 0.85693 \times 0.44768 \times 0.81461)^{1/6} \\
 &= 0.68655
 \end{aligned}$$

A  $D$ -value of 0.687 implied that the set conditions were ideal for a simultaneous extraction of the analytes from the donor phase into the acceptor phase across a supported liquid membrane impregnated with a carrier molecule. This was a fair result considering that only one of the responses was used to set the factor values. A different value could have been obtained if the purpose was to maximize EF values for all analytes.

When the three analytes were finally extracted simultaneously under the MUS-biased conditions, only the experimental EF value for TRP was within the predicted range as shown in Table 27. Most affected was the most polar MUS which dropped by 40% below the minimal experimental value. The percentage difference was calculated using equation 16.

$$Difference = \left| (EF_{predicted(\text{minimum})} - EF_{experimental}) / EF_{predicted(\text{minimum})} \right| \times 100 \quad (16)$$

Table 27 Comparison of predicted and experimental EF values when TA, MUS and TRP were extracted simultaneously under universal factor levels

	TA	MUS	TRP	PSI
Expected EF	145 - 215	10 - 15	31 - 41	ND
Experimental EF	140	6	33	ND
RSD	0.0251	0.0220	0.0167	-

Conditions: DP pH 4 with 0.001% (w/v) NaCl, 100 mM HCl AP, 20% (w/w) DEHPA in DHE and stirring at 800 rpm for 60 mins. ND – Not detected.

The experimental EF values were expected to be higher than the predicted range. The observed experimental EF values compared to predicted values might be that predictions from Minitab disregarded possibility of competition in binding to the carrier molecule. A reduction in the EF value for the extremely polar MUS was expected considering that mixing analytes in a single donor phase might result in analytes competing for the carrier molecule during extraction. During screening experiments, an increase in NaCl content in the DP reduced extraction of MUS. Thus the 10 – 15 predicted range was obtained in the absence of salt in the DP.

The EF values in Table 28 were obtained when the AP concentration was increased from 100 mM to 200 mM HCl. Increasing the AP concentration was most effective for the enrichment of the least polar TA with a 49% increase while it was less for the polar MUS and TRP. Enrichment of MUS increased by 33% and TRP increased by 9%. During screening experiments it was shown that AP concentration is not so effective in the extraction of polar analytes.

Table 28 EF values for simultaneous extraction of TA, MUS and TRP using 200 mM HCl as the acceptor phase (n=3).

	TA	MUS	TRP
Average EF value	208	8	36
SD	4.0161	0.3771	2.1524
RSD	0.0193	0.0464	0.0596
%RSD	1.93	4.64	5.96

## 5.7 Applying the method in urine samples

### 5.7.1 Spiked urine extraction results

A visual comparison of chromatograms from blank and spiked urine extractions in Figure 51 showed presence of co-extracted compounds some of which co-eluted with our analytes of interest. Most affected was MUS. A big peak was observed that eluted within 0.01 mins of MUS elution. This peak could not be separated from the MUS peak even when elution was done at 0.2 mL min<sup>-1</sup>. Deja et al. (2014) identify urea as the interfering compound responsible for this peak (Deja et al., 2014). The same was observed with interference on the TRP peak. While the TA peak was prominent at 1.19 ± 0.01 mins, there were two peaks that eluted at 1.10 mins and at 1.49 mins. The 1.10 mins elution time peak could not be baseline separated from the TA peak. The peaks for blank extraction chromatograms were considered to be representative of matrix effects.

Chromatograms marked (b) in Figure 51 were obtained by injecting the AP diluted six-fold and was used to quantify MUS and TRP. The AP was diluted 53-fold for chromatograms marked (a) and were used to quantify TA. Compared to the retention times obtained during column selection experiments (Figure 14), it was observed that there was a general decrease in retention of analytes. This was attributed to the amount of THF used for diluting the AP before injection into the HPLC system. During HILIC column optimization, dilution was up to 2000 times and the analytes were retained more in the column. The effect of the THF diluent



amount is also apparent for the 6-fold and the 53-fold dilution chromatograms. This observation further enhances the findings of this research that use of a relatively non-polar diluent is essential for retention and hence effective separation of polar compounds as given in section 5.1.

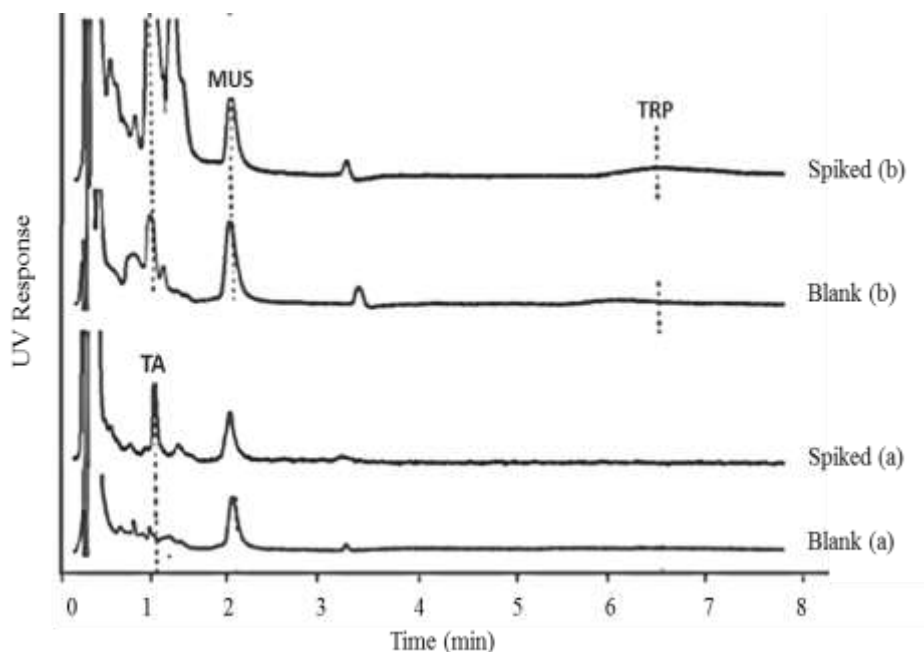


Figure 51 Comparison of blank urine peaks and the  $2 \mu\text{g mL}^{-1}$  spiked urine peaks for the extraction of TA (a) and, MUS and TRP (b)

Analytes extracted from a 20% (v/v) diluted urine sample using 200 mM HCl as the acceptor phase gave better peak areas of analytes compared to when either 100 mM HCl was used and also to when the analytes were extracted from a 50% (v/v) diluted urine solution. For MUS, it was observed that extraction was near impossible when urine was diluted at 50% (v/v). Table 29 is a comparison of peak areas for MUS obtained from blank and spiked urine extractions. The same was observed when 100 mM HCl was used with the peak of the interfering compound contributing  $29.021 \pm 0.0417$  in a total spiked extraction peak area of  $29.022 \pm 0.007$  ( $n=3$ , RSD). Thus further studies were carried on 20% (v/v) deionized water-diluted urine samples which equated to a dilution ratio of 1:4.

Table 29 Average peak areas for extraction of MUS from 2  $\mu\text{g mL}^{-1}$  spiked diluted urine solutions using 200 mM HCl as acceptor phase (n=3)

Urine dilution	Blank extraction		Spiked extraction		Peak area for MUS	
	50% (v/v)	20% (v/v)	50% (v/v)	20% (v/v)	50% (v/v)	20% (v/v)
Peak area	57.472	23.386	57.502	26.251	0.03	2.864
SD	0.3883	0.0100	0.0058	0.4596	0.0058	0.1255
RSD	0.0068	4.3E-04	1E-04	0.0175	0.1917	0.0438
%RSD	0.65	0.04	0.01	1.75	19.17	4.38

Generally there was a marked reduction in EF values for the three analytes when they were extracted from urine compared to when extracted from deionized water samples. Table 30 compares the EF values when 200 mM HCl was used to extract the analytes from water and from urine samples. The observed reduction in EF values for the three analytes was confirmation of the complexity of urine specimens and the matrix effect challenges associated with urinalysis. The hollow fibre is a size exclusion separation technique and therefore any low molecular weight compound would be expected to be found at the donor phase-SLM interface. This would reduce the surface area for analyte interaction with the carrier molecule. The anionic nature of the carrier molecule indicates selectivity for any positively charged component of urine like metallic cations, urea and creatinine. Similar scenario has been observed in most urinalysis chromatographic separation and quantification (Dziarkowska et al., 2008; Yamini et al., 2006). It should be noted that dark yellow urine was targeted in this investigation so as to maximize the matrix effects during method development. An average urine colour of a healthy person would be light yellow.

### 5.7.2 Calculating matrix effects

The extent of matrix effects when the method was applied on spiked 20% (v/v) diluted urine is given in Table 31. Equation 13 and 14 were used. The peak area that interfered with the MUS was extremely enhancing with a positive percentage matrix effect value of 840. This implied that the optimized conditions might have favoured the interfering compound however this could not be ascertained.

Surprisingly TA which experienced minimal matrix effects with a value of 3.4 had the highest percentage EF reduction as shown by the summary of percentage EF value reductions when extractions were done from 2  $\mu\text{g mL}^{-1}$  spiked urine using 200 mM HCl as the acceptor phase in Table 32. TRP with a median value for matrix effects experienced the least reduction in its EF value.

Table 30 Comparison of EF values of TA, MUS and TRP in water and diluted urine samples spiked at 2  $\mu\text{g mL}^{-1}$  (n=3)

	TA		MUS		TRP	
	Water	20% (v/v)	Water	20% (v/v)	Water	20% (v/v)
EF	208.4	25.5	8.4	4.2	36.1	21.6
SD	4.016	0.602	0.074	0.684	2.152	2.438
RSD	0.019	0.024	0.009	0.161	0.060	0.113
%RSD	1.9	2.4	0.9	16.1	6.0	11.3

Table 31 Percentage matrix effects on extraction of TA, MUS and TRP from a 2  $\mu\text{g mL}^{-1}$  spiked diluted urine sample using 200 mM HCl as the acceptor phase (n=3, RSD)

	TA	MUS	TRP
	20% v/v	20% v/v	20% v/v
Total peak area	24.037 $\pm$ 0.0228	26.251 $\pm$ 0.0176	29.962 $\pm$ 0.0817
Interfering compound	0.706 $\pm$ 0.0234	23.386 $\pm$ 0.0004	9.028 $\pm$ 0.0004
Analyte peak area	23.331 $\pm$ 0.0235	2.864 $\pm$ 0.1605	20.934 $\pm$ 0.1169
% matrix effect	3.026 $\pm$ 0.0235	840.331 $\pm$ 0.1773	43.773 $\pm$ 0.1269

Table 32 Summary of percentage reductions in EF values when TA, MUS and TRP were extracted from spiked diluted urine compared to spiked water samples

	TA	MUS	TRP
EF value from water	208.4	8.1	36.1
EF value from urine	25.5	4.2	21.6
% EF reduction	87.7	48.1	40.1

It was observed that the extent of matrix effects as shown in Table 33 was higher when the urine was less diluted and this was also observed when a more concentrated HCl acceptor phase was used. For a less diluted urine sample, the interfering compounds still exist in higher concentrations while a higher concentration of the acceptor phase maintains a high proton gradient essential for effective extraction of any cationic compound. However, the enrichment factor values showed that the use of a stronger HCl acceptor phase was more important than diluting the sample especially with TA and TRP. This could be attributed to the increased H<sup>+</sup> ion gradient which is actually the driving force in carrier mediated hollow fibre extraction.

Table 33 Comparison of matrix peak areas in EF values for TA, MUS and TRP in spiked diluted urine samples

HCl (mM)		TA		MUS		TRP	
		50%	20%	50%	20%	50%	20%
Matrix							
100	peak area	1.04	0.319	29.0	21.9	13.5	5.0
	EF value	5.5	10.1	ND*	1.5	14.3	16.7
Matrix							
200	peak area	2.55	0.706	57.5	23.4	27.6	9.0
	EF value	12.2	25.5	0.02	4.2	17.5	21.6

ND - Not detected

For MUS where diluting the urine sample seemed to be more effective, the explanation might lie in the extent of extraction of the interfering compound. The peak of the interfering compound was at least 99.9% of the total peak area for a 50% (v/v) dilution urine solution and between 95.3 – 96.4% for a 20% (v/v) urine solution. Diluting the urine helped by diluting the interfering compound thus allowing an increase in the extent of extraction of MUS. This observation also concurs with the observations made during optimization experiments where stirring rate was more important than AP concentration during extraction of more polar compounds. Muscimol is the most polar analyte in our study and diluting the interfering compound allows MUS to have more contact with the hollow fibre at the DP-SLM interface. For TA, the maximum percentage contribution of matrix effect to the total peak area was 18.7% where the urine had been diluted at 50% (v/v) and 200 mM HCl used as the acceptor phase. The maximum contribution due to matrix effects on TRP was 62.2% at the same extraction conditions. These percentage values due to matrix effects were considered very high and hence the decision to correct for the matrix effects using a matrix-based calibrator.

Having identified diluting the urine samples at 1:4 giving a urine solution of 20% (v/v) using 200 mM HCl as the acceptor phase as the minimal conditions that allow for effective enrichment of our analytes at a spiked concentration of 2  $\mu\text{g mL}^{-1}$ , the next step was to construct a matrix-based calibration curve for each analyte.

### **5.7.3 Matrix-based calibration curve for tryptamine**

Table 34 shows the average peak areas and EF values when TA was extracted from 20% (v/v) diluted urine solutions spiked at 0.1  $\mu\text{g mL}^{-1}$ , 0.5  $\mu\text{g mL}^{-1}$ , 1  $\mu\text{g mL}^{-1}$ , 2  $\mu\text{g mL}^{-1}$ , 5  $\mu\text{g mL}^{-1}$  and 10  $\mu\text{g mL}^{-1}$  using 200 mM HCl as an acceptor phase.

A matrix-based calibration was then constructed as a plot of spiking concentration versus average peak area and is given in Figure 52. Average total peak areas obtained by diluting the AP with 20  $\mu\text{L}$  of acetonitrile and 500  $\mu\text{L}$  of THF were used. For example, for a 10  $\mu\text{g mL}^{-1}$  spiked solution in Table 34, the peak area used for the calibration curve was 104.252. The peak area of the interfering

compound was included in the residual points as the response when the analyte spiking concentration was  $0 \mu\text{g mL}^{-1}$ . This point was also set as the y-intercept of the calibration curve. The manipulated regression line had an  $r^2$  value of 0.9986 while a true regression line had an  $R^2$  value of 0.9991.

Another calibration curve was plotted in which the final total peak areas assuming the AP phase was not diluted were used. In this case, the 104.252 peak area was multiplied by the dilution factor, 53 to obtain 5525.363. This value was then used for the calibration curve in Figure 53. The same was done with peak areas of other spiked concentration levels. Whether the calibration curve in Figure 52 or Figure 53 was used to predict concentration from a peak area, the result was the same. However the choice of Figure 52-type of calibration curve where the peak areas due to dilution of the acceptor phase were used allow for flexibility in terms of the extent of dilution. A dilution mistake made during analysis will not affect the outcome while a Figure 53-type approach is not flexible in that regard. Thus a matrix-based calibration curve plotted using the peak areas of diluted acceptor phase is recommended.

Table 34 Summary of data for calculating EF values for extracting TA from six different spiking concentrations (n=3, RSD)

Spiking concentration ( $\mu\text{g mL}^{-1}$ )	Average total peak area	Average interfering peak area	Average corrected peak area	Regression line	Dilution factor	Average final concentration ( $\mu\text{g mL}^{-1}$ )	Average EF value
0.1	1.731 $\pm 0.0485$	0.706 $\pm 0.0266$	1.025 $\pm 0.0820$		53	2.05 $\pm 0.089$	20.81 $\pm 0.088$
0.5	7.185 $\pm 0.0206$	0.706 $\pm 0.0266$	6.479 $\pm 0.0229$		53	14.039 $\pm 0.0231$	28.08 $\pm 0.023$
1	12.393 $\pm 0.0987$	0.706 $\pm 0.0266$	11.687 $\pm 0.1047$		53	25.455 $\pm 0.1054$	25.46 $\pm 0.105$
2	24.037 $\pm 0.0228$	0.706 $\pm 0.0266$	23.331 $\pm 0.0235$	$y = 24.176x + 4.0073$	53	50.982 $\pm 0.0236$	25.49 $\pm 0.024$
5	51.352 $\pm 0.0803$	0.706 $\pm 0.0266$	50.646 $\pm 0.0814$		53	110.863 $\pm 0.0815$	22.68 $\pm 0.081$
10	104.252 $\pm 0.0990$	0.706 $\pm 0.0266$	103.546 $\pm 0.0997$		53	226.835 $\pm 0.0997$	22.68 $\pm 0.100$

$y$  is the peak area and  $x$  is analyte concentration in  $\mu\text{g mL}^{-1}$

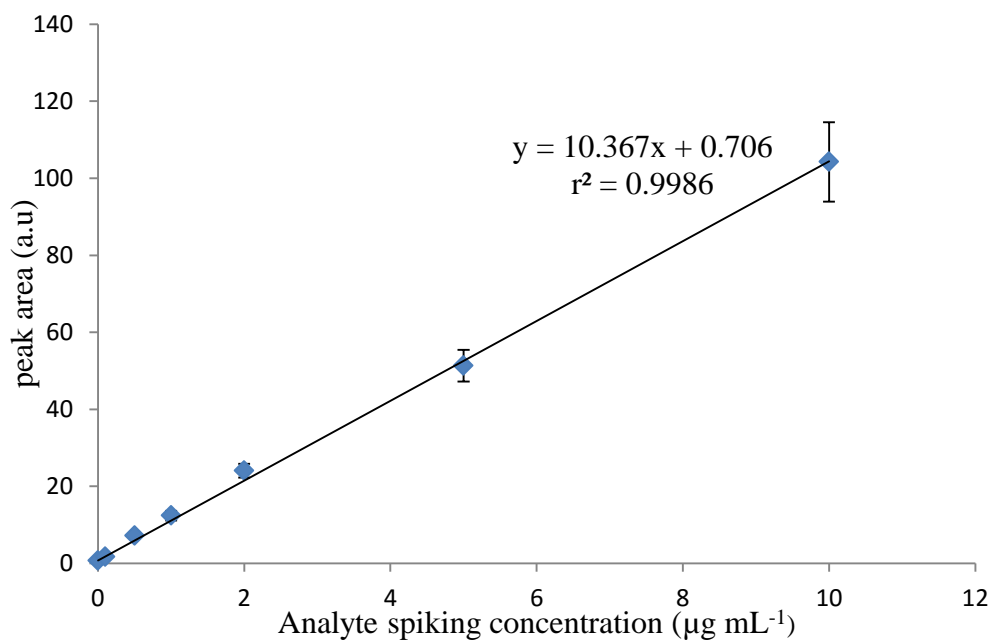


Figure 52 Matrix-based calibration curve for the extraction of TA from diluted urine samples; acceptor phase had been diluted 53 fold. (n=3, SD)

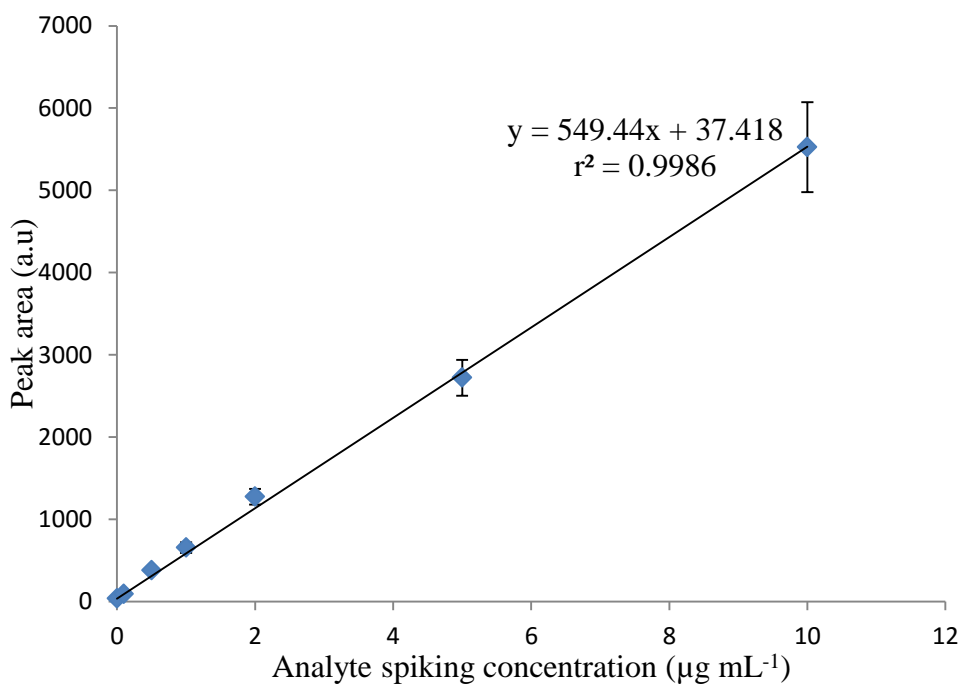


Figure 53 Matrix-based calibration curve for the extraction of TA from diluted urine samples assuming the AP was not diluted. (n=3, SD)



#### 5.7.4 Matrix-based calibration curve for muscimol

When the diluted urine solution was spiked at  $0.1 \mu\text{g mL}^{-1}$ , MUS could not be significantly enriched into the acceptor phase. Using single factor ANOVA it was shown that there was no significant difference between the blank and the  $0.1 \mu\text{g mL}^{-1}$  spiked results as shown in Table 35.

Table 35 Single Factor ANOVA for blank and  $0.1 \mu\text{g mL}^{-1}$  spiked results.

<i>Source of Variation</i>	<i>SS</i>	<i>df</i>	<i>MS</i>	<i>F</i>	<i>P-value</i>	<i>F crit</i>
Between						
Groups	0.5040	1	0.5040	1.087	0.3561	7.709
Within Groups	1.856	4	0.4639			
Total	2.360	5				

The F value was less than the F critical value and the P-value greater the set  $P = 0.05$  value implying that there was no significant difference between the means of peak areas for the blank and the  $0.1 \mu\text{g mL}^{-1}$  spiked result. Therefore MUS could not be sufficiently enriched into the acceptor phase when it was  $0.1 \mu\text{g mL}^{-1}$  of the matrix.

Table 36 shows the average peak areas and the EF values for MUS obtained when the 20% (v/v) diluted urine solution was spiked at  $0.5 \mu\text{g mL}^{-1}$ ,  $1 \mu\text{g mL}^{-1}$ ,  $2 \mu\text{g mL}^{-1}$ ,  $5 \mu\text{g mL}^{-1}$  and  $10 \mu\text{g mL}^{-1}$  respectively.

Table 36 Summary of data for calculating EF values for extracting MUS from six different spiking concentrations (n=3, RSD)

Spiking concentration ( $\mu\text{g mL}^{-1}$ )	Average total peak area	Average interfering peak area	Average corrected peak area	Regression line	Dilution factor	Average final concentration ( $\mu\text{g mL}^{-1}$ )	Average EF value
0.5	23.851 $\pm 0.0052$	23.386 $\pm 0.0004$	0.465 $\pm 0.2690$		6	1.331 $\pm 0.2796$	3.62 $\pm 0.409$
1	24.734 $\pm 0.0062$	23.386 $\pm 0.0004$	1.348 $\pm 0.1142$		6	3.958 $\pm 0.1158$	3.96 $\pm 0.116$
2	26.251 $\pm 0.0175$	23.386 $\pm 0.0004$	2.864 $\pm 0.1605$	$y = 2.0162x + 0.1052$	6	8.472 $\pm 0.1615$	4.24 $\pm 0.161$
5	30.736 $\pm 0.0170$	23.386 $\pm 0.0004$	7.350 $\pm 0.0597$		6	21.820 $\pm 0.0599$	4.36 $\pm 0.060$
10	35.483 $\pm 0.0170$	23.386 $\pm 0.0004$	12.096 $\pm 0.0499$		6	35.945 $\pm 0.0500$	3.59 $\pm 0.050$

$y$  is the peak area and  $x$  is analyte concentration in  $\mu\text{g mL}^{-1}$

A matrix-based calibration curve for the extraction of MUS from diluted urine is given in Figure 54. The peak area of the 10  $\mu\text{g mL}^{-1}$  spiked concentration was excluded from the calibration curve because it seemed to cause a deviation from linearity leading to an  $r^2$  value of 0.9868 compared to  $r^2$  value of 0.9975 as shown in Figure A1. The deviation from linearity due to the 10  $\mu\text{g mL}^{-1}$  spiked concentrations might have implied the beginning of a new linear region. However this was not confirmed. The peak area of the interfering compound was included in the residual points as the response when the analyte spiking concentration was 0  $\mu\text{g mL}^{-1}$ . This point was also set as the y-intercept of the calibration curve. The manipulated regression line had an  $r^2$  value of 0.9975 while a true regression line had an  $R^2$  value of 0.9996.

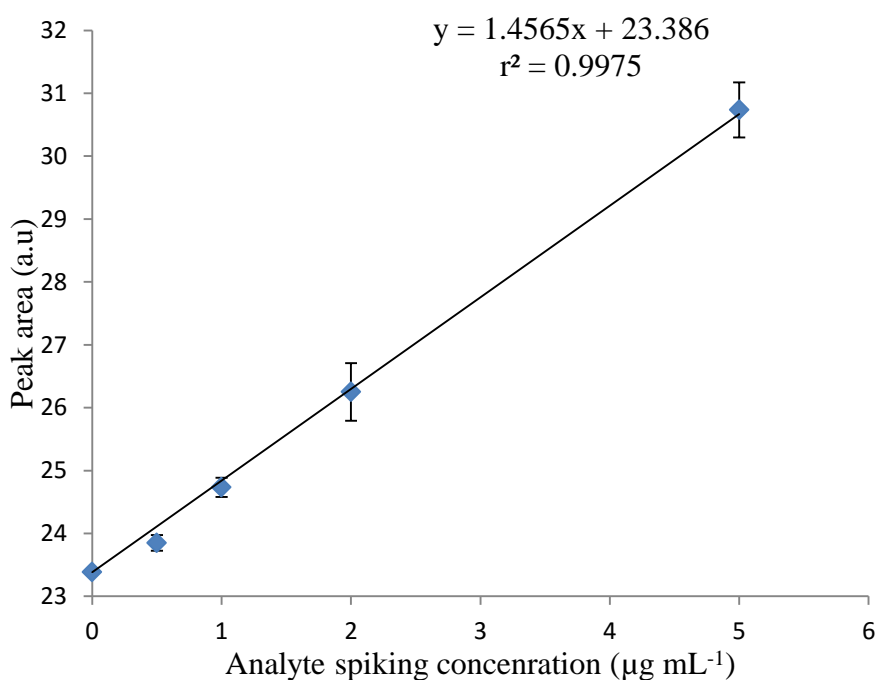


Figure 54 Matrix-based calibration curve for the extraction of MUS from diluted urine samples spiked up to a concentration of 5  $\mu\text{g mL}^{-1}$ . The acceptor phase had been diluted 6 fold. (n=3; SD)

### 5.7.5 Matrix-based calibration curve for tryptophan

The response for extraction from the  $0.1 \mu\text{g mL}^{-1}$  spiked sample had an RSD of 85% and the single factor ANOVA in Table 37 proved that there was no difference between the blank and the  $0.1 \mu\text{g mL}^{-1}$  peak areas. The  $0.1 \mu\text{g mL}^{-1}$  results were therefore excluded from calculation of the EF value and the construction of the matrix-based calibration curve. Table 38 shows the peak areas and EF values for TRP obtained when the 20% (v/v) diluted urine solution was spiked at  $0.1 \mu\text{g mL}^{-1}$ ,  $1 \mu\text{g mL}^{-1}$ ,  $2 \mu\text{g mL}^{-1}$ ,  $5 \mu\text{g mL}^{-1}$  and  $10 \mu\text{g mL}^{-1}$ .

A matrix-based calibration curve for the extraction of TRP from diluted urine is given in Figure 55. The peak area of the interfering compound was included in the residual points as the response when the analyte spiking concentration was  $0 \mu\text{g mL}^{-1}$ .

However when this point was set as the y-intercept of the calibration curve, it led to LOD and LOQ values of  $0.18 \mu\text{g mL}^{-1}$  and  $0.61 \mu\text{g mL}^{-1}$  respectively. This might have been due to bias towards false positives considering that  $0.5 \mu\text{g mL}^{-1}$  was one of the calibrators. Thus an unaltered regression equation was used for TRP.

Table 37 Single Factor ANOVA for blank and  $0.1 \mu\text{g mL}^{-1}$  spiked result.

<i>Source of Variation</i>	<i>SS</i>	<i>df</i>	<i>MS</i>	<i>F</i>	<i>P-value</i>	<i>F crit</i>
Between						
Groups	2.516	1	2.516	1.056	0.3622	7.709
Within Groups	9.529	4	2.382			
Total	12.044	5				

Table 38 Summary of data for calculating EF values for extracting TA from six different spiking concentrations (n=3, RSD)

Spiking concentration ( $\mu\text{g mL}^{-1}$ )	Average total peak area	Average interfering peak area	Average corrected peak area	Regression line	Dilution factor	Average final concentration ( $\mu\text{g mL}^{-1}$ )	Average EF value
0.5	13.096 $\pm 0.0471$	9.028 $\pm 0.0541$	4.068 $\pm 0.1517$		6	9.522 $\pm 0.1291$	19.04 $\pm 0.129$
1	21.088 $\pm 0.0486$	9.028 $\pm 0.0541$	12.060 $\pm 0.0849$		6	25.449 $\pm 0.0802$	25.45 $\pm 0.080$
2	29.962 $\pm 0.0817$	9.028 $\pm 0.0541$	20.934 $\pm 0.1169$	$y = 3.1063x - 4.2568$	6	43.135 $\pm 0.1131$	21.57 $\pm 0.1131$
5	48.677 $\pm 0.0268$	9.028 $\pm 0.0541$	38.901 $\pm 0.0386$		6	78.942 $\pm 0.0379$	16.09 $\pm 0.032$
10	89.283 $\pm 0.0904$	9.028 $\pm 0.0541$	80.255 $\pm 0.1006$		6	161.359 $\pm 0.0997$	16.14 $\pm 0.0997$

$y$  is the peak area and  $x$  is analyte concentration in  $\mu\text{g mL}^{-1}$

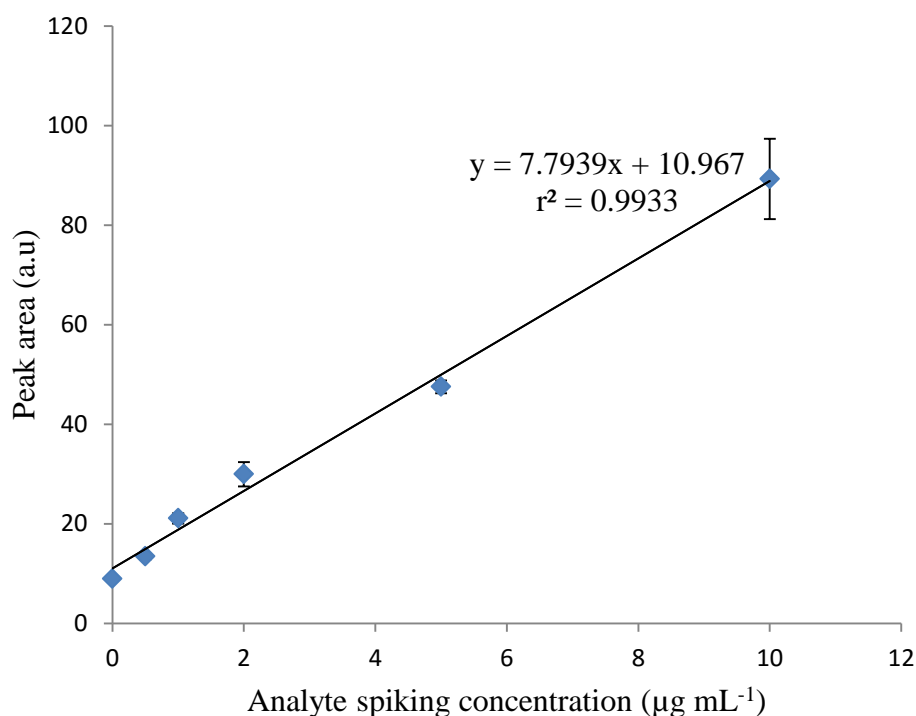


Figure 55 Matrix-based calibration curve for the extraction of TRP from diluted urine samples spiked up to a concentration of 10 µg mL<sup>-1</sup>. The acceptor phase had been diluted 6 fold.

### 5.7.6 Differences in peak area errors and EF value errors at each analyte spiking level

A closer look at the peak errors for three extractions per spiked concentration in Table 39 revealed that the results could be relied on with %RSD values ranging from 0.5% for extracting MUS from a 0.5 µg mL<sup>-1</sup> spiked urine solution to 9.90% when TA was enriched from a 10 µg mL<sup>-1</sup> spiked urine diluted sample. However in all extractions, the corresponding EF error values were higher than the peak area errors.

The extent of increase in the %RSD error value from peak area errors to EF value errors was reducing as concentration of the spiked solution was increasing. The most affected was MUS extraction with the EF value error going up to 40.9% when MUS was being extracted from a 0.5 µg mL<sup>-1</sup> spiked concentration. The most appropriate explanation might be carry-over effects or propagation of errors

during calculations. The low error values for peak areas is because these were obtained from raw data from the injection results while several calculation steps had to be followed until the EF value was obtained. Also dealing with AP volumes in the micro scale and small values of peak areas and later multiplying with larger dilution factors might have contributed to enhanced EF value errors. However the overall errors in the EF value for each analyte given as RSD were acceptable and ranged from 8.3% for MUS to 13.1% for TRP.

### **5.8 EF values for the simultaneous extractions from diluted urine samples**

The overall enrichments for the simultaneous extraction of MUS, TRP and TA using the developed HF-LPME approach under MUS-based universal factor levels are summarized in Table 40. The conditions of extraction were DP pH 4, 200 mM HCl as the AP, 20 %w/w DEHPA in DHE, 800 rpm stirring rate and 60 mins extraction time. Equation 17 was used.

Overall EF value for analyte

$$= (\text{sum of EF} - \text{number of spiking concentration}) \pm \text{RSD} \quad (17)$$

The relatively low EF value for MUS might be related to its polarity and pKa values. MUS is highly polar and exists in its neutral state between pH 4.8 and 8.4.

Table 39 Summary of errors when three extractions were performed per analyte spiked concentration (n=3).

Analyte spiked concentration ( $\mu\text{g mL}^{-1}$ )	TA		MUS		TRP	
	Peak area error (%RSD)	EF value error (%RSD)	Peak area error (%RSD)	EF value error (%RSD)	Peak area error (%RSD)	EF value error (%RSD)
0.1	4.9	8.8	-	-	-	-
0.5	2.1	2.3	0.5	40.9	4.7	12.9
1	9.9	10.5	0.6	11.6	4.9	8.0
2	2.3	2.4	1.8	16.1	8.2	11.3
5	8.0	8.1	1.4	6.0	2.7	3.2
10	9.90	9.97	1.7	5.0	9.04	9.97



Table 40 Summary of EF values for the simultaneous extraction of MUS, TRP and TA from diluted urine sample spiked in the 0.1 – 10  $\mu\text{g mL}^{-1}$ .

Analyte	Overall EF value	RSD (%)
MUS	4.1	8.3
TRP	19.7	13.1
TA	24.1	10.2

## 5.9 Method validation

Table 41 shows that our linear regression prediction model could be relied on for the quantification of MUS, TRP and TA from urine samples with  $r^2$  values ranging from 0.9933 for the TRP regression to 0.9986 for the least polar TA. These numeric linear association parameters from the matrix-based extractions were directly linked to the reproducibility of the EF values over a wide range of analyte concentration calibrators. The %RSD values for the overall EF values of each analyte after doing extraction from six different spiked urine samples ranged from 8.3% to 13.1%. This was satisfactory considering that the overall EF values were determined in the 0.1 – 10  $\mu\text{g mL}^{-1}$  using six spiking concentrations.

Table 41 Summary of method validation parameters.

Matrix based								
	regression equation	r <sup>2</sup>	LOD	LOQ	EF	SD	RSD	%RSD
MUS	$y = 1.4565x + 23.386$	0.9975	0.021	0.069	4.06	0.337	0.083	8.3
TRP	$y = 7.7939x + 10.967$	0.9933	-0.061	0.38	19.66	2.572	0.131	13.1
TA	$y = 10.33x + 0.706$	0.9986	0.005	0.018	24.12	2.453	0.102	10.2

$y$  is the peak area and  $x$  is analyte spiking concentration in  $\mu\text{g mL}^{-1}$

Table 42 Comparison of r<sup>2</sup> values, LODs and LOQs for the matrix-based calibration and the standard solution-based calibration.

r <sup>2</sup>			LOD			LOQ			Type of
TA	MUS	TRP	TA	MUS	TRP	TA	MUS	TRP	Calibration curve
0.9994	0.9868	0.9933	0.005	0.021	0.061	0.018	0.069	0.38	Matrix-based
0.9999	0.9929	0.9976	0.027	0.024	0.166	0.040	0.034	0.167	Standard-based

### 5.9.1 Limits of detection and quantification

Because blank determination is an interference-based analyte detection technique, the average peak areas of the interfering compounds were used in the calculation of LOD and LOQ. Equations 18 and 19 were used for LOD and LOQ respectively. The matrix-based linear regression equation for each analyte was then used to quantify LOD as a minimum quantifiable analyte concentration.

$$\text{LOD (peak area)} = \text{average peak area of interfering compound} + 3\text{SD} \quad (18)$$

$$\text{LOQ (peak area)} = \text{average peak area of interfering compound} + 10\text{SD} \quad (19)$$

One of the major disadvantages of the method-based approach is its inability to identify if the measured detection limit is biased towards a false negative or a false positive. Ripp 1996 observes that false negatives are a common feature in method detection limits (Ripp, 1996). TA which was least affected by matrix effects had the lowest detection and quantification limits compared to MUS and TRP. This could not be declared as the explanation to the observed scenario as TA was also the least polar of the three analytes.

While standard solution calibration curves gave better linearity, the matrix-based calibration curves presented better LOD and LOQ values as shown in Table 42. In the matrix-based calibration curves the baseline noise peak had already been accounted for in the peak of the interfering compound. The larger LOQ values for MUS and TRP might be due to the larger matrix effect contribution to the total peak areas.

### 5.9.2 Repeatability and reproducibility

All intra-day experiments were carried out in triplicate and repeatability expressed using RSD values. Table 43 shows the RSD values when diluted urine spiked at 2  $\mu\text{g mL}^{-1}$  preserved at 4<sup>0</sup>C was extracted after a day and results compared statistically with those from the fresh urine extractions done the previous day using RSD values.

Table 43 Reproducibility of EF values of TA, MUS and TRP extracted from the 2  $\mu\text{g mL}^{-1}$  spiked urine solution after 24 hrs.

	TA		MUS		TRP	
	Peak areas	EF value	Peak areas	EF value	Peak areas	EF value
Day 1	24.037	25.49	26.251	4.24	29.962	21.57
Day 2	21.612	22.83	22.680	-1.08	23.688	15.31
Average	22.824	24.16	24.465	1.579	26.825	18.44
SD	1.2125	1.329	1.785	2.657	3.1369	3.1258
RSD	0.0531	0.0550	0.0730	1.682	0.1169	0.1695
%RSD	5.31	5.50	7.30	168.2	11.69	16.95

A general decrease in the peak areas was observed even though the %RSD values for the average peak area was within acceptable values of 5.31% for the TA peak area to 11.69% for the TRP. This observation might be attributed to possibility of loss of analyte or even the interfering compounds through some biological processes. The stability of our analytes and the interfering compounds in urine preserved at 4<sup>0</sup>C was unknown. When the average peak areas for day 2 were equated to EF values, MUS gave a negative value with an inter-day RSD of 168.2%. This was an indication that the total peak area after 24 hrs was lower than the blank peak area calculated the previous day. The explanation might have been that the enhancing matrix effect had reduced due to loss of the interfering compound. The TRP EF value reduced from 21.57 to 15.31 giving an inter-day RSD value of 16.95%. These results are an indication that if the extraction were to be repeated after at least 24 hours of urine preservation, a new matrix-based calibration curve might be necessary using unspiked preserved urine in order to determine the extent of matrix changes. This procedure could not be done during this research as the amount of preserved urine was not enough to start new matrix-based calibration curves. A new urine sample could not be collected as it could have had different properties and quantities of interfering compounds and results from such a sample would have been distorted.

When enrichment of the three analytes was tested again after 5 days, both MUS and TRP gave negative EF values while the EF value for TA had dropped to 13.14 with the inter-day RSD rising to 25.9%. These results might have been an indication that urine from individuals suspected of hallucinogen consumption must be analysed as early as possible to avoid false negatives preferably on the day of urine sample collection. There might be need for new calibration curves if analysis is to be repeated after several hours of urine preservation. Alternatively, better preservation methods can be applied in order to minimize urine enzyme activity.

### **5.9.3 Comparative studies**

Table 44 below gives a comparison of LODs and LOQs for extraction of MUS from urine samples using the current method and other methods that have been used before. The results show that better LOD values were obtained when the current HF-LPME approach was used. In Table 45, EF values of several compounds with polarity as high as the current study compounds that have been extracted from urine samples using the carrier-mediated HF-LPME approach. It was obvious that the EF values obtained from the HF-LPME for the extraction of muscimol and its two precursors were in the acceptable region.

Table 44 Comparison of LODs and LOQs, repeatability and reproducibility, and  $r^2$  values for different methods that have used to extract MUS from urine samples.

$r^2$	LOD ( $\mu\text{g mL}^{-1}$ )	Method	Reference
0.9868	0.021	HF-LPME with HPLC-UV	Current
0.9996	13	NMR-NOESY spectroscopy	(Deja et al., 2014)
0.9992	0.05 ng mL <sup>-1</sup>	Capillary electrophoresis coupled with electrospray tandem mass spectrometry	(Ginterová et al., 2014)
>0.99	1	Cation exchanger with derivatization (Dowex® 50W X8) with GC-MS	(Stříbrný et al., 2012)
0.9999	0.0025 (in blood serum)	Solid phase extraction with LC-MS-MS from blood serum	(Hasegawa et al., 2013)
	Purpose was to quantify MUS and IBO from dog urine that had ingested mushrooms	1Urine:3 mixture of methylene chloride /methanol with agitation	(Rossmeisl et al., 2006)
	Purpose was to confirm presence of MUS in a patient's urine. No validation was done	Derivatization with N-methyl-N-(trimethylsilyl) trifluoroacetamide (MSTFA) GC-MS	(Garcia et al., 2015)

Table 45 EF values of polar compounds with  $X \log P_3 \leq 1.6$  that have been extracted from urine using carrier-mediated HF-LPME

Compounds & X log P3 values	SLM composition	EF values in urine	Urine dilution	Instrument	AP conc.	Reference
Muscimol, tryptophan, tryptamine (-1.4, - 1.1, 1.6)	20% (w/w) DEHPA in DHE	4.1, 19.7, 24.1	1.4	HPLC-UV	200 mM HCl	Current
Putrescine, cadaverine spermidine, spermine (-0.9, -0.6, -1, -1.1)	20% (w/w) DEHPA in DHE	11.0, 13.6 4.3, 13.1	-	HPLC-UV	200 mM HCl	(Dziarkowska et al., 2008)
Ephedrine (0.9)	10% (w/v) TEHP in Toluene	8	1:6	HPLC-UV	1mmol L <sup>-1</sup>	(Fotouhi et al., 2011)
Amphetamine, morphine, practolol (1.8, 0.8, 0.8)	Sodium octanoate in octanol	R (45–71%)	1:1	CE-UV	50 mM HCl	(Ho et al., 2003)
Morphine, codeine, thebaine, papaverine, noscapine, (0.8, 1.1, 2.2, 3.9, 2.7)	25 mM sodium octanoate in octanol	R (17-45%)	Undiluted	HPLC-UV	50 mM HCl	(Li et al., 2014)
Salbutamol, terbutaline (0.3, 0.9)	20% Aliquat 336 in DHE	52.9 213.1	(1:109)	LC-MS	1M NaBr	(Yamini et al., 2006)
Ephedrine (0.9)	15% TEHP in Toluene	35	1:6	HPLC-UV	100 mM HCl	(Fotouhi et al., 2011)

\* tris(2-ethylhexy)phosphate TEHP

## 6 CONCLUSIONS AND RECOMMENDATIONS

### 6.1 Conclusions

An HPLC-UV system with a HILIC column was selected for the separation and quantification of analytes from urine samples. The mobile phase was acetonitrile-buffer 90:10% (v/v) 10 mM formate. The results of this study showed that better separation in HILIC columns can be achieved if analyte diluents of relatively lower polarity are used to introduce analytes into a mobile phase of higher polarity. Tetrahydrofuran was recommended where acetonitrile is used as the organic component of the mobile phase. Extraction and enrichment of analytes from spiked urine samples was successfully achieved using a hollow fibre liquid phase microextraction. The conditions for a simultaneous extraction of muscimol, tryptophan and tryptamine were a 20% (v/v) diluted urine sample at pH 4, an acceptor concentration of 200 mM HCl, 20% (w/w) DEHPA in DHE supported on the walls of a hollow fibre and stirring at 800 rpm for 60 mins. These universal factor values were biased towards maximizing the extraction of muscimol.

The optimization procedure was meant to influence selectivity of the carrier-mediated microextraction towards muscimol, tryptophan and tryptamine. However the complexity of urine resulted in peaks that could not be completely resolved from the analyte peaks. This was an indication of inability of the hollow fibre and the carrier molecule to completely discriminate analytes from the matrix. Thus the lack of method specificity or selectivity was compensated by calculating matrix effects which were in turn used to construct matrix-based calibration curves.

Good coefficients of determination denoted by  $r^2$  were obtained from matrix-based calibration curves and ranged from 0.9933 to 0.9986. Compared to other methods that have been applied for the extraction and quantification of muscimol from urine samples, the developed method offered better limits of detection of  $0.021 \mu\text{g mL}^{-1}$  for the extraction of muscimol. The enrichment factor values of



4.1, 19.7 and 24.1 for muscimol, tryptophan and tryptamine respectively were comparable with carrier-mediated HF-LPME enrichments of other compounds of similar polarity in the presence of matrix. Fair repeatability RSD values of the enrichment factors of 8.3%, 13.1% and 10.2% respectively were obtained.

Dark yellow urine was used for matrix-based studies implying that the values reported in this research were the minimum possible for extraction of muscimol and its two precursors from a 20% (v/v) diluted urine solution. Also an acceptor of 200 mM HCl was considerably of lower acid concentration. A better H<sup>+</sup> ion gradient and hence higher enrichment values would be obtained if a more concentrated HCl acceptor phase was used.

The optimum factor values for individual extractions were different for each analyte. Because muscimol was the analyte of interest in this research, its optimum factor values were set as universal conditions for a simultaneous extraction. A compound desirability of 0.687 was considered acceptable considering that only one response output was used in determining the overall conditions of extraction.

The results of this study are an indication that the developed HF-LPME method can be a viable alternative in the extraction and quantification of muscimol from urine samples. The method is environmentally friendly and has a further advantage of ensuring that sample extraction and clean-up are achieved in a single step with no need for a derivatization step.

## **6.2 Recommendations**

Accuracy could have been addressed by applying the method on certified reference materials or comparing with another well-validated procedure. Hallucinogenic compounds are schedule 1 drugs and it was impossible to obtain their CRM in urine matrix. Neither could we obtain samples from individuals that had consumed hallucinogenic mushrooms. Administering MUS into volunteers could not be done as specialised monitoring procedures and appropriate therapy

protocol would have been required to address potential risks associated with hallucinating (Garcia et al., 2015; Johnson et al., 2008).

Peak identification was achieved by comparison of elution times of analytes when these analytes were spiked into the acceptor phase that had been diluted accordingly with specific diluents for injection into the HPLC. An HPLC-MS detector could have been a better instrument for analyte identification.

System suitability was limited to an HPLC-UV approach. An MS detector could have been used in order to identify the analytes and interfering compounds. A better H<sup>+</sup> ion gradient and hence higher EF values are predicted if a more concentrated HCl acceptor phase was used.

## 7 REFERENCES

- Abadi, M.D.M., Ashraf, N., Chamsaz, M., Shemirani, F., 2012. An overview of liquid phase microextraction approaches combined with UV–Vis spectrophotometry. *Talanta* 99, 1–12.
- Akers, B.P., Ruiz, J.F., Piper, A., Ruck, C.A., 2011. A Prehistoric Mural in Spain Depicting Neurotropic Psilocybe Mushrooms? 1. *Econ. Bot.* 65, 121–128.
- Al Azzam, K.M., Makahleah, A., Saad, B., Mansor, S.M., 2010. Hollow fiber liquid-phase microextraction for the determination of trace amounts of rosiglitazone (anti-diabetic drug) in biological fluids using capillary electrophoresis and high performance liquid chromatographic methods. *J. Chromatogr. A* 1217, 3654–3659.
- Anastos, N., Barnett, N., Pfeffer, F., Lewis, S., 2006. Investigation into the temporal stability of aqueous standard solutions of psilocin and psilocybin using high performance liquid chromatography. *Sci. Justice* 46, 91–96.
- Asensio-Ramos, M., Ravelo-Pérez, L.M., González-Curbelo, M.Á., Hernández-Borges, J., 2011. Liquid phase microextraction applications in food analysis. *J. Chromatogr. A* 1218, 7415–7437.
- Asselborn, G., Wennig, R., Yegles, M., 2000. Tragic flying attempt under the influence of “magic mushrooms.” *Probl Forensic Sci* 42, 41–6.
- Atkinson, A.C., Donev, A.N., Tobias, R.D., 2007. Optimum experimental designs, with SAS. Oxford University Press Oxford.
- Becker, A., Grecksch, G., Bernstein, H.-G., Höllt, V., Bogerts, B., 1999. Social behaviour in rats lesioned with ibotenic acid in the hippocampus: quantitative and qualitative analysis. *Psychopharmacology (Berl.)* 144, 333–338.
- Bello-López, M.Á., Ramos-Payán, M., Ocaña-González, J.A., Fernández-Torres, R., Callejón-Mochón, M., 2012. Analytical applications of hollow fiber liquid phase microextraction (HF-LPME): a review. *Anal. Lett.* 45, 804–830.
- Berge, J.T., 1999. Breakdown or breakthrough? A history of European research into drugs and creativity. *J. Creat. Behav.* 33, 257–276.

- Bezerra, M.A., Santelli, R.E., Oliveira, E.P., Villar, L.S., Escalera, L.A., 2008. Response surface methodology (RSM) as a tool for optimization in analytical chemistry. *Talanta* 76, 965–977.
- Bigwood, J., Beug, M.W., 1982. Variation of psilocybin and psilocin levels with repeated flushes (harvests) of mature sporocarps of *Psilocybe cubensis* (Earle) Singer. *J. Ethnopharmacol.* 5, 287–291.
- Björnstad, K., Beck, O., Helander, A., 2009. A multi-component LC–MS/MS method for detection of ten plant-derived psychoactive substances in urine. *J. Chromatogr. B* 877, 1162–1168.
- Box, G.E., Hunter, J.S., 1961. The 2<sup>k</sup>—p fractional factorial designs. *Technometrics* 3, 311–351.
- Box, G.E., Hunter, J.S., Hunter, W.G., 2005. *Statistics for experimenters: design, innovation, and discovery.* Wiley-Interscience New York.
- Brandt, S.D., Martins, C.P., 2010. Analytical methods for psychoactive N, N-dialkylated tryptamines. *TrAC Trends Anal. Chem.* 29, 858–869.
- Brunzel, N.A., 2013. *Fundamentals of urine and body fluid analysis.* Elsevier Health Sciences.
- Buszewski, B., Noga, S., 2012. Hydrophilic interaction liquid chromatography (HILIC)—a powerful separation technique. *Anal. Bioanal. Chem.* 402, 231–247.
- Carley, K.M., Kamneva, N.Y., Reminga, J., 2004. Response surface methodology. DTIC Document.
- Cheng, T., Zhao, Y., Li, X., Lin, F., Xu, Y., Zhang, X., Li, Y., Wang, R., Lai, L., 2007. Computation of octanol-water partition coefficients by guiding an additive model with knowledge. *J. Chem. Inf. Model.* 47, 2140–2148.
- Chen, J., Li, M., Yan, X., Wu, E., Zhu, H., Lee, K.J., Zhan, L., Lee, W., Kang, J.S., 2011. Determining the pharmacokinetics of psilocin in rat plasma using ultra-performance liquid chromatography coupled with a photodiode array detector after orally administering an extract of *Gymnopilus spectabilis*. *J. Chromatogr. B* 879, 2669–2672.
- Chen, Y., Pawliszyn, J., 2004. Kinetics and the on-site application of standards in a solid-phase microextraction fiber. *Anal. Chem.* 76, 5807–5815.

- Chiao, C.-H., Hamada, M., 2001. Analyzing experiments with correlated multiple responses. *J. Qual. Technol.* 33, 451.
- Chimuka, L., Cukrowska, E., Michel, M., Buszewski, B., 2011. Advances in sample preparation using membrane-based liquid-phase microextraction techniques. *TrAC Trends Anal. Chem.* 30, 1781–1792.
- Chimuka, L., Mathiasson, L., Jönsson, J.Å., 2000. Role of octanol–water partition coefficients in extraction of ionisable organic compounds in a supported liquid membrane with a stagnant acceptor. *Anal. Chim. Acta* 416, 77–86.
- Chimuka, L., Msagati, T.A., Cukrowska, E., Tutu, H., 2010. Critical parameters in a supported liquid membrane extraction technique for ionizable organic compounds with a stagnant acceptor phase. *J. Chromatogr. A* 1217, 2318–2325.
- Chirita, R.-I., West, C., Finaru, A.-L., Elfakir, C., 2010. Approach to hydrophilic interaction chromatography column selection: Application to neurotransmitters analysis. *J. Chromatogr. A* 1217, 3091–3104.
- Cochran, W.G., Cox, G.M., 1957. *Experimental designs* .
- Condra, L., 2001. *Reliability Improvement With Design of Experiment*. CRC Press.
- Cox, D.R., Reid, N., 2000. *The theory of the design of experiments*. CRC Press.
- Cui, S., Ouyang, G., Duan, G., Hou, J., Luan, T., Zhang, X., 2012. The mass transfer dynamics of hollow fiber liquid-phase microextraction and its application for rapid analysis of biological samples. *J. Chromatogr. A* 1266, 10–16.
- Czitrom, V., 1999. One-factor-at-a-time versus designed experiments. *Am. Stat.* 53, 126–131.
- Dadfarnia, S., Shabani, A.M.H., 2010. Recent development in liquid phase microextraction for determination of trace level concentration of metals—A review. *Anal. Chim. Acta* 658, 107–119.
- Deja, S., Jawień, E., Jasicka-Misiak, I., Halama, M., Wieczorek, P., Kafarski, P., Młynarz, P., 2014. Rapid determination of ibotenic acid and muscimol in human urine. *Magn Reson Chem* 52, 711–714.

- Del Castillo, E., Montgomery, D.C., McCarville, D.R., 1996. Modified desirability functions for multiple response optimization. *J. Qual. Technol.* 28, 337–345.
- Dinh, N.P., Jonsson, T., Irgum, K., 2013. Water uptake on polar stationary phases under conditions for hydrophilic interaction chromatography and its relation to solute retention. *J. Chromatogr. A* 1320, 33–47.
- Dziarkowska, K., Jönsson, J. Åke, Wieczorek, P.P., 2008. Single hollow fiber SLM extraction of polyamines followed by tosyl chloride derivatization and HPLC determination. *Anal. Chim. Acta* 606, 184–193.
- Ebrahimpour, B., Yamini, Y., Esrafil, A., 2011a. Extraction of azole antifungal drugs from milk and biological fluids using a new hollow fiber liquid-phase microextraction and analysis by GC-FID. *Chromatographia* 74, 281–289.
- Ebrahimpour, B., Yamini, Y., Esrafil, A., 2011b. Extraction of azole antifungal drugs from milk and biological fluids using a new hollow fiber liquid-phase microextraction and analysis by GC-FID. *Chromatographia* 74, 281–289.
- Ebrahimzadeh, H., Asgharinezhad, A.A., Abedi, H., Kamarei, F., 2011. Optimization of carrier-mediated three-phase hollow fiber microextraction combined with HPLC-UV for determination of propylthiouracil in biological samples. *Talanta* 85, 1043–1049.
- Ebrahimzadeh, H., Shekari, N., Saharkhiz, Z., Asgharinezhad, A.A., 2012. Simultaneous determination of chlorpheniramine maleate and dextromethorphan hydrobromide in plasma sample by hollow fiber liquid phase microextraction and high performance liquid chromatography with the aid of chemometrics. *Talanta* 94, 77–83.
- Emídio, E.S., de Menezes Prata, V., De Santana, F.J.M., Dórea, H.S., 2010. Hollow fiber-based liquid phase microextraction with factorial design optimization and gas chromatography–tandem mass spectrometry for determination of cannabinoids in human hair. *J. Chromatogr. B* 878, 2175–2183.

- Ferreira, S.L.C., Bruns, R.E., da Silva, E.G.P., dos Santos, W.N.L., Quintella, C.M., David, J.M., de Andrade, J.B., Breikreitz, M.C., Jardim, I.C.S.F., Neto, B.B., 2007. Statistical designs and response surface techniques for the optimization of chromatographic systems. *J. Chromatogr. A* 1158, 2–14.
- Fotouhi, L., Yamini, Y., Molaei, S., Seidi, S., 2011. Comparison of conventional hollow fiber based liquid phase microextraction and electromembrane extraction efficiencies for the extraction of ephedrine from biological fluids. *J. Chromatogr. A* 1218, 8581–8586.
- Franceschini, G., Macchietto, S., 2008. Model-based design of experiments for parameter precision: State of the art. *Chem. Eng. Sci.* 63, 4846–4872.
- Gable, R.S., 2004. Comparison of acute lethal toxicity of commonly abused psychoactive substances. *Addiction* 99, 686–696.
- Garcia, J., Costa, V.M., Costa, A.E., Andrade, S., Carneiro, A.C., Conceição, F., Paiva, J.A., de Pinho, P.G., Baptista, P., de Lourdes Bastos, M., 2015. Co-ingestion of amatoxins and isoxazoles-containing mushrooms and successful treatment: A case report. *Toxicol.* 103, 55–59.
- Gennaro, M., Giacosa, D., Gioannini, E., Angelino, S., 1997. Hallucinogenic species in *Amanita muscaria*. Determination of muscimol and ibotenic acid by ion-interaction HPLC. *J. Liq. Chromatogr. Relat. Technol.* 20, 413–424.
- Geyer, M.A., Vollenweider, F.X., 2008. Serotonin research: contributions to understanding psychoses. *Trends Pharmacol. Sci.* 29, 445–453.
- Ghaffarzaghan, T., Nyman, M., Jönsson, J.Å., Sandahl, M., 2014. Determination of bile acids by hollow fibre liquid-phase microextraction coupled with gas chromatography. *J. Chromatogr. B* 944, 69–74.
- Ghambarian, M., Yamini, Y., Esrafil, A., 2012. Developments in hollow fiber based liquid-phase microextraction: principles and applications. *Microchim. Acta* 177, 271–294.
- Ghambarian, M., Yamini, Y., Esrafil, A., 2011. Three-phase hollow fiber liquid-phase microextraction based on two immiscible organic solvents for

- determination of tramadol in urine and plasma samples. *J. Pharm. Biomed. Anal.* 56, 1041–1045.
- Ginterová, P., Sokolová, B., Ondra, P., Znaležiona, J., Petr, J., Ševčík, J., Maier, V., 2014. Determination of mushroom toxins ibotenic acid, muscimol and muscarine by capillary electrophoresis coupled with electrospray tandem mass spectrometry. *Talanta* 125, 242–247.
- Guideline, E., 1995. Note for Guidance on Validation of Analytical Procedures Methodology. CPMP/ICH/281/95.
- Gunst, R.F., Mason, R.L., 2009. Fractional factorial design. *Wiley Interdiscip. Rev. Comput. Stat.* 1, 234–244.
- Guo, Y., Gaiki, S., 2011. Retention and selectivity of stationary phases for hydrophilic interaction chromatography. *J. Chromatogr. A* 1218, 5920–5938.
- Guo, Y., Srinivasan, S., Gaiki, S., 2007. Investigating the effect of chromatographic conditions on retention of organic acids in hydrophilic interaction chromatography using a design of experiment. *Chromatographia* 66, 223–229.
- Guzmán, G., Allen, J.W., Gartz, J., 1998. A worldwide geographical distribution of the neurotropic fungi, an analysis and discussion. *Ann Mus Civ Rovereto* 14, 189–280.
- Hadjmohammadi, M., Ghambari, H., 2012. Three-phase hollow fiber liquid phase microextraction of warfarin from human plasma and its determination by high-performance liquid chromatography. *J. Pharm. Biomed. Anal.* 61, 44–49.
- Han, D.-D., Row, K.-H., 2010. Analysis of Matrine Alkaloids in Human Urine by Hollow Fiber Liquid-phase Microextraction with High-performance Liquid Chromatography. *J. Korean Chem. Soc.* 54, 38–42.
- Han, D., Row, K.H., 2012. Trends in liquid-phase microextraction, and its application to environmental and biological samples. *Microchim. Acta* 176, 1–22.
- Hasegawa, K., Gonmori, K., Fujita, H., Kamijo, Y., Nozawa, H., Yamagishi, I., Minakata, K., Watanabe, K., Suzuki, O., 2013. Determination of ibotenic



- acid and muscimol, the Amanita mushroom toxins, in human serum by liquid chromatography–tandem mass spectrometry. *Forensic Toxicol.* 31, 322–327.
- Hasler, F., Bourquin, D., Brenneisen, R., Vollenweider, F.X., 2002. Renal excretion profiles of psilocin following oral administration of psilocybin: a controlled study in man. *J. Pharm. Biomed. Anal.* 30, 331–339.
- Hasler, F., Grimberg, U., Benz, M.A., Huber, T., Vollenweider, F.X., 2004. Acute psychological and physiological effects of psilocybin in healthy humans: a double-blind, placebo-controlled dose–effect study. *Psychopharmacology (Berl.)* 172, 145–156.
- Hemström, P., Irgum, K., 2006. Hydrophilic interaction chromatography. *J. Sep. Sci.* 29, 1784–1821.
- Hinkelmann, K., Kempthorne, O., n.d. Fractional Factorial Designs. *Des. Anal. Exp. Adv. Exp. Des. Vol. 2* 507–563.
- Ho, T.S., Halvorsen, T.G., Pedersen-Bjergaard, S., Rasmussen, K.E., 2003. Liquid-phase microextraction of hydrophilic drugs by carrier-mediated transport. *J. Chromatogr. A* 998, 61–72.
- Ho, T.S., Reubsaet, J.L.E., Anthonsen, H.S., Pedersen-Bjergaard, S., Rasmussen, K.E., 2005. Liquid-phase microextraction based on carrier mediated transport combined with liquid chromatography–mass spectrometry: new concept for the determination of polar drugs in a single drop of human plasma. *J. Chromatogr. A* 1072, 29–36.
- Hyder, M., Jönsson, J.Å., 2012. Hollow-fiber liquid phase microextraction for lignin pyrolysis acids in aerosol samples and gas chromatography–mass spectrometry analysis. *J. Chromatogr. A* 1249, 48–53.
- Johnson, M.W., Richards, W.A., Griffiths, R.R., 2008. Human hallucinogen research: guidelines for safety. *J. Psychopharmacol. (Oxf.)*.
- Jönsson, J.Å., Mathiasson, L., 2000. Membrane-based techniques for sample enrichment. *J. Chromatogr. A* 902, 205–225.
- Kamata, T., Katagi, M., Tsuchihashi, H., 2010. Metabolism and toxicological analyses of hallucinogenic tryptamine analogues being abused in Japan. *Forensic Toxicol.* 28, 1–8.

- Khuri, A.I., Mukhopadhyay, S., 2010. Response surface methodology. Wiley Interdiscip. Rev. Comput. Stat. 2, 128–149.
- Kovács, A., Wojnárovits, L., Baranyai, M., Moussa, A., Othman, I., McLaughlin, W., 1999. Radiolytic reactions of nitro blue tetrazolium under oxidative and reductive conditions: a pulse radiolysis study. Radiat. Phys. Chem. 55, 795–798.
- Lee, J., Lee, H.K., Rasmussen, K.E., Pedersen-Bjergaard, S., 2008. Environmental and bioanalytical applications of hollow fiber membrane liquid-phase microextraction: a review. Anal. Chim. Acta 624, 253–268.
- Lezamiz, J., Barri, T., Jönsson, J.Å., Skog, K., 2008. A simplified hollow-fibre supported liquid membrane extraction method for quantification of 2-amino-1-methyl-6-phenylimidazo [4, 5-b] pyridine (PhIP) in urine and plasma samples. Anal. Bioanal. Chem. 390, 689–696.
- Lezamiz, J., Jönsson, J.Å., 2007. Development of a simple hollow fibre supported liquid membrane extraction method to extract and preconcentrate dinitrophenols in environmental samples at ngL<sup>-1</sup> level by liquid chromatography. J. Chromatogr. A 1152, 226–233.
- Li, B., Petersen, N.J., Payán, M.D.R., Hansen, S.H., Pedersen-Bjergaard, S., 2014. Design and implementation of an automated liquid-phase microextraction-chip system coupled on-line with high performance liquid chromatography. Talanta 120, 224–229.
- Lindenblatt, H., Krämer, E., Holzmann-Erens, P., Gouzoulis-Mayfrank, E., Kovar, K.-A., 1998. Quantitation of psilocin in human plasma by high-performance liquid chromatography and electrochemical detection: comparison of liquid–liquid extraction with automated on-line solid-phase extraction. J. Chromatogr. B. Biomed. Sci. App. 709, 255–263.
- Lin, H., Wang, J., Zeng, L., Li, G., Sha, Y., Wu, D., Liu, B., 2013. Development of solvent micro-extraction combined with derivatization. J. Chromatogr. A 1296, 235–242.
- Lin, S.-H., Chen, C.-N., 2006. Simultaneous reactive extraction separation of amino acids from water with D2EHPA in hollow fiber contactors. J. Membr. Sci. 280, 771–780.

- Manevski, N., Kurkela, M., Höglund, C., Mauriala, T., Yli-Kauhaluoma, J., Finel, M., 2010. Glucuronidation of psilocin and 4-hydroxyindole by the human UDP-glucuronosyltransferases. *Drug Metab. Dispos.* 38, 386–395.
- Marcano, V., Méndez, A.M., Castellano, F., Salazar, F., Martinez, L., 1994. Occurrence of psilocybin and psilocin in *Psilocybe pseudobullacea* (Petch) Pegler from the Venezuelan Andes. *J. Ethnopharmacol.* 43, 157–159.
- Marickar, Y.F., 2010. Electrical conductivity and total dissolved solids in urine. *Urol. Res.* 38, 233–235.
- Martin, R., Schürenkamp, J., Pfeiffer, H., Lehr, M., Köhler, H., 2014. Synthesis, hydrolysis and stability of psilocin glucuronide. *Forensic Sci. Int.* 237, 1–6.
- McCalley, D.V., 2010. Study of the selectivity, retention mechanisms and performance of alternative silica-based stationary phases for separation of ionised solutes in hydrophilic interaction chromatography. *J. Chromatogr. A* 1217, 3408–3417.
- McCalley, D.V., Neue, U.D., 2008. Estimation of the extent of the water-rich layer associated with the silica surface in hydrophilic interaction chromatography. *J. Chromatogr. A* 1192, 225–229.
- Michelot, D., Melendez-Howell, L.M., 2003. *Amanita muscaria*: chemistry, biology, toxicology, and ethnomycology. *Mycol. Res.* 107, 131–146.
- Miles, P.G., Chang, S.-T., 2004. *Mushrooms: cultivation, nutritional value, medicinal effect, and environmental impact.* CRC press.
- Miller, J.N., Miller, J.C., 2005. *Statistics and chemometrics for analytical chemistry.* Pearson Education.
- Miraeae, S.N., Qomi, M., Shamschiri, F., Raoufi, P., 2014. Hollow-Fiber liquid-phase Microextraction Followed By High Performance Liquid Chromatography For The Determination Of Trace Amounts Of Methylphenidate Hydrochloride in Biological Fluids. *Biomed. Pharmacol. J.* 7, 715–725.
- Montgomery, D.C., Runger, G.C., Hubele, N.F., 2009. *Engineering statistics.* John Wiley & Sons.

- Mursyid, M.A., Saberi, W.M., 2010. Comparison between method of one-factor-at-a-time (OFAT) & design of experiment (DOE) in screening of immunoglobulin production stimulating factors.
- Myers, W.R., Montgomery, D.C., 2003. Response surface methodology. *Encycl Biopharm Stat* 1, 858–869.
- Nichols, D.E., 2004. Hallucinogens. *Pharmacol. Ther.* 101, 131–181.
- Passie, T., Seifert, J., Schneider, U., Emrich, H.M., 2002a. The pharmacology of psilocybin. *Addict. Biol.* 7, 357–364.
- Passie, T., Seifert, J., Schneider, U., Emrich, H.M., 2002b. The pharmacology of psilocybin. *Addict. Biol.* 7, 357–364.
- Payán, M.R., López, M.Á.B., Fernández-Torres, R., González, J.A.O., Mochón, M.C., 2011a. Hollow fiber-based liquid phase microextraction (HF-LPME) as a new approach for the HPLC determination of fluoroquinolones in biological and environmental matrices. *J. Pharm. Biomed. Anal.* 55, 332–341.
- Payán, M.R., López, M.Á.B., Fernández-Torres, R., Mochón, M.C., Ariza, J.L.G., 2010. Application of hollow fiber-based liquid-phase microextraction (HF-LPME) for the determination of acidic pharmaceuticals in wastewaters. *Talanta* 82, 854–858.
- Payán, M.R., López, M.Á.B., Fernández-Torres, R., Navarro, M.V., Mochón, M.C., 2011b. Hollow fiber-based liquid phase microextraction (HF-LPME) for a highly sensitive HPLC determination of sulfonamides and their main metabolites. *J. Chromatogr. B* 879, 197–204.
- Pedersen-Bjergaard, S., Ho, T.S., Rasmussen, K.E., 2002. Fundamental studies on selectivity in 3-phase liquid-phase microextraction (LPME) of basic drugs. *J. Sep. Sci.* 25, 141–146.
- Pena-Pereira, F., Lavilla, I., Bendicho, C., 2010a. Liquid-phase microextraction approaches combined with atomic detection: A critical review. *Anal. Chim. Acta* 669, 1–16.
- Pena-Pereira, F., Lavilla, I., Bendicho, C., 2010b. Liquid-phase microextraction techniques within the framework of green chemistry. *TrAC Trends Anal. Chem.* 29, 617–628.

- Pichini, S., Marchei, E., García-Algar, O., Gomez, A., Di Giovannandrea, R., Pacifici, R., 2014. Ultra-high-pressure liquid chromatography tandem mass spectrometry determination of hallucinogenic drugs in hair of psychedelic plants and mushrooms consumers. *J. Pharm. Biomed. Anal.* 100, 284–289.
- Poliwoda, A., Krzyżak, M., Wieczorek, P.P., 2010. Supported liquid membrane extraction with single hollow fiber for the analysis of fluoroquinolones from environmental surface water samples. *J. Chromatogr. A* 1217, 3590–3597.
- Quintana, J.B., Rodil, R., Reemtsma, T., 2004. Suitability of hollow fibre liquid-phase microextraction for the determination of acidic pharmaceuticals in wastewater by liquid chromatography–electrospray tandem mass spectrometry without matrix effects. *J. Chromatogr. A* 1061, 19–26.
- Ripp, J., 1996. Analytical detection limit guidance & laboratory guide for determining method detection limits. Wisconsin Department of Natural Resources, Laboratory Certification Program.
- Rogers, R., 2011. *The fungal pharmacy: the complete guide to medicinal mushrooms and lichens of North America*. North Atlantic Books.
- Romero, R., Jönsson, J.Å., Gázquez, D., Bagur, M.G., Sánchez-Viñas, M., 2002. Multivariate optimization of supported liquid membrane extraction of biogenic amines from wine samples prior to liquid chromatography determination as dabsyl derivatives. *J. Sep. Sci.* 25, 584–592.
- Rossmesl, J.H., Higgins, M.A., Blodgett, D.J., Ellis, M., Jones, D.E., 2006. *Amanita muscaria* toxicosis in two dogs. *J. Vet. Emerg. Crit. Care* 16, 208–214.
- Rubel, W., Arora, D., 2008. A study of cultural bias in field guide determinations of mushroom edibility using the iconic mushroom, *Amanita muscaria*, as an example. *Econ. Bot.* 62, 223–243.
- Ruck, C.A., Bigwood, J., Staples, D., Ott, J., Wasson, R.G., 1979. *Entheogens*. *J. Psychoactive Drugs* 11, 145–146.
- Rueda, M., Sarabia, L., Herrero, A., Ortiz, M., 2003. Optimisation of a flow injection system with electrochemical detection using the desirability

- function: application to the determination of hydroquinone in cosmetics. *Anal. Chim. Acta* 479, 173–184.
- Saaid, M., Saad, B., Ali, A.S.M., Saleh, M.I., Basheer, C., Lee, H.K., 2009. In situ derivatization hollow fibre liquid-phase microextraction for the determination of biogenic amines in food samples. *J. Chromatogr. A* 1216, 5165–5170.
- Saito, K., Toyo'oka, T., Kato, M., Fukushima, T., Shiota, O., Goda, Y., 2005. Determination of psilocybin in hallucinogenic mushrooms by reversed-phase liquid chromatography with fluorescence detection. *Talanta* 66, 562–568.
- Shariati, S., Yamini, Y., Esrafil, A., 2009. Carrier mediated hollow fiber liquid phase microextraction combined with HPLC–UV for preconcentration and determination of some tetracycline antibiotics. *J. Chromatogr. B* 877, 393–400.
- Shrivastava, A., Gupta, V.B., 2011. Methods for the determination of limit of detection and limit of quantitation of the analytical methods. *Chron. Young Sci.* 2, 21.
- Sticht, G., Käferstein, H., 2000. Detection of psilocin in body fluids. *Forensic Sci. Int.* 113, 403–407.
- Stříbrný, J., Sokol, M., Merová, B., Ondra, P., 2012. GC/MS determination of ibotenic acid and muscimol in the urine of patients intoxicated with *Amanita pantherina*. *Int. J. Legal Med.* 126, 519–524.
- Tahmasebi, E., Yamini, Y., Saleh, A., 2009. Extraction of trace amounts of pioglitazone as an anti-diabetic drug with hollow fiber liquid phase microextraction and determination by high-performance liquid chromatography-ultraviolet detection in biological fluids. *J. Chromatogr. B* 877, 1923–1929.
- Tsujikawa, K., Kuwayama, K., Miyaguchi, H., Kanamori, T., Iwata, Y., Inoue, H., Yoshida, T., Kishi, T., 2007. Determination of muscimol and ibotenic acid in *Amanita* mushrooms by high-performance liquid chromatography and liquid chromatography-tandem mass spectrometry. *J. Chromatogr. B* 852, 430–435.

- US Food and Drug Administration, 1996. Guidance for industry: Q2B validation of analytical procedures: methodology. Rockv. MD Nov.
- van Amsterdam, J., Opperhuizen, A., van den Brink, W., 2011. Harm potential of magic mushroom use: a review. *Regul. Toxicol. Pharmacol.* 59, 423–429.
- Van Pinxteren, D., Teich, M., Herrmann, H., 2012. Hollow fibre liquid-phase microextraction of functionalised carboxylic acids from atmospheric particles combined with capillary electrophoresis/mass spectrometric analysis. *J. Chromatogr. A* 1267, 178–188.
- Vollenweider, F., VontobeJ, P., Leendersz, K., Hell, D., 1998. 5-HT stimulation increases basal ganglia dopamine release in human humel psychosis: A pet study with [11 C] raclopride. *Schizophr. Res.* 29, 96.
- Wittmann, M., Carter, O., Hasler, F., Cahn, B.R., Grimberg, U., Spring, P., Hell, D., Flohr, H., Vollenweider, F.X., 2007. Effects of psilocybin on time perception and temporal control of behaviour in humans. *J. Psychopharmacol. (Oxf.)* 21, 50–64.
- Wurst, M., Kysilka, R., Koza, T., 1992. Analysis and isolation of indole alkaloids of fungi by high-performance liquid chromatography. *J. Chromatogr. A* 593, 201–208.
- Wu, W., Cui, G., Lu, B., 2000. Optimization of multiple evariables: application of central composite design and overall desirability. *Chin. Pharm. J.-BEIJING-* 35, 530–532.
- Xiao-Wang, T., Yan-Xi, S., Rui-Ping, W., Gu-Yang, Y., 2012. Determination of trace bisphenol A in water using three-phase hollow fiber liquid-phase microextraction coupled with high performance liquid chromatography. *Chin. J. Anal. Chem.* 40, 1409–1414.
- Xu, B., Chen, M., Hou, J., Chen, X., Zhang, X., Cui, S., 2015. Calibration of pre-equilibrium HF-LPME and its application to the rapid determination of free analytes in biological fluids. *J. Chromatogr. B* 980, 28–33.
- Yamini, Y., Reimann, C.T., Vatanara, A., Jönsson, J.Å., 2006. Extraction and preconcentration of salbutamol and terbutaline from aqueous samples using hollow fiber supported liquid membrane containing anionic carrier. *J. Chromatogr. A* 1124, 57–67.

- Yang, Y., Chen, J., Shi, Y.-P., 2010. Determination of aconitine, hypaconitine and mesaconitine in urine using hollow fiber liquid-phase microextraction combined with high-performance liquid chromatography. *J. Chromatogr. B* 878, 2811–2816.
- Ziegel, E.R., 2004. *Statistics and Chemometrics for Analytical Chemistry*. Technometrics 46, 498–499.



## APPENDIX

Table A 1 Randomized design table showing 32 experimental runs. The two levels of each of the six factors are sign coded

Run	A	B	C	D	E	F
1	-	+	-	-	-	+
2	+	-	-	-	+	-
3	-	-	+	+	-	-
4	+	+	+	+	+	+
5	-	+	-	+	+	+
6	+	+	-	-	-	-
7	-	-	+	+	+	+
8	-	-	+	-	+	-
9	+	-	-	+	+	+
10	+	-	+	-	+	+
11	-	-	-	-	-	-
12	+	-	+	+	+	-
13	-	-	-	+	-	+
14	-	-	+	-	-	+
15	+	-	+	+	-	+
16	-	+	-	-	+	-
17	-	+	+	+	+	-
18	+	-	-	+	-	-
19	+	-	-	-	-	+
20	+	+	-	-	+	+
21	-	-	-	+	+	-
22	+	+	-	+	-	+
23	+	+	-	+	+	-

24	-	+	+	-	-	-
25	-	+	+	+	-	+
26	-	+	-	+	-	-
27	+	-	+	-	-	-
28	-	-	-	-	+	+
29	+	+	+	+	-	-
30	-	+	+	-	+	+
31	+	+	+	-	-	+
32	+	+	+	-	+	-

---

Table A 2 Randomized central composite design for the essential factors for MUS at  $\alpha = 2$

Run	A	B	C	D
1	-2	0	0	0
2	0	2	0	0
3	0	0	0	-2
4	0	-2	0	0
5	0	0	-2	0
6	0	0	2	0
7	0	0	0	2
8	0	0	0	0
9	0	0	0	0
10	2	0	0	0
11	-1	1	-1	1
12	0	0	0	0
13	0	0	0	0
14	1	-1	-1	-1
15	1	-1	1	-1
16	-1	1	1	1
17	1	1	1	-1
18	-1	-1	1	-1
19	-1	-1	1	1
20	1	1	-1	1
21	1	-1	1	1
22	-1	-1	-1	1
23	0	0	0	0
24	-1	-1	-1	-1
25	1	-1	-1	1
26	1	1	1	1
27	-1	1	-1	-1
28	1	1	-1	-1
29	0	0	0	0
30	-1	1	1	-1

Table A 3 Randomized coded CCD for the essential factors for MUS at  $\alpha = 2$

Run	A	B	C	D
1	0	0	0	2
2	2	0	0	0
3	0	0	-2	0
4	0	0	0	-2
5	0	0	0	0
6	0	-2	0	0
7	-2	0	0	0
8	0	0	2	0
9	0	0	0	0
10	0	2	0	0
11	-1	1	-1	-1
12	1	1	-1	-1
13	1	1	1	1
14	0	0	0	0
15	-1	1	1	1
16	1	1	1	1
17	1	1	-1	1
18	-1	1	-1	1
19	-1	-1	1	-1
20	-1	-1	1	1
21	-1	1	1	-1
22	-1	-1	-1	-1
23	1	1	1	-1
24	0	0	0	0
25	1	-1	-1	-1
26	0	0	0	0
27	1	-1	1	1
28	-1	-1	-1	1
29	1	-1	1	-1
30	0	0	0	0

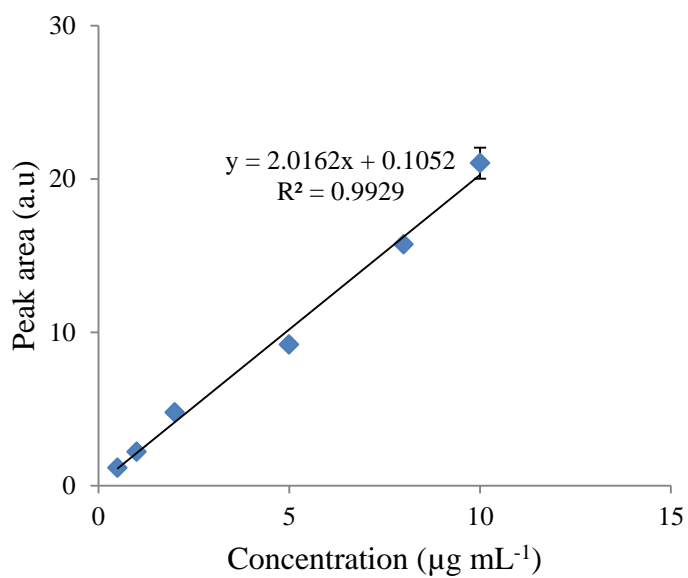


Figure A 1 Calibration curve for MUS (n = 3, SD)

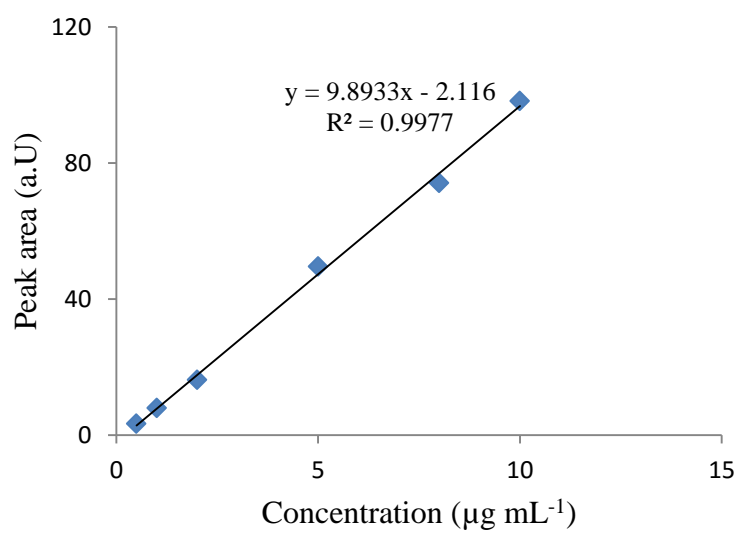


Figure A 2 Calibration curve for PSI (n = 3, SD)

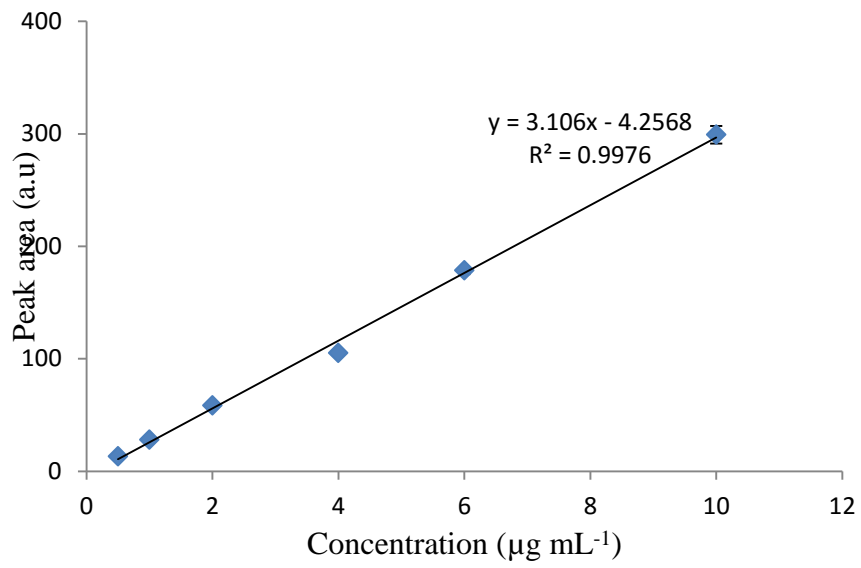


Figure A 3 Calibration curve for TRP (n = 3, SD)

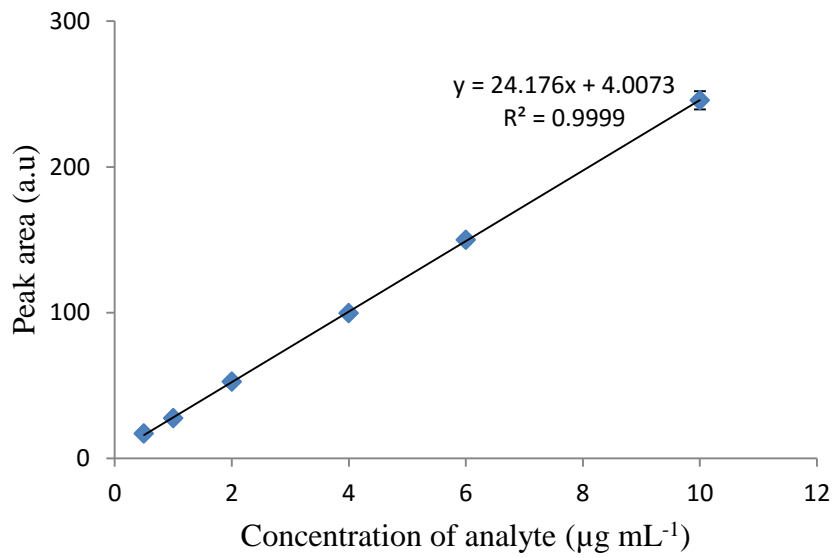


Figure A 4 Calibration curve for TA (n= 3, SD)

Table A 4 Peak areas for TA when 32 runs were investigated.

Run	DP	AP HCl	SLM	Extraction	Stirring					
Order	pH	conc	compo	time	rate	%NaCl	Peak Area 1	Peak Area 2	Peak Area 3	Average
1	3	100	5	10	600	0.01	59.866	53.866	56.296	56.676
2	7	10	5	10	800	0.001	31.709	33.705	29.847	31.754
3	3	10	20	30	600	0.001	71.662	74.426	74.092	73.393
4	7	100	20	30	800	0.01	441.497	456.479	449.002	448.993
5	3	100	5	30	800	0.01	61.521	61.057	62.157	61.578
6	7	100	5	10	600	0.001	16.204	18.820	19.479	18.168
7	3	10	20	30	800	0.01	71.563	73.190	71.784	72.179
8	3	10	20	10	800	0.001	80.475	80.725	80.578	80.593
9	7	10	5	30	800	0.01	69.610	68.289	68.713	68.871
10	7	10	20	10	800	0.01	110.686	111.577	110.830	111.031
11	3	10	5	10	600	0.001	33.437	31.668	31.937	32.347
12	7	10	20	30	800	0.001	96.446	95.746	95.631	95.941
13	3	10	5	30	600	0.01	34.644	35.736	35.049	35.143
14	3	10	20	10	600	0.01	76.848	76.954	76.599	76.800
15	7	10	20	30	600	0.01	123.207	122.530	123.637	123.125
16	3	100	5	10	800	0.001	55.323	59.056	55.874	56.751
17	3	100	20	30	800	0.001	289.361	290.385	291.201	290.316

18	7	10	5	30	600	0.001	27.766	26.030	26.893	26.896
19	7	10	5	10	600	0.01	47.753	39.743	39.649	42.382
20	7	100	5	10	800	0.01	67.659	71.480	69.346	69.495
21	3	10	5	30	800	0.001	47.842	48.286	47.978	48.035
22	7	100	5	30	600	0.01	72.697	71.890	73.295	72.627
23	7	100	5	30	800	0.001	61.973	64.573	64.149	63.565
24	3	100	20	10	600	0.001	170.143	168.789	169.310	169.414
25	3	100	20	30	600	0.01	333.275	329.136	327.376	329.929
26	3	100	5	30	600	0.001	34.062	29.230	33.027	32.106
27	7	10	20	10	600	0.001	87.369	91.882	91.573	90.275
28	3	10	5	10	800	0.01	34.030	32.233	34.536	33.600
29	7	100	20	30	600	0.001	479.605	456.772	467.892	468.090
30	3	100	20	10	800	0.01	165.085	164.553	170.857	166.832
31	7	100	20	10	600	0.01	230.043	221.228	227.793	226.355
32	7	100	20	10	800	0.001	294.154	300.395	299.356	297.968

---



Table A 5 Summary of variances of 32 runs done at 3 repeat experiments each

<i>Run</i>	<i>Count</i>	<i>Sum of peak areas</i>	<i>Average peak area</i>	<i>Variance</i>
1	3	170.028	56.676	9.108
2	3	95.261	31.754	3.723
3	3	220.18	73.393	2.276
4	3	1346.978	448.993	56.115
5	3	184.735	61.578	0.305
6	3	54.503	18.168	3.001
7	3	216.537	72.179	0.779
8	3	241.778	80.593	0.016
9	3	206.612	68.871	0.455
10	3	333.093	111.031	0.229
11	3	97.042	32.347	0.909
12	3	287.823	95.941	0.195
13	3	105.429	35.143	0.305
14	3	230.401	76.800	0.033
15	3	369.374	123.125	0.311
16	3	170.253	56.751	4.061
17	3	870.947	290.316	0.850
18	3	80.689	26.896	0.753
19	3	127.145	42.382	21.641
20	3	208.485	69.495	3.667
21	3	144.106	48.035	0.052
22	3	217.882	72.627	0.497
23	3	190.695	63.565	1.946
24	3	508.242	169.414	0.466
25	3	989.787	329.929	9.171
26	3	96.319	32.106	6.473
27	3	270.824	90.275	6.356
28	3	100.799	33.600	1.465
29	3	1404.269	468.090	130.366
30	3	500.495	166.832	12.223
31	3	679.064	226.355	20.978
32	3	893.905	297.968	11.182

Table A 6 Enrichment factor values for TA when 32 runs were investigated.

Run	DP	AP HCl	SLM	Extraction	Stirring		
Order	pH	conc	compo	time	rate	%NaCl	EF values
1	3	100	5	10	600		15.5
2	7	10	5	10	800	0.01	28.9
3	3	10	20	30	600	0.001	32.1
4	7	100	20	30	800	0.001	204.2
5	3	100	5	30	800	0.01	27.9
6	7	100	5	10	600	0.01	8.5
7	3	10	20	30	800	0.001	36.8
8	3	10	20	10	800	0.01	55.3
9	7	10	5	30	800	0.001	36.7
10	7	10	20	10	800	0.01	61.9
11	3	10	5	10	600	0.01	19.8
12	7	10	20	30	800	0.001	51.1
13	3	10	5	30	600	0.001	15.3
14	3	10	20	10	600	0.01	36.2
15	7	10	20	30	600	0.01	60.4
16	3	100	5	10	800	0.01	26.7
17	3	100	20	30	800	0.001	148.4
18	7	10	5	30	600	0.001	18.4
19	7	10	5	10	600	0.001	26.0
20	7	100	5	10	800	0.01	31.5
21	3	10	5	30	800	0.01	24.5
22	7	100	5	30	600	0.001	33.0
23	7	100	5	30	800	0.01	29.9
24	3	100	20	10	600	0.001	74.3
25	3	100	20	30	600	0.001	226.8
26	3	100	5	30	600	0.01	15.1
27	7	10	20	10	600	0.001	46.1
28	3	10	5	10	800	0.001	17.1
29	7	100	20	30	600	0.01	221.0
30	3	100	20	10	800	0.001	102.7
31	7	100	20	10	600	0.01	106.8
32	7	100	20	10	800	0.01	166.3

Table A 7 Peak area values for MUS when 32 runs were investigated.

Run	DP	AP HCl	SLM	Extraction	Stirring					
Order	pH	conc	compo	time	rate	%NaCl	Peak Area 1	Peak Area 2	Peak Area 3	Average
1	3	100	5	10	600	0.01	7.915	7.088	7.313	7.439
2	7	10	5	10	800	0.001	17.957	18.559	19.561	18.692
3	3	10	20	30	600	0.001	16.242	16.267	16.127	16.212
4	7	100	20	30	800	0.01	4.024	4.901	5.069	4.665
5	3	100	5	30	800	0.01	10.393	11.246	12.476	11.372
6	7	100	5	10	600	0.001	4.776	4.776	4.698	4.750
7	3	10	20	30	800	0.01	18.340	20.541	19.568	19.483
8	3	10	20	10	800	0.001	8.476	8.956	9.599	9.010
9	7	10	5	30	800	0.01	5.638	5.176	5.712	5.509
10	7	10	20	10	800	0.01	8.517	9.927	10.859	9.768
11	3	10	5	10	600	0.001	3.690	4.224	4.168	4.027
12	7	10	20	30	800	0.001	11.729	12.089	9.384	11.067
13	3	10	5	30	600	0.01	6.812	7.075	7.106	6.998
14	3	10	20	10	600	0.01	4.527	3.690	4.256	4.158
15	7	10	20	30	600	0.01	6.490	7.961	6.490	6.980
16	3	100	5	10	800	0.001	11.924	12.452	10.598	11.658
17	3	100	20	30	800	0.001	12.818	12.890	12.839	12.849
18	7	10	5	30	600	0.001	5.971	11.338	9.578	8.962

19	7	10	5	10	600	0.01	3.501	2.082	2.130	2.571
20	7	100	5	10	800	0.01	9.991	10.672	9.869	10.177
21	3	10	5	30	800	0.001	27.352	27.900	27.984	27.745
22	7	100	5	30	600	0.01	5.664	3.398	1.836	3.633
23	7	100	5	30	800	0.001	13.290	13.154	13.199	13.214
24	3	100	20	10	600	0.001	16.573	17.942	15.783	16.766
25	3	100	20	30	600	0.01	17.018	21.644	-	19.331
26	3	100	5	30	600	0.001	14.584	33.224	-	23.904
27	7	10	20	10	600	0.001	12.454	13.024	13.107	12.862
28	3	10	5	10	800	0.01	4.179	4.482	4.350	4.337
29	7	100	20	30	600	0.001	10.224	11.364	9.978	10.522
30	3	100	20	10	800	0.01	28.867	28.063	-	28.465
31	7	100	20	10	600	0.01	19.452	18.724	-	19.088
32	7	100	20	10	800	0.001	10.182	8.702	10.258	9.714

---

Table A 8 Summary of variances of 32 runs done at 3 repeat experiments each for MUS

<i>Run</i>	<i>Count</i>	<i>Sum of peak areas</i>	<i>Average peak area</i>	<i>Variance</i>
1	3	56.077	18.692	0.657
2	3	22.316	7.439	0.183
3	3	48.636	16.212	0.006
4	3	13.994	4.665	0.315
5	3	34.115	11.372	1.097
6	3	14.250	4.750	0.002
7	3	58.449	19.483	1.217
8	3	27.031	9.010	0.317
9	3	16.526	5.509	0.084
10	3	29.303	9.768	1.390
11	3	12.082	4.027	0.086
12	3	33.202	11.067	2.158
13	3	20.993	6.998	0.026
14	3	12.473	4.158	0.182
15	3	20.941	6.980	0.721
16	3	34.974	11.658	0.912
17	3	38.547	12.849	0.001
18	3	26.887	8.962	7.485
19	3	7.713	2.571	0.649
20	3	30.532	10.177	0.187
21	3	83.236	27.745	0.118
22	3	10.898	3.633	3.705
23	3	39.643	13.214	0.005
24	3	50.298	16.766	1.193
25	3	38.662	19.331	10.700
26	3	47.808	23.904	173.725
27	3	38.585	12.862	0.126
28	3	13.011	4.337	0.023
29	3	31.566	10.522	0.547
30	3	56.930	28.465	0.323
31	3	29.142	9.714	0.265
32	3	38.176	19.088	0.770

Table A 9 Enrichment factor values for MUS when 32 runs were investigated.

Run	AP HCl	SLM	Extraction	Stirring			
Order	DP pH	conc	compo	time	rate	%NaCl	EF values
1	3	100	5	10	600	0.01	9.2
2	7	10	5	10	800	0.001	3.7
3	3	10	20	30	600	0.001	8.0
4	7	100	20	30	800	0.01	2.3
5	3	100	5	30	800	0.01	5.6
6	7	100	5	10	600	0.001	2.3
7	3	10	20	30	800	0.01	9.6
8	3	10	20	10	800	0.001	4.4
9	7	10	5	30	800	0.01	2.7
10	7	10	20	10	800	0.01	4.8
11	3	10	5	10	600	0.001	2.0
12	7	10	20	30	800	0.001	5.5
13	3	10	5	30	600	0.01	3.4
14	3	10	20	10	600	0.01	2.0
15	7	10	20	30	600	0.01	3.4
16	3	100	5	10	800	0.001	5.8
17	3	100	20	30	800	0.001	6.3
18	7	10	5	30	600	0.001	4.4
19	7	10	5	10	600	0.01	1.2
20	7	100	5	10	800	0.01	5.0
21	3	10	5	30	800	0.001	13.7
22	7	100	5	30	600	0.01	1.8
23	7	100	5	30	800	0.001	6.5
24	3	100	20	10	600	0.001	8.3
25	3	100	20	30	600	0.01	9.6
26	3	100	5	30	600	0.001	11.8
27	7	10	20	10	600	0.001	6.4
28	3	10	5	10	800	0.01	2.1
29	7	100	20	30	600	0.001	5.2
30	3	100	20	10	800	0.01	14.1
31	7	100	20	10	600	0.01	4.8
32	7	100	20	10	800	0.001	9.4

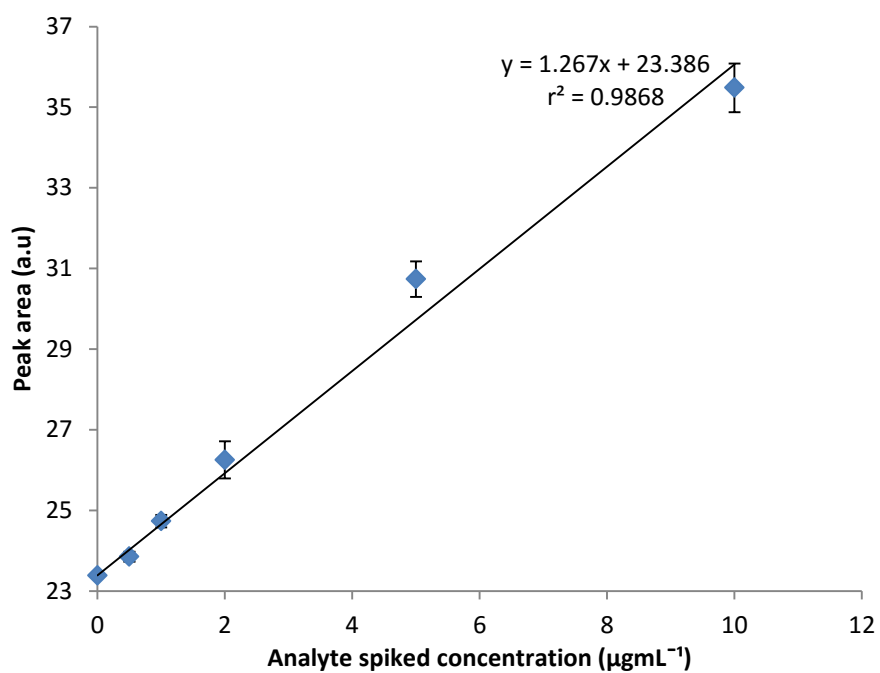


Figure A 5 Matrix-based calibration curve for the extraction of MUS from diluted urine samples and spiked up to a concentration of 10 µg L<sup>-1</sup>. The acceptor phase had been diluted 6 fold (n = 3, SD).